# Density-functional formulation of the generalized pseudopotential theory. III. Transition-metal interatomic potentials

John A. Moriarty
*Lawrence Livermore National Laboratory, University of California, Livermore, California 94550*
(Received 2 November 1987; revised manuscript received 24 February 1988)

The first-principles, density-functional version of the generalized pseudopotential theory (GPT) developed in papers I and II of this series [Phys. Rev. B **16**, 2537 (1977); **26**, 1754 (1982)] for empty- and filled-$d$-band metals is here extended to pure transition metals with partially filled $d$ bands. The present focus is on a rigorous, real-space expansion of the bulk total energy in terms of widely transferable, *structure-independent* interatomic potentials, including both central-force pair interactions and angular-force triplet and quadruplet interactions. To accomplish this expansion, a specialized set of starting equations is derived from the basic local-density formalism for a pure metal, including refined expansions for the exchange-correlation terms and a simplified yet accurate representation of the cohesive energy. The parent pseudo-Green's-function formalism of the GPT is then used to develop these equations in a plane-wave, localized-$d$-state basis. In this basis, the cohesive energy divides quite naturally into a large volume component and a smaller structural component. The volume component,which includes all one-ion *intra-atomic* energy contributions, already gives a good description of the cohesion in lowest order. The structural component is expanded in terms of weak *interatomic* matrix elements and gives rise to a multi-ion series which establishes the interatomic potentials. Special attention is focused on the dominant $d$-electron contributions to this series and complete formal results for the two-ion, three-ion, and four-ion $d$-state potentials ($v_2^d$, $v_3^d$, and $v_4^d$) are derived. In addition, a simplified model is used to demonstrate that while $v_3^d$ can be of comparable importance to $v_2^d$, $v_4^d$ is inherently small and the series is rapidly convergent beyond three-ion interactions. Analytic model forms are also derived for $v_2^d$ and $v_3^d$ in the case of canonical $d$ bands. In this limit, $v_2^d$ is purely attractive and varies with interatomic distance as $r^{-10}$, while $v_3^d$ is weak and attractive for almost empty or filled $d$ bands and maximum in strength and repulsive for half-filled $d$ bands. Full first-principles expressions are then developed for the total two-ion and three-ion potentials and implemented for all 20 $3d$ and $4d$ transition metals. The first-principles potentials qualitatively display all of the trends predicted by the model results, but they also reflect additional effects, including long-range hybridization tails which must be suitably screened in real-space calculations. Finally, illustrative application of the first-principles potentials is made to the calculation of the [100] phonon spectrum for V and Cr, where the importance of three-ion angular forces is explicitly demonstrated.

## I. INTRODUCTION

The generalization of pseudopotential expansion techniques to $d$-band metals[1-3] has been successfully developed in the past ten years for materials near the beginning and end of the transition series in the limits of empty and filled $d$ bands, respectively.[3-7] Our own work in this regard has taken the form of a first-principles, generalized pseudopotential theory (GPT) which has been fully integrated with the Kohn-Sham local-density-functional formalism[8] in the first two papers of this series[4,5] (hereinafter referred to as papers I and II). The parent theory[2] from which the density-functional GPT has evolved, however, is a quite general synthesis of nearly-free-electron concepts for $s$ and $p$ electrons and localized-orbital concepts for $d$ electrons and applies, in principle, to all $d$-band metals. In the present paper, we address the remaining problem of rigorously extending of the density-functional GPT to the more difficult case of pure transition metals with partially filled $d$ bands.

The focal point of the present theory is an accurate real-space representation of the total energy for a transition metal in terms of well-defined interatomic potentials. Specifically, we consider a homogeneous, elemental metal with an atomic volume $\Omega$ and seek to develop the total energy of the system as a multi-ion expansion involving its $N$ individual ion coordinates $\mathbf{R}_i$. The essential feature of our approach which permits this expansion is the characterization of the electronic structure in terms of effectively weak potentials, corresponding to small $sp$ band gaps and narrow $d$ bands in the metal, so that while *intra-atomic* $d$-state effects are large, all *interatomic* matrix elements coupling different sites are small. As a result, the series we shall derive is formally analogous to that obtained for nontransition metals:

$$E_{\rm tot}(\mathbf{R}_1,\mathbf{R}_2,\ldots,\mathbf{R}_N)=E_0(\Omega)+\tfrac{1}{2}\sum_{i,j}{}' v_2(R_{ij})+\tfrac{1}{6}\sum_{i,j,k}{}' v_3(R_{ij},R_{jk},R_{ki})+\tfrac{1}{24}\sum_{i,j,k,l}{}' v_4(R_{ij},R_{jk},R_{kl},R_{li},R_{ki},R_{lj})+\cdots . \quad (1)$$

 

Here, $E_0$ represents a volume term (including all intra-atomic, one-ion contributions) and $v_2$, $v_3$, $v_4$, etc. are two-ion, three-ion, four-ion, etc. interatomic potentials which are implicitly volume dependent, but explicitly *structure independent*. That is, the potentials themselves are independent of the absolute ion positions $\mathbf{R}_i$ and depend only on relative separations $R_{ij}=|\mathbf{R}_i-\mathbf{R}_j|$, etc. They are thus completely *transferable* at fixed volume and the entire structure dependence of the total energy then appears *analytically* through the summations, which extend over all $N$ ions in each case. The prime on each summation denotes the exclusion of all self-interaction terms where two indices are equal.

The ability of the local-density formalism to describe the energetics of transition metals has been rather well established through direct nonperturbative total-energy calculations of cohesion,[9] structural phase stability,[10] and high-symmetry phonons.[11] The introduction of the additional expansion (1), while necessarily a more approximate representation of the total energy, offers the possibility of greatly extending the range of application to include a complete description of structural, thermal, and mechanical properties of both the solid and liquid state, as has been possible for nontransition metals.[3–7,12] For these latter materials, one can readily express both the volume term $E_0$ and the central-force, pair potential $v_2$ in terms of appropriate nonlocal pseudopotentials. Furthermore, the neglect of $v_3$, $v_4$, and higher potentials has proved to be an excellent approximation in most applications. For pure transition metals, on the other hand, not only are the individual functionals necessarily more complicated and difficult to obtain, but one expects *a priori* that the angular forces associated with the multi-ion terms to be more important due to the strong-scattering nature of the $d$ electrons. This expectation is confirmed here, and, in particular, the three-ion triplet potential $v_3$ entering Eq. (1) will play a vital role in our development. At the same time, the series we shall obtain is rapidly convergent in the sense that the four-ion quadruplet potential $v_4$ is small and higher potentials appear to be negligible.

To our knowledge, this is the first *ab initio* theory of interatomic potentials for transition metals which has been *completely derived* from basic quantum-mechanical principles. In particular, we should contrast at the outset the present approach with the numerous attempts through the years to construct *ad hoc* interatomic potentials for transition metals from less fundamental perspectives. Most early representations of the total energy were given entirely in terms of empirical pair potentials [i.e., with $E_0=v_3=v_4=\cdots=0$ in Eq. (1)], typically with arbitrary forms for $v_2$ containing a number of adjustable parameters.[13] Such potentials are implicitly *structure dependent* and hence their transferability is always in serious doubt. Carlsson *et al.*[14] attempted to derive pair potentials more systematically by inverting energy-band calculations of $E_{\rm tot}$ as a function of volume. While such a potential is parameter-free and reproduces the cohesive properties of the metal by construction, it does not deal correctly with more subtle energetic properties such as phonons or structural energy differences. Moreover, pure pair potentials of this type suffer two fundamental weaknesses. First, they are required to satisfy the Cauchy elastic-constant relations (i.e., $C_{44}=C_{12}$), whereas it is well known that these relations are not obeyed in real transition metals (e.g., $C_{12}/C_{44}\approx 3$ for V, $\approx 5$ for Nb, $\approx 0.35$ for Cr, and $\approx 1.5$ for Mo). Second, such potentials require that the (unrelaxed) vacancy-formation energy $E_{\rm vac}$ is equal in magnitude to the cohesive energy $E_{\rm coh}$, whereas observed values of $E_{\rm vac}$ are typically only a small fraction of $E_{\rm coh}$ (e.g., $|E_{\rm vac}/E_{\rm coh}|\approx 0.3$ for Cr, Nb, and Mo).

An attempt has also been made to invert the experimental phonon spectrum of a metal into a pair potential.[15] This proved to be rather successful for simple metals, where a pair potential can indeed accurately describe the phonon spectrum, but the results are considerably more suspect for transition metals, where the anomalous phonon behavior driven by the multi-ion interactions is not well described. In addition, other attempts to explain observed properties for the central transition metals in terms of empirical potentials, including phonons and x-ray scattering data[16] and cohesion, defect energies, and elastic constants,[17] led directly to the conclusion that angular forces were indeed required in these materials. More recent empirical efforts[18,19] have attempted to effectively sum the multi-ion interactions by introducing local-volume potentials which depend nonlinearly on the local electron density. Such methods are inspired by density-functional theory and claim to have enough variational freedom to treat simultaneously not only the bulk and defect environments (including the lowering of $E_{\rm vac}$ below $E_{\rm coh}$), but free surfaces as well, where Eq. (1) is not expected to apply. However, as used in practice these methods depend on arbitrary functional forms with many adjustable parameters.

Other recent work on transition-metal interatomic potentials has begun to make a closer association with the real electronic structure of transition metals. Tight-binding concepts have been invoked in an attempt to tie the $d$-bonding component of the potentials to either the $d$-band energy or to moments of the density of states.[20–22] While the ideas presented are suggestive, the actual connection between these quantities and the potentials must ultimately be assumed rather than derived, and a number of the assumptions made are not well supported by the present theory. In related work, Dagens[23] has used liquid-metal theory and statistical concepts in an attempt to distribute the $d$-bonding energy among $E_0$, $v_2$, etc. in a more general way. His approach has only been carried out at the pair-potential level (i.e., with $v_3=v_4=\cdots=0$), but it does produce one result which is supported by our theory, namely, that in the limit of canonical tight-binding $d$ bands the short-range, $d$-bonding component of $v_2(r)$ should vary as $r^{-10}$.

A brief, preliminary account of the present work was published earlier,[24] in which prototype results for the pair ($v_2$) and triplet ($v_3$) potentials entering Eq. (1) were reported for $3d$ transition metals together with successful tests on the fundamental aspects of cohesion, structural phase stability, and the phonon spectrum. Additional applications to the recently observed anomalous phonon be-

havior in Ba and to the high-pressure properties of Cu have also appeared[25–27] and more will be forthcoming. The primary purpose of this paper is to establish, in complete detail, the full theory behind these results. We begin in Sec. II with the basic equations of density-functional theory governing the total energy of a metal and derive several important general results needed to accomplish our desired expansion. In Sec. III we add those elements of the parent GPT formalism from Ref. 2 required to obtain specific forms for the various components of the electron density and total energy of a transition metal. We also demonstrate for real $3d$ and $4d$ transition metals that the zero-order system from which our expansion proceeds is an excellent starting point and, in particular, accurately describes the large volume component of the total energy associated with cohesion. Then, in Sec. IV we focus in on the most important feature of the present development, namely, the multi-ion expansion of the $d$-band energy. There we derive precise formal results for the $d$-band components of the interatomic potentials ($v_2^d$, $v_3^d$, $v_4^d$, etc.) and add insight into why the expansion works through a simplified model. The latter allows us to explicitly address the question of convergence of our series as well as to make contact with many of the recent tight-binding ideas.[20–23] In particular, we show in the context of this model that while $v_3^d$ can be comparable to $v_2^d$ in importance, $v_4^d$ is relatively small and higher potentials are negligible. In Sec. V we return to the full theory and obtain complete expressions for $E_0$ and the dominant interatomic potentials $v_2$ and $v_3$ entering Eq. (1). We then present and discuss calculated first-principles potentials for all of the $3d$ and $4d$ transition metals, and briefly illustrate their application. We conclude in Sec. VI with a discussion about the range of expected applications of these potentials and possible extensions, as well as limitations, of the theory as a whole.

## II. ELEMENTS OF DENSITY-FUNCTIONAL THEORY

### A. General equations in the local-density approximation

We begin with the usual nonrelativistic Kohn-Sham local-density equations[8] specialized to a nonmagnetic, elemental metal of atomic number $Z_a$. The total energy can be written in the form

$$E_{\rm tot}=\tfrac{1}{2}\sum_{i,j}{}'\frac{(Z_a e)^2}{|\mathbf{R}_i-\mathbf{R}_j|}+\sum_\alpha E_\alpha-\tfrac{1}{2}\int\int\frac{e^2 n(\mathbf{r})n(\mathbf{r}')}{|\mathbf{r}-\mathbf{r}'|}d\mathbf{r}\,d\mathbf{r}'+\int n(\mathbf{r})[\varepsilon_{\rm xc}(n(\mathbf{r}))-\mu_{\rm xc}(n(\mathbf{r}))]d\mathbf{r}+NZ_aV_0\ , \tag{2}$$

where the $E_\alpha$ are one-electron eigenvalues of the Schrödinger equation

$$\left[-\frac{\hbar^2}{2m}\nabla^2+V\right]|\psi_\alpha\rangle=E_\alpha|\psi_\alpha\rangle\ , \tag{3}$$

with $V$ the total self-consistent one-electron potential

$$V(\mathbf{r})=-\sum_i\frac{Z_a e^2}{|\mathbf{r}-\mathbf{R}_i|}+\int\frac{e^2 n(\mathbf{r}')}{|\mathbf{r}-\mathbf{r}'|}d\mathbf{r}'+\mu_{\rm xc}(n(\mathbf{r}))-V_0\ , \tag{4}$$

$n$ the total electron density

$$n(\mathbf{r})=\sum_\alpha\langle\mathbf{r}|\psi_\alpha\rangle\langle\psi_\alpha|\mathbf{r}\rangle\ , \tag{5}$$

and $\mu_{\rm xc}$ the exchange-correlation potential

$$\mu_{\rm xc}(n)=\frac{d}{dn}[n\varepsilon_{\rm xc}(n)]\ . \tag{6}$$

The sums in Eqs. (2) and (5) are over all occupied states $\alpha$ and $\varepsilon_{\rm xc}(n)$ in Eqs. (2) and (6) is the exchange-correlation energy of the uniform electron gas of density $n$. When a specific form is required for $\varepsilon_{\rm xc}(n)$, we shall use here, as previously, the interpolation formula developed by Hedin and Lundqvist.[28] The constant $V_0$ in the potential $V$ permits an arbitrary choice of the zero of energy in Eq. (3), while the final term in Eq. (2) insures that $E_{\rm tot}$ is independent of this choice.

### B. Multi-ion expansion of $\mu_{\rm xc}$ and $E_{\rm xc}$

A fundamental requirement in the present work is to approximate the inherently nonlinear exchange-correlation functionals entering Eqs. (2)–(6) in forms that are both accurate and commensurate with the total-energy expansion we seek, Eq. (1). To do this, we first write the electron density in the form

$$n=n_{\rm val}+\sum_i n_i\ , \tag{7}$$

where we envisage that $n_i$ is a *localized* inner-core plus occupied valence $d$-state density centered about the site $i$ and that $n_{\rm val}$ includes all remaining valence-electron density, which is then primarily $s$ and $p$ in character and more or less uniform outside the inner-core regions. This represents no additional approximation at present, but only reflects the anticipated partitioning of electron density which will enter our theory below in Sec. III. We next define the functionals

$$\mu_{\rm xc}^*(n_i)\equiv\mu_{\rm xc}(n_{\rm val}+n_i)-\mu_{\rm xc}(n_{\rm val}) \tag{8}$$

and

$$\varepsilon_{\rm xc}^*(n_i)\equiv\varepsilon_{\rm xc}(n_{\rm val}+n_i)-\varepsilon_{\rm xc}(n_{\rm val})\ . \tag{9}$$

Both of these quantities are well localized about the site $i$ and vanish as $n_i$ does. We can then develop $\mu_{\rm xc}(n)$ and $\varepsilon_{\rm xc}(n)$ in appropriate multi-ion expansions involving the overlap of the $n_i$ from different sites. To do this, we for-

mally proceed as in paper I and consider the limit of large ion separation. We then expand in powers of $\sum_i n_i/n_{\rm val}$, isolate all overlap terms with a common structural dependence, and finally, continue the result analytically to arbitrary separation by resumming each group of structurally similar terms. This leads to the desired clusterlike expansion

$$\mu_{\rm xc}(n)=\mu_{\rm xc}(n_{\rm val})+\sum_i \mu^*_{\rm xc}(n_i)+\tfrac{1}{2}\sum_{i,j}{}' \delta\mu^*_{\rm xc}(n_i,n_j)+\cdots , \tag{10}$$

where

$$\delta\mu^*_{\rm xc}(n_i,n_j)\equiv\mu^*_{\rm xc}(n_i+n_j)-\mu^*_{\rm xc}(n_i)-\mu^*_{\rm xc}(n_j) . \tag{11}$$

As demonstrated in paper I, the linear superposition approximation represented by the first two terms in Eq. (10) is already reasonably accurate for real $d$-band metals due to the slowly varying nature of the functional $\mu_{\rm xc}$. The third term in Eq. (10) makes the result exact for two-ion overlap, as can be verified by inspection. The correction functional $\delta\mu^*_{\rm xc}(n_i,n_j)$ is localized in the interstitial region between sites $i$ and $j$ and is retained here as a desirable improvement for pure transition metals. Three-ion and higher overlap terms may be systematically obtained by a continuation of this procedure, but are here neglected as small.

A similar development can be made for $\varepsilon_{\rm xc}(n)$ and the corresponding exchange-correlation energy

$$E_{\rm xc}=\int n(\mathbf{r})\varepsilon_{\rm xc}(n(\mathbf{r}))d\mathbf{r}\equiv n\varepsilon_{\rm xc}(n) , \tag{12}$$

where the latter equality represents a shorthand notation which we shall adopt everywhere below. To the level of two-ion overlap, we find

$$E_{\rm xc}=n_{\rm val}\varepsilon_{\rm xc}(n_{\rm val})+\sum_i n_i\varepsilon_{\rm xc}(n_i)+\sum_i \delta\varepsilon^{\text{val-core}}_{\rm xc}(n_i)+\tfrac{1}{2}\sum_{i,j}{}'[n_i\mu^*_{\rm xc}(n_j)+\delta\varepsilon^*_{\rm xc}(n_i,n_j)]+\cdots , \tag{13}$$

where

$$\delta\varepsilon^{\text{val-core}}_{\rm xc}(n_i)\equiv(n_{\rm val}+n_i)\varepsilon_{\rm xc}(n_{\rm val}+n_i)-n_{\rm val}\varepsilon_{\rm xc}(n_{\rm val})-n_i\varepsilon_{\rm xc}(n_i) \tag{14}$$

and

$$\delta\varepsilon^*_{\rm xc}(n_i,n_j)\equiv(n_{\rm val}+n_i+n_j)[\varepsilon^*_{\rm xc}(n_i+n_j)-\varepsilon^*_{\rm xc}(n_i)-\varepsilon^*_{\rm xc}(n_j)]+n_i[\varepsilon^*_{\rm xc}(n_j)-\tfrac{1}{2}\mu^*_{\rm xc}(n_j)]+n_j[\varepsilon^*_{\rm xc}(n_i)-\tfrac{1}{2}\mu^*_{\rm xc}(n_i)] . \tag{15}$$

The first two terms in Eq. (13) represent the exchange-correlation energies of isolated densities $n_{\rm val}$ and $n_i$, the third term is the correction for valence-core overlap on a single site, and the final term is the contribution of two-ion overlap, which adds directly to the two-ion pair potential $v_2$ in Eq. (1). The valence-core–overlap energy $\delta\varepsilon^{\text{val-core}}_{\rm xc}(n_i)$ derives its principal contribution from the inner-core region where $n_{\rm val}$ is small. In papers I and II this energy was implicitly neglected; a better approximation, in general, is to arrange a direct cancellation of this quantity in the cohesive energy, as discussed below. In addition, the two-ion-overlap correction term $\delta\varepsilon^*_{\rm xc}(n_i,n_j)$, which was also neglected in papers I and II, makes a significant positive contribution to $v_2$ in transition metals, as illustrated in Fig. 1 for the case of Cu, and is therefore explicitly retained in the present work.

### C. Cohesive energy and valence binding energy

To extract the small structural components of the total energy which contribute to the interatomic potentials in Eq. (1), it is desirable to remove at the outset the large one-ion corelike contributions in $E_{\rm tot}$. With the electron density expressed in the form (7), this can be done most cleanly by considering the cohesive energy. We begin by indexing the total energy per atom in the solid,

$$E_{\rm solid}(Z)\equiv\frac{1}{N}E^{\rm solid}_{\rm tot} , \tag{16}$$

by the $sp$ valence $Z$, here defined as

$$Z\equiv\frac{1}{N}\int n^{\rm solid}_{\rm val}(\mathbf{r})d\mathbf{r} . \tag{17}$$

Physically, $Z$ is a measure of the number of valence $s$ and $p$ electrons per atom and must be determined self-consistently. In addition, this valence is an environmentally dependent quantity, depending in the present theory explicitly on volume for a given material. Representative values for the $3d$ and $4d$ transition metals at their observed equilibrium volumes are given in Table I; the pre-

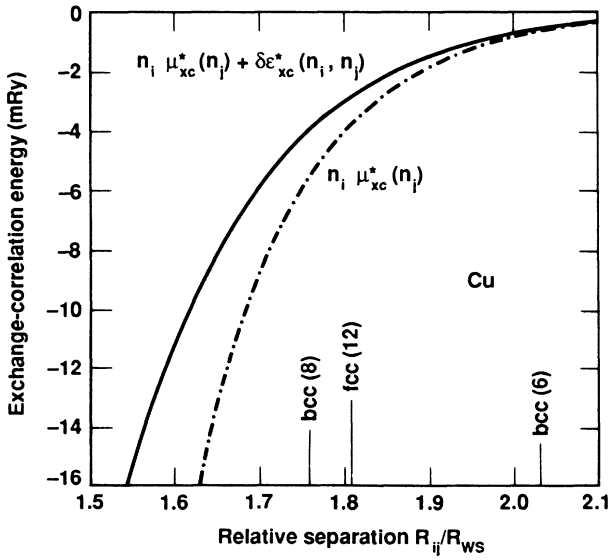


FIG. 1. Direct exchange-correlation contributions from Eq. (13) to the two-ion interatomic potential $v_2(R_{ij})$ for the case of Cu. Here, $R_{\rm WS}$ is the Wigner-Seitz radius, and the location and number of near neighbors in the fcc and bcc structures are indicated.

TABLE I. Free-atom and metallic valences and atomic components of the cohesive energy for the $3d$ and $4d$ transition metals, as discussed in the text. The values of $Z_0$ are those predicted by the LSD calculations of Ref. 9. The values of $Z$ correspond to a $d$-state logarithmic derivative of $D_2^* = -3$ (see Sec. III D). All energies are given in Ry.

| Element | $Z_0$ | $Z$ | $\delta E_{sp}$ | $E_{pro}$ | $E_{prep}$ | $E_{bind}^{atom}(Z)-E_{prep}$ |
|---|---|---|---|---|---|---|
| $3d$ series | | | | | | |
| Ca | 2.0 | 1.565 | 0.0 | 0.060 | 0.060 | −0.904 |
| Sc | 2.0 | 1.617 | 0.012 | 0.029 | 0.041 | −1.019 |
| Ti | 1.0 | 1.516 | 0.159 | −0.049 | 0.110 | −1.036 |
| V | 1.0 | 1.425 | 0.262 | −0.029 | 0.233 | −1.104 |
| Cr | 1.0 | 1.411 | 0.400 | −0.015 | 0.385 | −1.278 |
| Mn | 2.0 | 1.485 | 0.395 | −0.049 | 0.346 | −1.359 |
| Fe | 1.6 | 1.474 | 0.219 | −0.011 | 0.208 | −1.242 |
| Co | 1.1 | 1.463 | 0.098 | 0.024 | 0.122 | −1.174 |
| Ni | 1.0 | 1.487 | 0.043 | 0.043 | 0.086 | −1.200 |
| Cu | 1.0 | 1.654 | 0.025 | 0.089 | 0.114 | −1.504 |
| $4d$ series | | | | | | |
| Sr | 2.0 | 1.508 | 0.0 | 0.072 | 0.072 | −0.822 |
| Y | 2.0 | 1.541 | 0.014 | 0.044 | 0.058 | −0.919 |
| Zr | 1.0 | 1.382 | 0.147 | −0.028 | 0.119 | −0.879 |
| Nb | 1.0 | 1.210 | 0.227 | −0.007 | 0.220 | −0.856 |
| Mo | 1.0 | 1.141 | 0.330 | 0.002 | 0.332 | −0.928 |
| Tc | 1.0 | 1.125 | 0.224 | 0.008 | 0.232 | −0.829 |
| Ru | 1.0 | 1.132 | 0.139 | 0.016 | 0.155 | −0.771 |
| Rh | 0.0 | 1.146 | 0.016 | 0.138 | 0.154 | −0.795 |
| Pd | 0.0 | 1.179 | 0.0 | 0.203 | 0.203 | −0.886 |
| Ag | 1.0 | 1.617 | 0.021 | 0.206 | 0.227 | −1.443 |

cise origin of these results will be discussed in Sec. III. For the present, note only that the range of values is between 1.1 and 1.7 for all 20 elements, including the alkaline-earth and noble metals at the series endpoints.[27] Similarly, in the isolated free atom we write

$$E_{atom}(Z_0) \equiv E_{tot}^{atom} , \tag{18}$$

with

$$Z_0 \equiv \int n_{val}^{atom}(\mathbf{r}) d\mathbf{r} . \tag{19}$$

For transition metals, $Z_0$ represents the number of outer valence $s$ electrons in the ground state. In the usual case, an $s \rightarrow d$ or $d \rightarrow s$ transfer of electrons will occur as the solid is formed, so that $Z_0$ will differ from $Z$. Furthermore, in the context of density-functional theory $Z_0$ will necessarily reflect the effects of spin polarization. In order to deal with the latter complication, we here adopt the values of $Z_0$ determined by Moruzzi *et al.*[9] using the local-spin-density (LSD) formulation of density-functional theory and a treatment of exchange and correlation consistent with the Hedin-Lundqvist prescription[28] in the non-spin-polarized case. These values are listed in Table I for the $3d$ and $4d$ transition-series elements. We also define a corresponding spin-polarization energy $\delta E_{sp}$ as the difference in total energy between the non-spin-polarized atom calculated in the present local-density (LD) approximation and the spin-polarized atom calculated in the LSD approximation for the same atomic configuration with valence $Z_0$:

$$\delta E_{sp} \equiv E_{atom}(Z_0;\mathrm{LD}) - E_{atom}(Z_0;\mathrm{LSD}) . \tag{20}$$

Then, $\delta E_{sp}$ is a positive constant for each element, which may be evaluated once and for all, and the remaining total-energy considerations may be made in the LD approximation. Values of $\delta E_{sp}$ that we have obtained from the LSD free-atom total energies of Moruzzi *et al.*[9] and our own LD results for the same atomic configurations are given in Table I.

The next step is to transfer the appropriate number of $d$ electrons to valence $s$ orbitals (or vice versa where necessary) to match the valence $Z$ of the solid.[29] Then the inner-core plus occupied $d$-state density of the promoted atom closely approximates $n_i$, the localized density associated with a single ion in the solid. The corresponding promotion energy is simply

$$E_{pro} \equiv E_{atom}(Z) - E_{atom}(Z_0) , \tag{21}$$

where the LD approximation is now implied in the total energies. There is no difficulty in evaluating $E_{pro}$ directly, but we have developed a simple yet very accurate approximation formula for this quantity:

$$E_{pro} = \tfrac{1}{2} \sum_m (\alpha_m - \alpha_m^0)(\varepsilon_m + \varepsilon_m^0) , \tag{22}$$

where $\alpha_m$ and $\alpha_m^0$ are the occupation numbers and $\varepsilon_m$ and $\varepsilon_m^0$ the one-electron orbital energies of the promoted and unpromoted atoms, respectively. The derivation of this result in the context of the density-functional theory, as well as its accuracy for real materials, is discussed in

Appendix A. Note that only the states whose occupation numbers change (i.e., the outer $d$ and $s$ states) contribute to the sum in Eq. (22), so that energies several orders of magnitude smaller than the total energy are involved in the result. Values of $E_{\rm pro}$ obtained from Eq. (22) for the $3d$ and $4d$ elements are given in Table I. The largest promotion energies here occur for elements on the right-hand side of each series and the smallest for the central elements. The slight negative values of some of the latter occur because $E_{\rm atom}(Z_0)$ is *not* the lowest total energy of the non-spin-polarized free atom. The total atomic preparation energy,

$$E_{\rm prep} \equiv E_{\rm pro} + \delta E_{\rm sp} \ , \tag{23}$$

is, of course, always positive and is maximum near the center of each series.

One may now write the cohesive energy as the total energy of the solid relative to that of the free atom:

$$\begin{aligned} E_{\rm coh} &= E_{\rm solid}(Z) - E_{\rm atom}(Z_0) + \delta E_{\rm sp} \\ &= E_{\rm solid}(Z) - E_{\rm atom}(Z) + E_{\rm prep} \ . \end{aligned} \tag{24}$$

The second form of Eq. (24) then allows us to accomplish the desired cancellations. To do this, we break both the solid and promoted-atom total energies into valence-binding, core, and valence-core–overlap contributions:

$$E_{\rm solid}(Z) = E^{\rm solid}_{\rm bind}(Z) + E_{\rm core} + E_{\rm val\text{-}core} \tag{25}$$

and

$$E_{\rm atom}(Z) = E^{\rm atom}_{\rm bind}(Z) + E_{\rm core} + E_{\rm val\text{-}core} \ . \tag{26}$$

In the solid with the electron density given by Eq. (7), one can anticipate that the sum over occupied states in Eq. (2) will have the form

$$\sum_\alpha E_\alpha = E^{\rm val}_{\rm band} + \sum_i \left( T[n_i] + n_i V \right) \ , \tag{27}$$

which defines an effective valence contribution $E^{\rm val}_{\rm band}$ to the total band-structure energy, where $T[n_i]$ is the kinetic energy of the electron density $n_i$. Equation (27) thus divides the total $d$-electron contribution to the band-structure energy into a large corelike component contained in the final two terms and a cohesive component implicit in $E^{\rm val}_{\rm band}$. Then using Eqs. (7), (10), (13), and (27) in Eq. (2), one can derive the following results *without further approximation*:

$$E^{\rm solid}_{\rm bind}(Z) = \frac{1}{N} \left\{ E^{\rm val}_{\rm band} - \tfrac{1}{2} n_{\rm val} V_{\rm val} + n_{\rm val} [\varepsilon_{\rm xc}(n_{\rm val}) - \mu_{\rm xc}(n_{\rm val})] + \tfrac{1}{2} {\sum_{i,j}}' [n_i \mu^*_{\rm xc}(n_j) + \delta\varepsilon^*_{\rm xc}(n_i, n_j) - n_{\rm val} \delta\mu^*_{\rm xc}(n_i, n_j)] \right.$$

$$\left. + \tfrac{1}{2} {\sum_{i,j}}' \left[ \frac{(Z_a e)^2}{|\mathbf{R}_i - \mathbf{R}_j|} + 2 n_i \left[ -\frac{Z_a e^2}{|\mathbf{r} - \mathbf{R}_j|} \right] + n_i v_j \right] \right\} + Z V_0 \ , \tag{28}$$

$$E_{\rm core} = \frac{1}{N} \sum_i \left[ T[n_i] + n_i \left[ -\frac{Z_a e^2}{|\mathbf{r} - \mathbf{R}_i|} + \tfrac{1}{2} v_i + \varepsilon_{\rm xc}(n_i) \right] \right] \ , \tag{29}$$

and

$$E_{\rm val\text{-}core} = \frac{1}{N} \sum_i [\delta\varepsilon^{\rm val\text{-}core}_{\rm xc}(n_i) - n_{\rm val} \mu^*_{\rm xc}(n_i)] \ . \tag{30}$$

Here, $V_{\rm val}$ and $v_i$ are the Coulomb potentials arising from $n_{\rm val}$ and $n_i$, respectively. Likewise, for the promoted atom with valence density $n^{\rm at}_{\rm val}$ one obtains (with $V_0 = 0$)

$$\begin{aligned} E^{\rm atom}_{\rm bind}(Z) = & \sum_{m = \rm val} \varepsilon_m - \tfrac{1}{2} n^{\rm at}_{\rm val} V^{\rm at}_{\rm val} \\ & + n^{\rm at}_{\rm val} [\varepsilon_{\rm xc}(n^{\rm at}_{\rm val}) - \mu_{\rm xc}(n^{\rm at}_{\rm val})] \ , \end{aligned} \tag{31}$$

with similar expressions to Eqs. (29) and (30) for $E_{\rm core}$ and $E_{\rm val\text{-}core}$. The solid and atomic core energies are equal so long as $n_i$ in the solid closely approximates the corresponding promoted-atom density, as will be the case here. The respective valence-core–overlap energies are approximately equal because (i) in both cases the additional second term in Eq. (30) tends to cancel the first in the important inner-core region where $n_i \gg n_{\rm val}$ and (ii) in the inner-core region $n_{\rm val}$ approximates $n^{\rm at}_{\rm val}$ due to the constraints of valence-core wave-function orthogonality.

Canceling the $E_{\rm core}$ and $E_{\rm val\text{-}core}$ terms in the cohesive energy (24), we are thus left with the simplified result we desire:

$$E_{\rm coh} = E^{\rm solid}_{\rm bind}(Z) - E^{\rm atom}_{\rm bind}(Z) + E_{\rm prep} \ . \tag{32}$$

The explicit advantage of Eq. (32) is that all three components on the right-hand side are already within an order of magnitude of the cohesive energy itself and the multi-ion expansion we seek can now be developed from Eq. (28). The small price that has been paid is that the final two atomic terms depend on $Z$ and hence must be recalculated for each volume of interest.

Equations (23), (28), (31), and (32) generalize our previous results[30] obtained for simple, empty-$d$-band, and filled-$d$-band metals in the limit $Z = Z_0$, with $\delta\varepsilon^*_{\rm xc} = \delta\mu^*_{\rm xc} = 0$. For such metals, both the normal cohesive properties (cohesive energy, equilibrium atomic volume, and bulk modulus) and the zero-temperature equation of state are thereby accurately described.[5,6,30] For transition metals, a similar test of the present equations has been made in the case of Cu up to very high pressure.[26] Except at extreme compression, where the

core overlap becomes large, these equations are found to produce results comparable to those obtained from the full density-functional formalism, Eqs. (2)–(6), as implemented by self-consistent band-structure techniques.

## III. ELEMENTS OF GENERALIZED PSEUDOPOTENTIAL THEORY

### A. Mixed-basis representation and pseudo Green's functions

The inner-core electrons governed by the one-electron Schrödinger equation (3) are amenable to a purely atomiclike treatment. We invoke the usual small-core approximation, in which such localized states $|\phi_c\rangle$ are assumed to be exact eigenstates of the full metal Hamiltonian $H$. This allows one to transform Eq. (3) to an exactly equivalent pseudo-Schrödinger equation

$$\left[-\frac{\hbar^2}{2m}\nabla^2+W\right]|\phi_\alpha\rangle=E_\alpha|\phi_\alpha\rangle \tag{33}$$

for the remaining valence $s$, $p$, and $d$ electrons, where in optimized form $W$ is the nonlocal pseudopotential

$$W=(1-P_c)V\ , \tag{34}$$

with $P_c$ the inner-core-state projection operator

$$P_c\equiv\sum_c|\phi_c\rangle\langle\phi_c|\ . \tag{35}$$

Some of the important properties of this form of pseudopotential in the present context are discussed in Appendix B, but here we need only note that in transition metals $W$ is effectively weak for the nearly-free-electron $s$ and $p$ electrons, as in simple metals, but is strong for the more localized $d$ electrons which still largely see the full potential $V$. An appropriate basis set with which to represent $|\phi_\alpha\rangle$ then is one including both plane waves $|\mathbf{k}\rangle$ and five localized $d$ states $|\phi_d\rangle$ centered on each ion site. The latter are chosen to be exact eigenstates of a suitable atomiclike reference Hamiltonian:

$$\left[-\frac{\hbar^2}{2m}\nabla^2+v_{\rm at}\right]|\phi_d\rangle=E_d^0|\phi_d\rangle\ . \tag{36}$$

A second effectively weak potential is then

$$\Delta\equiv\delta V-\langle\phi_d|\delta V|\phi_d\rangle\ , \tag{37}$$

where

$$\delta V\equiv v_{\rm at}-V\ . \tag{38}$$

Conceptually, one may identify the reference Hamiltonian in Eq. (36) with the promoted atom introduced above. In practice, the actual choice of $v_{\rm at}$ and the calculation of $|\phi_c\rangle$ and $|\phi_d\rangle$ are specified through a closely related zero-order pseudoatom construction, as used in papers I and II, and as discussed in Sec. III D below for transition metals. For this choice of $v_{\rm at}$, the $d$-state hybridization potential $\Delta$ is indeed small in the interior region of the atomic site on which it is centered and only becomes large in the exterior region. Thus the product $\Delta|\phi_d\rangle$ is everywhere small. The entire structure of the $d$ bands in the metal and their hybridization with the nearly-free-electron $s$ and $p$ bands can be fully characterized in terms of the $d$-state energy

$$E_d\equiv\langle\phi_d|H|\phi_d\rangle =E_d^0-\langle\phi_d|\delta V|\phi_d\rangle\ , \tag{39}$$

small $d$-state overlap matrix elements

$$S_{dd'}(R_{ij})\equiv\langle\phi_d(\mathbf{r}-\mathbf{R}_i)|\phi_{d'}(\mathbf{r}-\mathbf{R}_j)\rangle \tag{40}$$

and

$$\Delta_{dd'}(R_{ij})\equiv\langle\phi_d(\mathbf{r}-\mathbf{R}_i)|\Delta|\phi_{d'}(\mathbf{r}-\mathbf{R}_j)\rangle \tag{41}$$

between $d$ states centered on sites $i$ and $j$, and small plane-wave–$d$-state (or $sp$-$d$) hybridization matrix elements

$$S_{\mathbf{k}d}\equiv\langle\mathbf{k}|\phi_d\rangle \tag{42}$$

and

$$\Delta_{\mathbf{k}d}\equiv\langle\mathbf{k}|\Delta|\phi_d\rangle\ . \tag{43}$$

The $d$ states centered on a given site are orthonormal functions, so that for $R_{ij}=0$ one has $S_{dd}=1$ and $\Delta_{dd}=0$.

In order to obtain the central theoretical quantities of interest here, namely, the electron density and the valence band-structure energy, it is convenient to introduce a pseudo-Green's-function formalism based on Eq. (33). We follow Ref. 2, where in a $|\mathbf{k}\rangle$, $|\phi_d\rangle$ basis the appropriate Green's-function equations are found to be

$$(E-E_d)G_{dd'}=S_{dd'}+\sum_{\mathbf{k}'}V'_{d\mathbf{k}'}G_{\mathbf{k}'d'}+\sum_{d''}{}'V'_{dd''}G_{d''d'}\ , \tag{44a}$$

$$(E-\varepsilon_{\mathbf{k}})G_{\mathbf{k}d}=S_{\mathbf{k}d}+\sum_{\mathbf{k}'}W_{\mathbf{k}\mathbf{k}'}G_{\mathbf{k}'d}+\sum_{d'}V'_{\mathbf{k}d'}G_{d'd}\ , \tag{44b}$$

$$(E-\varepsilon_{\mathbf{k}})G_{\mathbf{k}\mathbf{k}'}=\delta_{\mathbf{k}\mathbf{k}'}+\sum_{\mathbf{k}''}W_{\mathbf{k}\mathbf{k}''}G_{\mathbf{k}''\mathbf{k}'}+\sum_{d'}V'_{\mathbf{k}d'}G_{d'\mathbf{k}'}\ , \tag{44c}$$

$$(E-E_d)G_{d\mathbf{k}}=S_{d\mathbf{k}}+\sum_{\mathbf{k}'}V'_{d\mathbf{k}'}G_{\mathbf{k}'\mathbf{k}}+\sum_{d'}{}'V'_{dd'}G_{d'\mathbf{k}}\ , \tag{44d}$$

with $W_{\mathbf{k}\mathbf{k}'}\equiv\langle\mathbf{k}|W|\mathbf{k}'\rangle$ and $V'\equiv H-E$, so that

$$V'_{\mathbf{k}d}=-(E-E_d)S_{\mathbf{k}d}-\Delta_{\mathbf{k}d} \tag{45}$$

and

$$V'_{dd'}=-(E-E_d)S_{dd'}-\Delta_{dd'}\ . \tag{46}$$

The formal solution of the coupled equations (44a)–(44d) for the four Green's-function elements $G_{\mathbf{k}\mathbf{k}'}$, $G_{\mathbf{k}d}$, $G_{d\mathbf{k}}$, and $G_{dd'}$ is discussed in Ref. 2 and we shall apply those results directly in our derivations below. The summations over localized inner-core and $d$ states in all these equations implicitly include a sum both over ion sites and individual quantum numbers (excluding spin), and we shall maintain this convention[31] in the remainder of Sec. III. Also, in all results derived from the Green's-function equations, $E$ has the meaning $E+i0^+$.

### B. Density of states and valence band-structure energy $E_{\rm band}^{\rm val}$

If we now choose the constant $V_0$ in the potential $V$ such that the zero of energy in Eqs. (44a)–(44d) is at the bottom of the valence bands, then the density of states for $E>0$ (i.e., excluding the inner-core states) is given by Eq. (48) of Ref. 2:

$$\rho(E)=-\frac{2}{\pi}\mathrm{Im}\left[\sum_{\mathbf{k}} G_{\mathbf{kk}}+\sum_{d} G_{dd}\right] =-\frac{2}{\pi}\mathrm{Im}\left[\sum_{\mathbf{k}}\frac{1}{E-\varepsilon_{\mathbf{k}}}+\sum_{\mathbf{k}}\frac{\Sigma_{\mathbf{kk}}}{(E-\varepsilon_{\mathbf{k}})^2} +\frac{d}{dE}\ln D(E)\right], \tag{47}$$

where the spin factor of 2 has been taken out explicitly and we have defined the energy-dependent functionals

$$\Sigma_{\mathbf{kk}}\equiv W_{\mathbf{kk}}+\sum_{\mathbf{k}'}\frac{W_{\mathbf{kk}'}W_{\mathbf{k}'\mathbf{k}}}{E-\varepsilon_{\mathbf{k}'}}+\cdots \tag{48}$$

and

$$D(E)=\det[-(V'_{dd'}+\Gamma_{dd'}+\Lambda_{dd'})], \tag{49}$$

with

$$\Gamma_{dd'}(R_{ij},E)\equiv\sum_{\mathbf{k}}\frac{V'_{d\mathbf{k}}V'_{\mathbf{k}d'}}{E-\varepsilon_{\mathbf{k}}} \tag{50}$$

and

$$\Lambda_{dd'}(R_{ij},E)\equiv\sum_{\mathbf{k},\mathbf{k}'}\frac{V'_{d\mathbf{k}}\Sigma_{\mathbf{kk}'}V'_{\mathbf{k}'d'}}{(E-\varepsilon_{\mathbf{k}})(E-\varepsilon_{\mathbf{k}'})}\ . \tag{51}$$

Note that $\Sigma_{\mathbf{kk}}$ involves an infinite series expansion in powers of $W_{\mathbf{kk}'}$ and that $D(E)$ is a $5N\times 5N$ determinant. Thus Eq. (47), although formally exact, cannot readily be used in this form to numerically calculate the density of states for a real material. The usefulness of this result comes rather through its powerful analytic properties, which we now seek to exploit in developing a multi-ion expansion for the valence band-structure energy.

In writing Eq. (27) for the sum of one-electron energies in the metal, we separated out the corelike component associated with the localized inner-core and $d$-state electron density $n_i$. If the $d$-state contribution to $n_i$ is now identified with the partial occupation of our basis states $|\phi_d\rangle$, corresponding to $Z_d$ electrons per site, then the effective valence band-structure energy defined in Eq. (27) is exactly

$$E_{\rm band}^{\rm val}=\int_0^{E_F}E\rho(E)dE-NZ_dE_d\ , \tag{52}$$

where $E_F$ is the Fermi energy. Here, one can avoid the energy derivative in Eq. (47) for $\rho(E)$ by introducing the integrated density of states

$$\mathcal{N}(E)\equiv\int_0^E\rho(E)dE\ . \tag{53}$$

Then using $\rho(E)=d\mathcal{N}(E)/dE$, integrating once by parts, and adding the conservation-of-electrons condition

$$\mathcal{N}(E_F)=N(Z+Z_d)\ , \tag{54}$$

one has without approximation

$$E_{\rm band}^{\rm val}=NZE_F+NZ_d(E_F-E_d)-\int_0^{E_F}\mathcal{N}(E)dE\ . \tag{55}$$

The next step is to break $\rho(E)$ and $\mathcal{N}(E)$ into separate components:

$$\rho(E)=\rho_0(E)+\delta\rho_{sp}(E)+\rho_d(E)+\delta\rho_d(E) \tag{56}$$

and

$$\mathcal{N}(E)=\mathcal{N}_0(E)+\delta\mathcal{N}_{sp}(E)+\mathcal{N}_d(E)+\delta\mathcal{N}_d(E)\ . \tag{57}$$

We identify $\rho_0$ and $\delta\rho_{sp}$ with the first two terms in Eq. (47), where $\rho_0$ is just the free-electron density of states. It readily follows that

$$\mathcal{N}_0(E)=\left[\frac{2m}{\hbar^2}\right]^{3/2}\frac{N\Omega}{3\pi^2}E^{3/2} \tag{58}$$

and, using Eq. (59) of Ref. 2, that

$$\delta\mathcal{N}_{sp}(E)=\frac{2}{\pi}\mathrm{Im}\left[\sum_{\mathbf{k}}\frac{W_{\mathbf{kk}}}{E-\varepsilon_{\mathbf{k}}}+\tfrac{1}{2}\sum_{\mathbf{k}}\frac{W_{\mathbf{kk}}^2}{(E-\varepsilon_{\mathbf{k}})^2} +\sum_{\mathbf{k},\mathbf{k}'}{}'\frac{W_{\mathbf{kk}'}W_{\mathbf{k}'\mathbf{k}}}{(E-\varepsilon_{\mathbf{k}})(\varepsilon_{\mathbf{k}}-\varepsilon_{\mathbf{k}'})}+\cdots\right]. \tag{59}$$

We then identify $\rho_d$ and $\delta\rho_d$ with the final term in Eq. (47), such that $\rho_d$ is the one-ion $d$-state component of the density of states. In order to do this, we first note that the one-ion $R_{ij}=0$ terms in $\ln D(E)$ can be extracted in the form

$$\ln D(E)=\sum_d\ln(E-E_d-\Gamma_{dd}-\Lambda_{dd})+\ln[\det(t_{dd'})]\ , \tag{60}$$

where $t_{dd'}$ is the relative $d$-state coupling strength between different sites:

$$t_{dd'}(R_{ij},E)\equiv\frac{-V'_{dd'}-\Gamma_{dd'}-\Lambda_{dd'}}{E-E_d-\Gamma_{dd}-\Lambda_{dd}}\ . \tag{61}$$

It is then necessary to remove the residual structure dependence in the first term in Eq. (60) by carefully separating all matrix elements into volume and structure components. We proceed exactly as in paper II and write $\delta V=\delta V_{\rm vol}+\delta V_{\rm struc}$, so that

$$E_d=E_d^{\rm vol}+E_d^{\rm struc}\ , \tag{62a}$$

$$\Delta_{\mathbf{k}d}=\Delta_{\mathbf{k}d}^{\rm vol}+\Delta_{\mathbf{k}d}^{\rm struc}\ , \tag{62b}$$

and similarly for all remaining $d$-state quantities. In each case the volume component is dominant and the much smaller structural component can be formally considered to be 1 order smaller in magnitude. Isolating the largest structure-independent one-ion contributions, we are thus motivated to define

$$\mathcal{N}_d(E)\equiv-\frac{2}{\pi}\mathrm{Im}\sum_d\ln(E-E_d^{\rm vol}-\Gamma_{dd}^{\rm vol})\ , \tag{63}$$

and hence

$$\delta\mathcal{N}_d(E)\equiv-\frac{2}{\pi}\mathrm{Im}\left[\sum_d \ln\left[1-\frac{E_d^{\mathrm{struc}}+\Gamma_{dd}^{\mathrm{struc}}+\Lambda_{dd}}{E-E_d^{\mathrm{vol}}-\Gamma_{dd}^{\mathrm{vol}}}\right]+\ln[\det(t_{dd'})]\right] . \quad (64)$$

Here, the volume component of the $d$-state self-energy, $\Gamma_{dd}^{\mathrm{vol}}$, is given by Eq. (50) with $E_d$ and $\Delta_{kd}$ replaced by $E_d^{\mathrm{vol}}$ and $\Delta_{kd}^{\mathrm{vol}}$, respectively. The real and imaginary parts of $\Gamma_{dd}^{\mathrm{vol}}(E)$ are displayed in Fig. 2(a) for the case of Cu and are similar in form for all of the transition metals. The volume term $\mathcal{N}_d(E)$ may then be readily interpreted as

$$\mathcal{N}_d(E)=N\frac{10}{\pi}\delta_2(E) , \quad (65)$$

where $\delta_2$ is the $l=2$ phase shift associated with a single site. For very narrow $d$ bands, $\delta_2(E)$ will have a sharp resonancelike behavior in the vicinity of $E=E_d^{\mathrm{vol}}$, as shown in Fig. 2(b) for Cu. More generally, the magnitude of the imaginary part of $\Gamma_{dd}^{\mathrm{vol}}(E)$ near the Fermi energy is comparable to half of the width of the $d$ bands, so that $\mathcal{N}_d(E_F)$ alone is a measure of the total number of $d$ electrons present. The structural term $\delta\mathcal{N}_d(E)$ is consequently small and oscillatory in nature.

To fully isolate the purely volume contributions in $E_{\mathrm{band}}^{\mathrm{val}}$, we finally introduce a zero-order Fermi energy $\varepsilon_F$ such that $Z$, $Z_d$, and $\varepsilon_F$ are self-consistently related by the equations

$$Z+Z_d=Z_a-Z_c , \quad (66)$$

$$\mathcal{N}_0(\varepsilon_F)=NZ , \quad (67)$$

and

$$\mathcal{N}_d(\varepsilon_F)=NZ_d . \quad (68)$$

In Eq. (66), $Z_c$ represents the number of inner-core electrons per atom, which is fixed, so that $Z+Z_d$ is a constant for a particular element. Equation (67) is the familiar free-electron relationship between $\varepsilon_F$ and the valence $Z$ and is consistent with Eq. (17). The final condition (68) is just the phase-shift relationship $Z_d=(10/\pi)\delta_2(\varepsilon_F)$. This condition is invoked by our zero-order pseudoatom construction, as discussed in Sec. III D, and is consistent with Eq. (52). Straightforward manipulation of Eq. (55) then yields, *still without approximation,* the interesting and useful result

$$E_{\mathrm{band}}^{\mathrm{val}}=\tfrac{3}{5}NZ\varepsilon_F+NE_{\mathrm{vol}}^d-\int_0^{\varepsilon_F}\delta\mathcal{N}_{sp}(E)dE-\int_0^{\varepsilon_F}\delta\mathcal{N}_d(E)dE-NZ_dE_d^{\mathrm{struc}}+\delta E_{\mathrm{band}} , \quad (69)$$

where we have now separated out the principal volume component of the $d$-state energy,

$$E_{\mathrm{vol}}^d\equiv Z_d(\varepsilon_F-E_d^{\mathrm{vol}})-\frac{10}{\pi}\int_0^{\varepsilon_F}\delta_2(E)dE , \quad (70)$$

and a Fermi-energy correction term

$$\delta E_{\mathrm{band}}\equiv N(Z+Z_d)(E_F-\varepsilon_F)-\int_{\varepsilon_F}^{E_F}\mathcal{N}(E)dE . \quad (71)$$

The increased cohesion in transition metals over simple metals is already largely contained in $E_{\mathrm{vol}}^d$, as we shall quantitatively demonstrate in Sec. III D below. The smaller components of $E_{\mathrm{band}}^{\mathrm{val}}$ which will contribute to our interatomic potentials are mostly derived from the integrals over $\delta\mathcal{N}_{sp}$ and $\delta\mathcal{N}_d$ for the $s$ and $p$ electrons and for the $d$ electrons, respectively. The former contribution is essentially the same as one obtains for simple metals. The latter contribution, in the full general form of Eq. (64), however, is new and the most vital feature in the

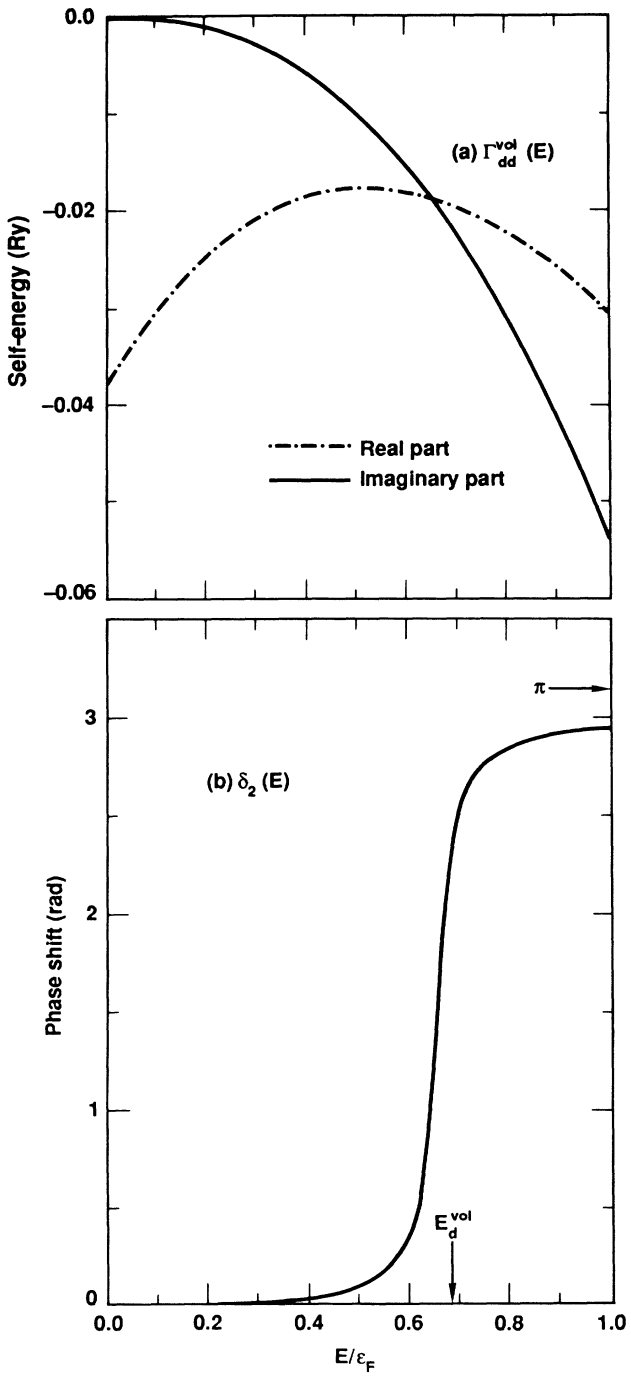


FIG. 2. (a) Complex $d$-state self-energy functional $\Gamma_{dd}^{\mathrm{vol}}(E)$ for Cu. (b) Corresponding $l=2$ phase shift $\delta_2(E)$ from Eqs. (63) and (65).

present development. We shall devote considerable special attention to this contribution in Sec. IV. The correction term $\delta E_{\text{band}}$ turns out to be of order $(E_F-\varepsilon_F)^2$ and is small so long as $\varepsilon_F$ is indeed a good approximation to $E_F$, which will be the case in practice. This contribution is considered in Appendix C.

### C. Valence-electron density $n_{\text{val}}$

The localized electron density $\sum_i n_i$ in Eq. (7) contains both an inner-core contribution,

$$\sum_i n_c(\mathbf{r}-\mathbf{R}_i)\equiv 2\sum_c \langle \mathbf{r}\mid \phi_c\rangle\langle\phi_c\mid \mathbf{r}\rangle = 2\langle \mathbf{r}\mid P_c\mid \mathbf{r}\rangle \ , \tag{72}$$

and a $d$-state contribution,

$$\sum_i n_d(\mathbf{r}-\mathbf{R}_i)\equiv \frac{Z_d}{5}\sum_d \langle \mathbf{r}\mid \phi_d\rangle\langle\phi_d\mid \mathbf{r}\rangle \ . \tag{73}$$

An exact expression for the remaining valence density can be obtained from Eq. (97) of Ref. 2, subtracting out the $d$-state contribution directly:

$$\begin{aligned} n_{\text{val}}(\mathbf{r}) = -\frac{2}{\pi}\operatorname{Im}\int_0^{E_F}\Bigg[\sum_{\mathbf{k},\mathbf{k}'}\big(\langle \mathbf{r}\mid \mathbf{k}\rangle\langle \mathbf{k}'\mid \mathbf{r}\rangle + \langle \mathbf{r}\mid P_c\mid \mathbf{k}\rangle\langle \mathbf{k}'\mid P_c\mid \mathbf{r}\rangle \\ - \langle \mathbf{r}\mid P_c\mid \mathbf{k}\rangle\langle \mathbf{k}'\mid \mathbf{r}\rangle - \langle \mathbf{r}\mid \mathbf{k}\rangle\langle \mathbf{k}'\mid P_c\mid \mathbf{r}\rangle\big)G_{\mathbf{k}\mathbf{k}'} \\ + \sum_{d,\mathbf{k}}\langle \mathbf{r}\mid \phi_d\rangle G_{d\mathbf{k}}\langle \mathbf{k}\mid (1-P_c)\mid \mathbf{r}\rangle\Bigg]dE - \sum_i n_d(\mathbf{r}-\mathbf{R}_i) \ . \end{aligned} \tag{74}$$

Equation (74), in turn, can be developed into an appropriate form for application here by using Eqs. (39) and (41) of Ref. 2 for $G_{\mathbf{k}\mathbf{k}'}$ and $G_{d\mathbf{k}}$, respectively, separating volume and structure contributions as above, and manipulating the term involving $n_d$ through Eqs. (50), (63), (68), and (73). Further defining the complex $d$-state or resonance energy

$$E_r(E)\equiv E_d^{\text{vol}}+\Gamma_{dd}^{\text{vol}}(E) \ , \tag{75}$$

one finds

$$\begin{aligned} n_{\text{val}}(\mathbf{r}) = -\frac{2}{\pi}\operatorname{Im}\int_0^{\varepsilon_F}\Bigg[\sum_{\mathbf{k}}\frac{\langle \mathbf{r}\mid \mathbf{k}\rangle\langle \mathbf{k}\mid \mathbf{r}\rangle}{E-\varepsilon_{\mathbf{k}}} + \sum_{\mathbf{k},\mathbf{k}'}\frac{\langle \mathbf{r}\mid \mathbf{k}\rangle W_{\mathbf{k}\mathbf{k}'}\langle \mathbf{k}'\mid \mathbf{r}\rangle}{(E-\varepsilon_{\mathbf{k}})(E-\varepsilon_{\mathbf{k}'})} \\ + \sum_{\mathbf{k}}\left[\frac{\langle \mathbf{r}\mid P_c\mid \mathbf{k}\rangle\langle \mathbf{k}\mid P_c\mid \mathbf{r}\rangle - \langle \mathbf{r}\mid P_c\mid \mathbf{k}\rangle\langle \mathbf{k}\mid \mathbf{r}\rangle - \langle \mathbf{r}\mid \mathbf{k}\rangle\langle \mathbf{k}\mid P_c\mid \mathbf{r}\rangle}{E-\varepsilon_{\mathbf{k}}}\right] \\ + \sum_d\frac{1}{E-E_r}\Bigg[\sum_{\mathbf{k},\mathbf{k}'}\frac{\langle \mathbf{r}\mid \mathbf{k}\rangle v'_{\mathbf{k}d}v'_{d\mathbf{k}'}\langle \mathbf{k}'\mid \mathbf{r}\rangle}{(E-\varepsilon_{\mathbf{k}})(E-\varepsilon_{\mathbf{k}'})} - \sum_{\mathbf{k}}\frac{\langle \mathbf{r}\mid \phi_d\rangle v'_{d\mathbf{k}}v'_{\mathbf{k}d}\langle \phi_d\mid \mathbf{r}\rangle}{(E-\varepsilon_{\mathbf{k}})^2} \\ + \sum_{\mathbf{k}}\frac{\langle \mathbf{r}\mid \phi_d\rangle v'_{d\mathbf{k}}(\langle \mathbf{k}\mid \mathbf{r}\rangle - S_{\mathbf{k}d}\langle \phi_d\mid \mathbf{r}\rangle)+\text{c.c.}}{E-\varepsilon_{\mathbf{k}}}\Bigg]\Bigg]dE + \delta n_{\text{band}}(\mathbf{r}) + \cdots \ . \end{aligned} \tag{76}$$

Here, $v'$ represents the volume component of $V'$, so that $v'_{\mathbf{k}d}$ is given by Eq. (45) with $E_d$ and $\Delta_{\mathbf{k}d}$ replaced by $E_d^{\text{vol}}$ and $\Delta_{\mathbf{k}d}^{\text{vol}}$, respectively. The quantity $\delta n_{\text{band}}$ in Eq. (76) is a Fermi-energy correction term analogous to $\delta E_{\text{band}}$ for the valence band-structure energy. The evaluation of $\delta n_{\text{band}}$ is discussed in Appendix C. Equation (76) is the beginning of a multi-ion series of the form

$$n_{\text{val}}(\mathbf{r}) = n_{\text{unif}} + \sum_i \delta n_{\text{val}}^i(\mathbf{r}-\mathbf{R}_i) + \cdots \ , \tag{77}$$

where $n_{\text{unif}}$ is the uniform density arising from the first term,

$$n_{\text{unif}}\equiv Z/\Omega = -\frac{2}{\pi}\operatorname{Im}\int_0^{\varepsilon_F}\sum_{\mathbf{k}}\frac{\langle \mathbf{r}\mid \mathbf{k}\rangle\langle \mathbf{k}\mid \mathbf{r}\rangle}{E-\varepsilon_{\mathbf{k}}}dE \ , \tag{78}$$

and $\delta n_{\text{val}}^i$ is the additional one-ion oscillatory density associated with the remaining terms. The latter will be broken down into separate self-consistent-screening and orthogonalization-hole contributions in Sec. V when the full theory of our interatomic potentials is assembled. Multi-ion contributions to $n_{\text{val}}$ can be obtained from the higher-order components of $G_{\mathbf{k}\mathbf{k}'}$ and $G_{d\mathbf{k}}$ in Eq. (74), but these are here neglected as small. In principle, these neglected terms contribute to $v_3$, $v_4$, and higher potentials, but in practice both the electron density and the total energy already appear to be well described without them, especially if the choice of $d$-basis state $\mid \phi_d\rangle$ is optimized.

### D. Zero-order pseudoatoms

Our desired expansions of $E_{\text{band}}^{\text{val}}$ and $n_{\text{val}}$ can only succeed to the extent that the zero-order system from which they are made is already a good representation of a real transition metal. We accomplish this goal through a zero-order pseudoatom construction, which (i) defines appropriate inner-core states $\mid \phi_c\rangle$ and $d$ states $\mid \phi_d\rangle$ and permits the evaluation of all matrix elements entering the theory, (ii) ensures that the self-consistency requirements

(66)–(68) are exactly satisfied and hence provides values of $Z$, $Z_d$, and $\varepsilon_F$, and (iii) leads a good first estimate of both the electron density and cohesive energy of the metal. The zero-order pseudoatom is effectively defined by Eq. (36) with the atomic reference potential $v_{at}$ taken in the form

$$v_{at}(r)=v_{pa}(r)+v_{loc}(r)-V_0' \ , \tag{79}$$

with $V_0' \equiv V_0-\mu_{xc}(n_{unif})$. Here, as in papers I and II,[4,5] the pseudoatom potential $v_{pa}$ represents the neutral one-ion self-consistent field

$$v_{pa}(r)=v_{unif}(r)+v_{ion}(r) \ , \tag{80}$$

where $v_{unif}$ is the Coulomb potential arising from the portion of $n_{unif}$ inside an atomic Wigner-Seitz sphere of radius $R_{WS}$ and $v_{ion}$ is the remaining ionic potential, as given by Eqs. (15) and (16) of paper II. The latter contains appropriate one-ion Coulomb and exchange-correlation contributions from $n_c$ and $n_d$. The constant exchange-correlation potential $\mu_{xc}(n_{unif})$ has here been absorbed into $V_0'$ rather than $v_{pa}$, making $V_0'$ a very small constant in practice (see Appendix B). The additional localization potential $v_{loc}$ in $v_{at}$ is also taken as previously and is given by Eq. (62) of paper II. This quantity is a repulsive barrier potential which operates only for $r>R_{WS}$ and serves to localize $\phi_d(\mathbf{r})$ to any desired degree while smoothly shaping its tail in a convenient Gaussian-like form. The strength of $v_{loc}$ is effectively characterized by a logarithmic derivative at $r=R_{WS}$, which we here precisely define[32] as

$$D_2^* \equiv R_{WS}\frac{d}{dr}[\ln \mathcal{R}_2(R_{WS},E_d^{vol})] \ . \tag{81}$$

The quantity $\mathcal{R}_2(r,E)$ is the solution of the radial Schrödinger equation associated with Eq. (36) for $r<R_{WS}$ and energy $E$, and, in the notation of paper II,

$$\begin{aligned} E_d^{vol} &= E_d^{pa}-\langle \phi_d \mid \delta V_{unif} \mid \phi_d \rangle - V_0' \\ &= E_d^0-\langle \phi_d \mid v_{loc}+\delta V_{unif} \mid \phi_d \rangle \ , \end{aligned} \tag{82}$$

where $-\delta V_{unif}$ is the additional Coulomb potential arising from the uniform density outside the atomic sphere, as given by Eqs. (7) and (13) of paper II. The definition (81) allows one to make a useful correspondence with fundamental ideas of band theory. In particular, if $E_d^{vol}$ marks the center of the $d$ bands, then one should expect the Andersen canonical boundary condition, $D_2^*=-3$ $[=-(l+1)$ for $l=2]$, to be appropriate.[33,34] This expectation is realized in practice and such a choice leads to a generally good zero-order description of the $d$ bands, as we demonstrate below. Competing optimization criteria can be elaborated on, however, as discussed in paper II, and the most important of these concerns the quality of the zero-order electron density. Experience to date suggests that for the central transition metals a slightly more bonding $d$ state, corresponding to values of $D_2^*$ closer to $-2$, is optimum, although as yet we do not have a universal scheme for obtaining definitive values in this regard. In the present work, we utilize the nominal choice $D_2^*=-3$, except where noted.

The zero-order pseudoatom immediately provides the ingredients needed to obtain both the $sp$-$d$ hybridization and $d$-state overlap matrix elements relevant to the $d$ bands, particularly $\Delta_{kd}^{vol}$ and $\Delta_{dd'}^{vol}$. The former matrix element is evaluated here exactly as in paper II, while the latter is refined slightly from Eq. (53) of paper II to the form

$$\Delta_{dd'}^{vol}(R_{ij})=\int \phi_d^*(\mathbf{r}-\mathbf{R}_i)[v_{loc}(\mid \mathbf{r}-\mathbf{R}_j \mid)-v_{pa}(\mid \mathbf{r}-\mathbf{R}_i \mid)-\delta v_{xc}(\mathbf{r}-\mathbf{R}_i,\mathbf{r}-\mathbf{R}_j)]\phi_{d'}(\mathbf{r}-\mathbf{R}_j)d\mathbf{r} \ , \tag{83}$$

where $\delta v_{xc}(\mathbf{r}-\mathbf{R}_i,\mathbf{r}-\mathbf{R}_j)$ is the lowest-order approximation to $\delta\mu_{xc}^*(n_i,n_j)$ as given by Eq. (11) with $n_{val}$ replaced by $n_{unif}$. A figure of merit for the matrix element $\Delta_{dd'}^{vol}$ is the predicted value of the unhybridized $d$-band width $W_d$ in the tight-binding approximation. For the fcc structure $W_d$ is the $X_5$-$X_3$ energy difference, and retaining only nearest-neighbor matrix elements one has from Eqs. (B7) and (B9) of paper II the result

$$W_d=-6(dd\sigma)+4(dd\pi)+2(dd\delta) \ , \tag{84}$$

where $dd\sigma$, $dd\pi$, and $dd\delta$ are the $m=0$, 1, and 2 components of $-\Delta_{dd'}^{vol}$ evaluated at $R_{ij}=1.809R_{WS}$, the fcc nearest-neighbor distance. Equation (84) is in close agreement with the $d$-band width estimated directly from Wigner-Seitz boundary conditions applied to $v_{pa}$. That is,

$$W_d^*=E_t-E_b \ , \tag{85}$$

with the top $E_t$ and bottom $E_b$ of the $d$ band determined from the usual antibonding and bonding conditions:

$$\frac{d}{dr}[\ln \mathcal{R}_2(R_{WS},E_t)]=-\infty \tag{86a}$$

and

$$\frac{d}{dr}[\ln \mathcal{R}_2(R_{WS},E_b)]=0 \ . \tag{86b}$$

For all 20 $3d$ and $4d$ transition metals, we find that Eqs. (84) and (85) agree to better than 1% with the choice $D_2^*=-3$ in defining the pseudoatom. Furthermore, the $d$-band width $W_d^*$ yielded by the pseudoatom potential $v_{pa}$ is also in good agreement with that determined from a full self-consistent band-structure potential. To show this explicitly, we have performed parallel linear-muffin-tin-orbital (LMTO) band-structure calculations,[35] which provide appropriate values for comparison. Figure 3 compares our GPT zero-order pseudoatom and our LMTO values of $W_d^*$ for the $3d$ and $4d$ metals. For pseudoatoms with $D_2^*=-3$, the GPT and LMTO results agree to within 20%, but except for Cu and Ag there is a small systematic overestimate of $W_d^*$ by the GPT, which

is greatest for central elements. Physically, this overestimate corresponds to the $d$ bands lying slightly too high in energy. Increasing $D_2^*$ to $-2$ for the central elements lowers both $E_d^{\text{vol}}$ and $W_d^*$ and moves the GPT and LMTO results into close agreement, as also shown in Fig. 3.

Of equal interest regarding the zero-order pseudoatom are the predicted values of the self-consistent valence $Z$. Figure 4 displays our calculated GPT values of $Z$ for the $3d$ and $4d$ transition metals, as obtained from zero-order pseudoatoms with $D_2^* = -3$ and, for the central elements, with $D_2^* = -2$ as well. For comparison, we have also shown in Fig. 4 for each element the number of non-$d$ valence electrons contained within one atomic sphere obtained from our parallel LMTO band-structure calculations.[35,36] In the case of the $3d$ metals, with the narrower $d$ bands and more localized $d$-electron density, there is always a rather good correspondence between the GPT and LMTO results, with an approximately constant value of $Z$ near 1.5 predicted in both cases and little sensitivity of the GPT results to $D_2^*$. For the $4d$ metals, on the other hand, with broader $d$ bands and more diffuse $d$-electron density, the correspondence is more subtle. The LMTO values have magnitudes similar to the $3d$ series and again show little variation with atomic number, except for a dip at Pd. In contrast, the GPT values with $D_2^* = -3$ display an extended dip over six elements from Nb to Pd. However, with $D_2^* = -2$ the GPT values for the central $4d$ metals are raised considerably and then agree with the LMTO values as well as do the corresponding results for the $3d$ series.

The volume dependence of $Z$ is also revealing. For example, all of the early and central transition metals are expected to undergo an $s \rightarrow d$ transfer of electrons under compression as the nearly-free-electron $sp$ bands are pushed up faster in energy than the $d$ bands. One should expect, therefore, that the zero-order pseudoatom value of $Z$ will decrease in such metals with decreasing volume, and we indeed find this to be so, as illustrated in Fig. 5 for Mo. Furthermore, in the case of Mo with $D_2^* = -2$, the correspondence with energy-band predictions is quantitative as well. That is, we find $Z \rightarrow 0$ and the end of the $s \rightarrow d$ transition at about the same volume that additional parallel LMTO calculations[35,36] predict the bottom the $sp$ bands to be moved above the Fermi level. The reverse situation, in which a $d \rightarrow s$ transfer of electrons takes

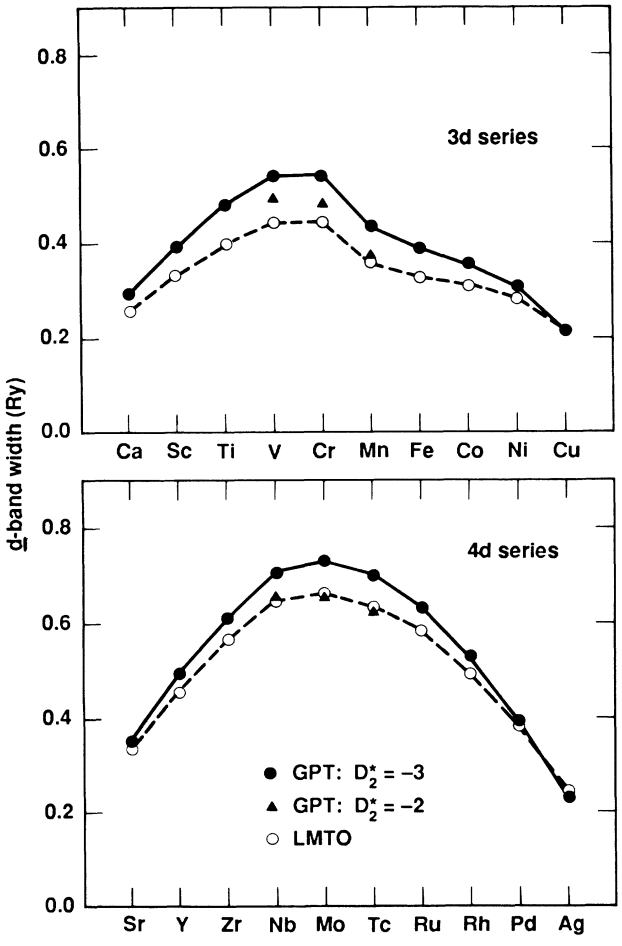


FIG. 3. Width of the $d$ bands for $3d$ and $4d$ transition metals, as obtained from Eqs. (85) and (86) using the zero-order pseudoatom potentials of the GPT and using parallel LMTO band-structure potentials (see Ref. 35).

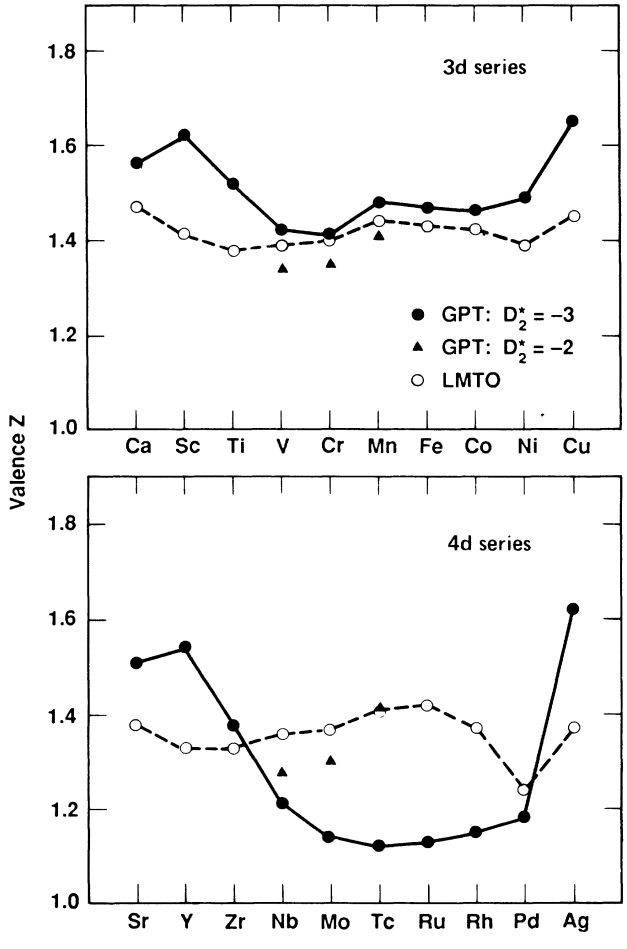


FIG. 4. Self-consistent valence $Z$ for the $3d$ and $4d$ transition metals, as obtained from the zero-order pseudoatoms of the GPT and as inferred from parallel LMTO energy-band calculations (see Refs. 35 and 36). In the latter case, $Z$ represents the number of non-$d$ valence electrons contained within the atomic sphere.

place, occurs at the end of each series in the noble metals, as also shown in Fig. 5 for Cu. Again, the predicted increase in $Z$ with decreasing volume from our zero-order pseudoatom approach is in accord with band-structure calculations.[37]

The entire evolution from the free atom through the promoted atom and the zero-order pseudoatom to the metal can be conceptually summarized as a simple three-step process. This is shown in Fig. 6 in terms of the one-electron energy levels of Cu, and is similar for all transition metals. In the first step, the appropriate transfer of $s$ and $d$ electrons is made to create the promoted atom. The $s$ and $d$ orbitals are largely unchanged at this stage, but the corresponding energy levels are shifted considerably. For a $d \rightarrow s$ transfer of electrons, as occurs in the case of Cu, the $s$ and $d$ levels fall in energy (even though $E_{\text{pro}} > 0$) because well-localized $d$ electrons are moved to less localized $s$ orbitals. In the second step of creating the zero-order pseudoatom, one permits the $s$-electron density to be spread out uniformly at a density $Z/\Omega$, while holding the $d$-electron density approximately constant. This transfers electrons from outside the atomic sphere to within, pushing the $d$ level higher in energy, and generally above its position in the free atom, and spreading out the $s$ level symmetrically into an occupied free-electron continuum of width $\varepsilon_F$. The total electron density as well as the position and occupation of the energy levels in the pseudoatom now simulate the conditions found in the actual metal. The final step is then to allow pseudoatoms centered on different sites to interact and thereby complete the remaining structural details of the energy bands.

Figure 6 strongly suggests that physical properties of the metal such as the cohesive energy, which are mostly

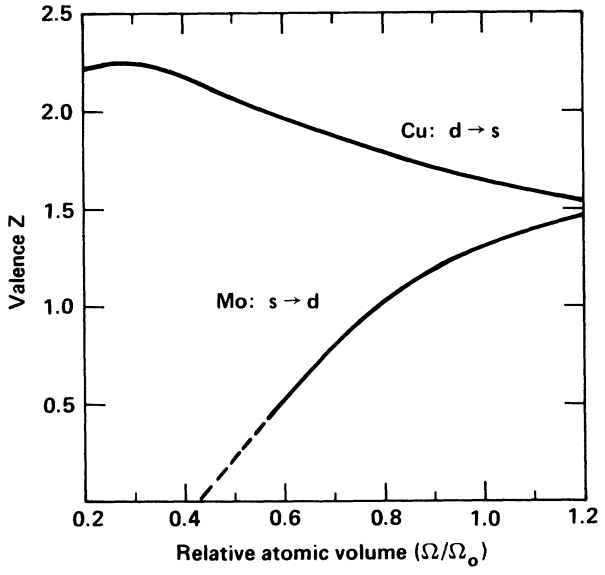


FIG. 5. Volume dependence of the self-consistent valence $Z$ for Cu and Mo, as obtained from the zero-order pseudoatoms of the GPT with $D_2^* = -3$ for Cu and $= -2$ for Mo. Here, $\Omega_0$ represents the observed equilibrium atomic volume. The dashed portion of the Mo curve is an extrapolation to $Z = 0$, where the $s \rightarrow d$ transition is completed.

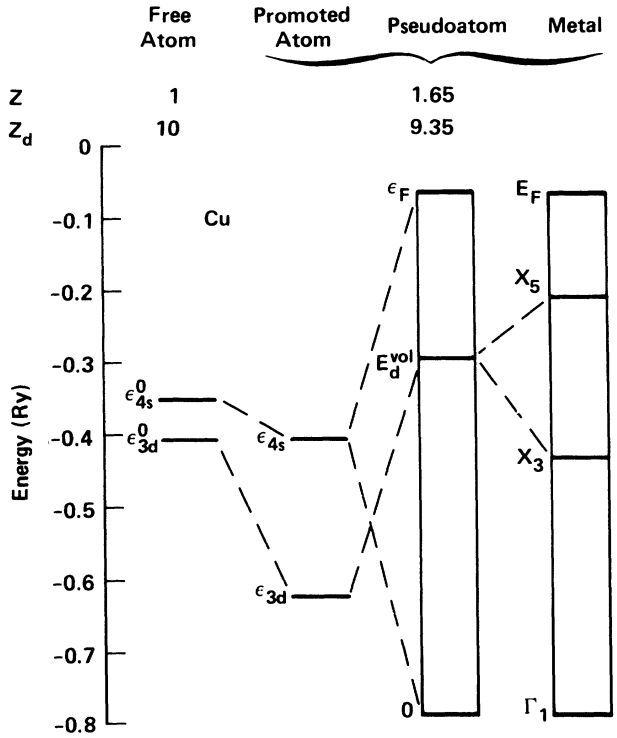


FIG. 6. Evolution of the valence energy levels from the free atom through the promoted atom and the zero-order pseudoatom to the metal in Cu. In the latter three cases, $Z = 1.65$ and $Z_d = 9.35$, corresponding to the observed equilibrium atomic volume.

dependent on volume rather than structure, should already be well approximated at the zero-order pseudoatom step. We can now demonstrate that this is indeed the case. The appropriate expression for the pseudoatom component of the cohesive energy, $E_{\text{coh}}^{\text{pa}}$, may be readily derived from Eqs. (28), (32), (59), and (69) with $n_{\text{val}} = n_{\text{unif}}$. We find

$$E_{\text{coh}}^{\text{pa}} \equiv E_{\text{fe}} + E_{\text{vol}}^{d} + \frac{2\Omega}{(2\pi)^3} \int_{k<k_F} \langle \mathbf{k} \mid w_{\text{pa}} \mid \mathbf{k} \rangle d\mathbf{k} - E_{\text{bind}}^{\text{atom}}(Z) + E_{\text{prep}} , \tag{87}$$

where $E_{\text{fe}}$ is the free-electron binding energy

$$E_{\text{fe}} \equiv \tfrac{3}{5} Z \varepsilon_F + Z \varepsilon_{\text{xc}}(n_{\text{unif}}) - \tfrac{3}{5}(Ze)^2 / R_{\text{WS}} + Z V_0' \tag{88}$$

and $w_{\text{pa}}$ is the one-ion component of the total pseudopotential $W$ with $V$ replaced by $v_{\text{pa}} - V_0'$. Calculations of $| E_{\text{coh}}^{\text{pa}} |$ for all of the $3d$ and $4d$ transition metals are presented in Fig. 7 and compared with parallel LMTO results based on our full self-consistent energy-band calculations.[35] For each element there is quantitative agreement to within 20%, and all trends, including the double-humped structure of each series, are reproduced by Eq. (87). Moreover, inspection of the last column of Table I shows that the latter structure is not simply an atomic trend but is, instead, a subtle feature involving *both* the

atom and the solid, which our zero-order calculation has correctly simulated. It is also interesting to note that the GPT results show little sensitivity to the choice of $D_2^*$, especially for the $4d$ metals.

## IV. MULTI-ION EXPANSION OF THE $d$-BAND STRUCTURAL ENERGY

### A. Formal results

We now focus in directly on the most important $d$-band structural contribution to the valence band-structure energy $E_{\rm band}^{\rm val}$; this arises from the fourth term in Eq. (69) involving $\delta\mathcal{N}_d$. Specifically, we consider the energy

$$NE_{\rm struc}^{d}\equiv\frac{2}{\pi}{\rm Im}\int_0^{\epsilon_F}\ln[\det(t_{dd'}^{\rm vol})]dE\ , \tag{89}$$

which results from the dominant contribution to $\delta\mathcal{N}_d$ in Eq. (64). Here $t_{dd'}^{\rm vol}$ is the appropriate volume component of $t_{dd'}$ and is given by the expression

$$t_{dd'}^{\rm vol}(R_{ij},E)=\frac{(E-E_d^{\rm vol})S_{dd'}(R_{ij})+\Delta_{dd'}^{\rm vol}(R_{ij})-\Gamma_{dd'}^{\rm vol}(R_{ij},E)}{E-E_d^{\rm vol}-\Gamma_{dd}^{\rm vol}(E)}\ . \tag{90}$$

Both $S_{dd'}(R_{ij})$ and $\Delta_{dd'}^{\rm vol}(R_{ij})$ are short-range functions of the separation distance $R_{ij}$ between sites $i$ and $j$, while $\Gamma_{dd'}^{\rm vol}(R_{ij},E)$ is a long-range hybridization interaction which depends on energy as well as distance. This latter quantity reduces to $\Gamma_{dd}^{\rm vol}(E)$ for $R_{ij}=0$, so that $t_{dd}^{\rm vol}(0,E)=1$. In addition, $|t_{dd'}^{\rm vol}|<1$ for all $R_{ij}$ of interest and $t_{dd'}^{\rm vol}\to 0$ as $R_{ij}\to\infty$.

Equation (89) may be formally developed into a multi-ion series as follows. First we note that the determinant in this equation involves a $5N\times 5N$ matrix made up of symmetric $5\times 5$ blocks. The diagonal blocks are simply unit matrices $I$ resulting from the orthogonality of $d$ states on a given site, while the off-diagonal blocks are $5\times 5$ matrices $T_{ij}$ linking sites $i$ and $j$ with components $t_{dd'}^{\rm vol}$. The determinant may be developed blockwise about its rows and columns and readily folds down into $5\times 5$ form:

$$L(E)\equiv\ln[\det(t_{dd'}^{\rm vol})]=\ln\left[\det\left[I-\tfrac{1}{2}{\sum_{i,j}}'\phi_{ij}+\tfrac{1}{6}{\sum_{i,j,k}}'\phi_{ijk}-\tfrac{1}{24}{\sum_{i,j,k,l}}'\phi_{ijkl}+\cdots\right]\right]\ , \tag{91}$$

where we have defined the matrix products

$$\phi_{ij}\equiv T_{ij}T_{ji}\ , \tag{92}$$

$$\phi_{ijk}\equiv T_{ij}T_{jk}T_{ki}+T_{ik}T_{kj}T_{ji}\ , \tag{93}$$

and

$$\phi_{ijkl}\equiv T_{ij}T_{jk}T_{kl}T_{li}+T_{il}T_{lk}T_{kj}T_{ji}+T_{ik}T_{kl}T_{lj}T_{ji}+T_{ij}T_{jl}T_{lk}T_{ki}+T_{il}T_{lj}T_{jk}T_{ki}+T_{ik}T_{kj}T_{jl}T_{li}-\phi_{ij}\phi_{kl}-\phi_{ik}\phi_{jl}-\phi_{il}\phi_{jk}\ . \tag{94}$$

We then consider the asymptotic limit of large $R_{ij}$, where the elements of $T_{ij}$ are arbitrarily small, and use the general expansion for any small, square matrix $A$:

$$\ln[\det(I+A)]={\rm Tr}(A-\tfrac{1}{2}AA+\tfrac{1}{3}AAA-\cdots)\ , \tag{95}$$

where Tr denotes the trace of the matrix which follows. Expanding the right-hand side of Eq. (91) via Eq. (95), collecting terms with a common structural dependence, and then resumming and analytically continuing the result to arbitrary $R_{ij}$ yields our desired multi-ion expansion of the $d$-band structural energy:

$$NE_{\rm struc}^{d}=\tfrac{1}{2}{\sum_{i,j}}'v_2^d(R_{ij})+\tfrac{1}{6}{\sum_{i,j,k}}'v_3^d(R_{ij},R_{jk},R_{ki})+\tfrac{1}{24}{\sum_{i,j,k,l}}'v_4^d(R_{ij},R_{jk},R_{kl},R_{li},R_{ki},R_{lj})+\cdots\ . \tag{96}$$

The two-ion potential $v_2^d$ in Eq. (96) is a one-dimensional function given by

$$v_2^d(i,j)\equiv v_2^d(R_{ij})=\frac{2}{\pi}{\rm Im}\int_0^{\epsilon_F}L_{ij}(E)dE\ , \tag{97}$$

with

$$L_{ij}(E)\equiv\ln[\det(I-\phi_{ij})]\ . \tag{98}$$

The three-ion potential $v_3^d$ is a three-dimensional function given by[38]

$$v_3^d(i,j,k)\equiv v_3^d(R_{ij},R_{jk},R_{ki})=\frac{2}{\pi}{\rm Im}\int_0^{\epsilon_F}\{L_{ijk}(E)-[L_{ij}(E)+L_{jk}(E)+L_{ki}(E)]\}dE\ , \tag{99}$$

with

$$L_{ijk}(E)\equiv\ln\{\det[I-(\phi_{ij}+\phi_{jk}+\phi_{ki})+\tilde{\phi}_{ijk}]\}\ , \tag{100}$$

where $\tilde{\phi}_{ijk}$ is the symmetrized matrix product

$$\tilde{\phi}_{ijk}\equiv\tfrac{1}{3}(\phi_{ijk}+\phi_{jki}+\phi_{kij})\ . \tag{101}$$

Finally, the four-ion potential $v_4^d$ is a six-dimensional function given by[38]

$$v_4^d(i,j,k,l)\equiv v_4^d(R_{ij},R_{jk},R_{kl},R_{li},R_{ki},R_{lj})$$
$$=\frac{2}{\pi}\mathrm{Im}\int_0^{\epsilon_F}\{L_{ijkl}(E)-[L_{ijk}(E)+L_{jkl}(E)+L_{kli}(E)+L_{lij}(E)]$$
$$+[L_{ij}(E)+L_{jk}(E)+L_{kl}(E)+L_{li}(E)+L_{ki}(E)+L_{lj}(E)]\}dE\ , \tag{102}$$

with

$$L_{ijkl}(E)\equiv\ln\{\det[I-(\phi_{ij}+\phi_{jk}+\phi_{kl}+\phi_{li}+\phi_{ki}+\phi_{lj})$$
$$+(\tilde{\phi}_{ijk}+\tilde{\phi}_{jkl}+\tilde{\phi}_{kli}+\tilde{\phi}_{lij})-\tilde{\phi}_{ijkl}]\}\ , \tag{103}$$

where

$$\tilde{\phi}_{ijkl}\equiv\tfrac{1}{4}(\phi_{ijkl}+\phi_{jkli}+\phi_{klij}+\phi_{lijk})\ . \tag{104}$$

Simplified forms of the formal results Eqs. (97)–(104) are frequently useful. One possible approximation is to note from Eq. (95) that

$$\det(I+A)=1+\mathrm{Tr}(A)+\cdots\ . \tag{105}$$

Using this result in the above expressions for $L_{ij}$, $L_{ijk}$, and $L_{ijkl}$ removes the determinants, replaces the matrix $I$ with unity, and replaces each remaining matrix product with its trace. This approximation is the origin of Eqs. (3) and (4) in Ref. 24 for $v_2^d$ and $v_3^d$, respectively, and has been used in all of our preliminary applications of the present theory.[24–26] The approximation itself is most satisfactory in practice for early and late transition metals where $A$ is effectively the smallest. Similar approximate results can be obtained by using Eq. (95) directly to generate asymptotic series. To fourth order in $T_{ij}$ one then finds

$$v_2^d(i,j)=-\frac{2}{\pi}\mathrm{Im}\int_0^{\epsilon_F}\mathrm{Tr}[\phi_{ij}+\tfrac{1}{2}(\phi_{ij})^2+\cdots]dE\ , \tag{106}$$

$$v_3^d(i,j,k)=-\frac{2}{\pi}\mathrm{Im}\int_0^{\epsilon_F}\mathrm{Tr}[-\phi_{ijk}$$
$$+(\phi_{ij}\phi_{jk}+\phi_{jk}\phi_{ki}+\phi_{ki}\phi_{ij})$$
$$+\cdots]dE\ , \tag{107}$$

and

$$v_4^d(i,j,k,l)=-\frac{2}{\pi}\mathrm{Im}\int_0^{\epsilon_F}\mathrm{Tr}[\phi_{ijkl}$$
$$+(\phi_{ij}\phi_{kl}+\phi_{ik}\phi_{jl}+\phi_{il}\phi_{jk})$$
$$+\cdots]dE\ . \tag{108}$$

These latter expressions can be used to gain considerable insight into the nature of our interatomic potentials, as we show in the next section. In writing Eqs. (107) and (108), we have noted that $\mathrm{Tr}(\tilde{\phi}_{ijk})=\mathrm{Tr}(\phi_{ijk})$ and $\mathrm{Tr}(\tilde{\phi}_{ijkl})=\mathrm{Tr}(\phi_{ijkl})$.

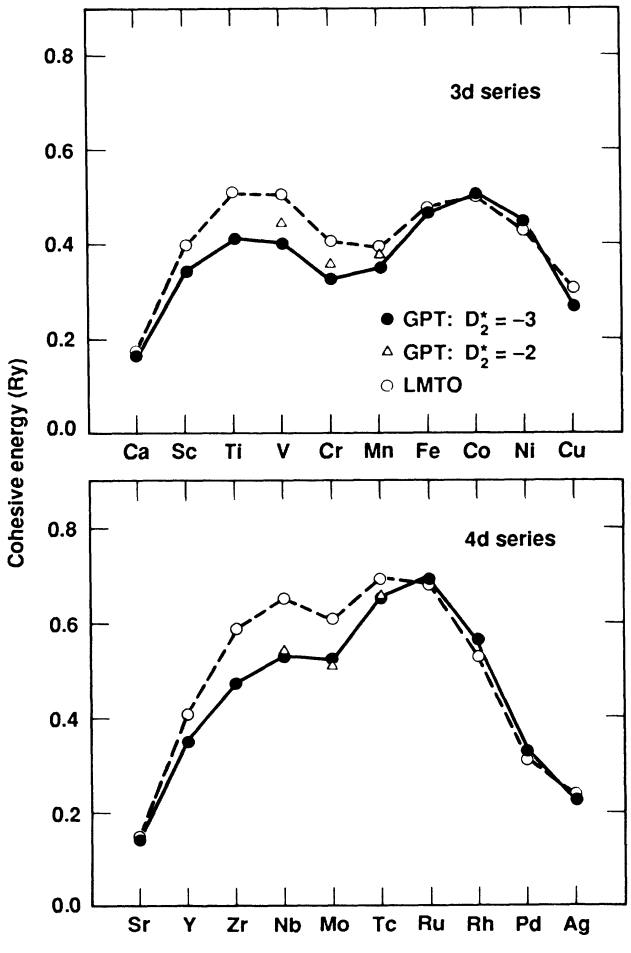


FIG. 7. Magnitude of the cohesive energy for the 3*d* and 4*d* transition metals, as obtained from the zero-order pseudoatoms of the GPT via Eq. (87) and as obtained from parallel LMTO energy-band calculations (see Ref. 35).

### B. Insight from a simple model

In this section we briefly consider the consequences of the above formal results in the context of a simple model for $t_{dd'}^{\mathrm{vol}}$. This will allow us to draw some immediate conclusions about the convergence of our multi-ion expansion Eq. (96), as well as to elucidate the behavior of the dominant potentials $v_2^d$ and $v_3^d$. Moreover, the model is sufficiently realistic that it well accounts for the results of full first-principles calculations on $v_2^d$ and $v_3^d$ in the absence of hybridization [$\Gamma_{dd'}^{\mathrm{vol}}(R_{ij},E)=0$], as we shall demonstrate, and is currently being used as a basis for developing a parametrized version of the transition-metal GPT.[39] It should be emphasized, however, that *the simplfying approximations introduced in this section apply only to this section*; the full theory will be restored in Sec. V.

Our model for $t_{dd'}^{\mathrm{vol}}$ is obtained by ignoring all of the

complicating features of Eq. (90), namely, the overlap term $S_{dd'}$, the hybridization term $\Gamma^{\rm vol}_{dd'}$, and the energy dependence of $\Gamma^{\rm vol}_{dd}$. Specifically, we let

$$t^{\rm vol}_{dd'}(R_{ij},E)\rightarrow\frac{\Delta^{\rm vol}_{dd'}(R_{ij})}{E-E^{\rm vol}_d+i\Gamma_0}\ , \tag{109}$$

where $\Gamma_0\equiv-i\Gamma^{\rm vol}_{dd}(\varepsilon_F)$ and the real part of $\Gamma^{\rm vol}_{dd}$ has been effectively absorbed into $E^{\rm vol}_d$. This form is sufficiently simple that the energy integrals in Eqs. (106)–(108) can now all be done analytically.[40] The quantity $\Gamma_0$ is a positive constant on the order of one-half of the $d$-band width, while the numerator of $t^{\rm vol}_{dd'}$ now involves only the energy-independent, tight-binding–type matrix elements $\Delta^{\rm vol}_{dd'}$ linking sites $i$ and $j$. The contributions of the latter to the $d$-band structural energy $E^d_{\rm struc}$ can be conveniently expressed in terms of moments. Specifically, one can define a dimensionless partial moment $M^{(s)}_n$ of order $n$ linking $s$ distinct sites for each of the terms in Eqs. (106)–(108), such that

$$M^{(2)}_2\equiv\frac{1}{2N}\sum_{i,j}{}'\,\alpha^2\,{\rm Tr}(\phi_{ij})$$

$$=\frac{1}{2N}\sum_{i,j}{}'\sum_{d,d'}\frac{\Delta^{\rm vol}_{dd'}(R_{ij})\Delta^{\rm vol}_{d'd}(R_{ij})}{\Gamma_0^2}\ , \tag{110a}$$

where $\alpha\equiv(E-E^{\rm vol}_d+i\Gamma_0)/\Gamma_0$ is a normalization factor which effectively replaces the denominator of $t^{\rm vol}_{dd'}$ with $\Gamma_0$ in Eq. (109).[31] Similarly,

$$M^{(2)}_4\equiv\frac{1}{2N}\sum_{i,j}{}'\,\alpha^4\,{\rm Tr}(\tfrac{1}{2}\phi_{ij}\phi_{ij})\ , \tag{110b}$$

$$M^{(3)}_3\equiv\frac{1}{6N}\sum_{i,j,k}{}'\,\alpha^3\,{\rm Tr}(\phi_{ijk})\ , \tag{110c}$$

$$M^{(3)}_4\equiv\frac{1}{6N}\sum_{i,j,k}{}'\,\alpha^4\,{\rm Tr}(\phi_{ij}\phi_{jk}+\phi_{jk}\phi_{ki}+\phi_{ki}\phi_{ij})\ , \tag{110d}$$

and

$$M^{(4)}_4\equiv\frac{1}{24N}\sum_{i,j,k,l}{}'\,\alpha^4\,{\rm Tr}(\phi_{ijkl}+\phi_{ij}\phi_{kl}+\phi_{ik}\phi_{jl}+\phi_{il}\phi_{jk})\ . \tag{110e}$$

Each moment has a simple graphical representation in which the matrix element $\Delta^{\rm vol}_{dd'}(R_{ij})$ is denoted by a solid line segment connecting sites $i$ and $j$. Thus, $M^{(s)}_n$ is a lattice sum of topologically similar graphs, each involving $n$ line segments linking $s$ sites. The graphs corresponding to the five moments defined in Eq. (110) are illustrated in Fig. 8.

In order to express $E^d_{\rm struc}$ in terms of the moments $M^{(s)}_n$, we further introduce the normalized energy

$$\tilde{\varepsilon}\equiv\frac{E-E^{\rm vol}_d}{\Gamma_0}=\alpha-i \tag{111}$$

and the energy-integral–related functions

$$F_n(\tilde{\varepsilon})\equiv-{\rm Im}[(\tilde{\varepsilon}+i)^{-n}]=-{\rm Im}(\alpha^{-n})\ . \tag{112}$$

Then, writing

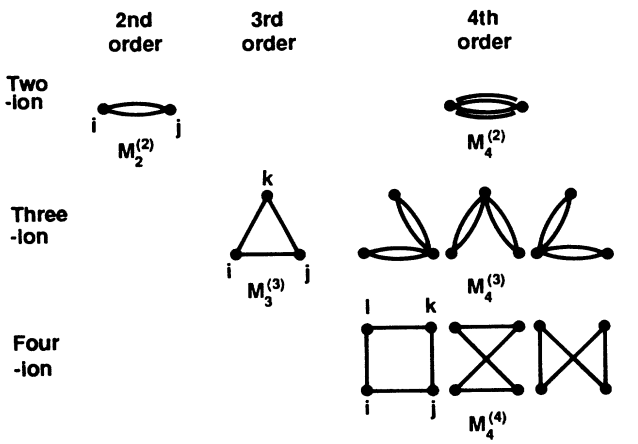


FIG. 8. Graphs associated with the partial moments $M^{(s)}_n$ defined in Eq. (110) and the corresponding interatomic potentials $v^d_n$ given by Eqs. (106)–(108). Each solid line represents a matrix element $\Delta^{\rm vol}_{dd'}$ (or, more generally, $t^{\rm vol}_{dd'}$) linking two sites.

$$E^d_{\rm struc}=E_2+E_3+E_4+\cdots\ , \tag{113}$$

where $E_2$, $E_3$, etc. are the two-ion, three-ion, etc. contributions to $E^d_{\rm struc}$, it is completely straightforward to show from Eqs. (96) and (106)–(108) that

$$E_2=\frac{2}{\pi}[-M^{(2)}_2F_1(\tilde{\varepsilon}_F)-\tfrac{1}{3}M^{(2)}_4F_3(\tilde{\varepsilon}_F)+\cdots]\Gamma_0\ , \tag{114a}$$

$$E_3=\frac{2}{\pi}[\tfrac{1}{2}M^{(3)}_3F_2(\tilde{\varepsilon}_F)-\tfrac{1}{3}M^{(3)}_4F_3(\tilde{\varepsilon}_F)+\cdots]\Gamma_0\ , \tag{114b}$$

and

$$E_4=\frac{2}{\pi}[-\tfrac{1}{3}M^{(4)}_4F_3(\tilde{\varepsilon}_F)+\cdots]\Gamma_0\ . \tag{114c}$$

The functions $F_n(\tilde{\varepsilon})$ are oscillatory in nature and the factors $F_n(\tilde{\varepsilon}_F)$ in Eq. (114) reflect the effects of $d$-band filling on the various energy components. The number of oscillations in $F_n(\tilde{\varepsilon})$ increases linearly with $n$, but the magnitude of each function is bounded through the condition $-1\le F_n\le 1$, as shown in Fig. 9 for $n=1$, 2, and 3. Consequently, the convergence of our multi-ion expansion for $E^d_{\rm struc}$ is govern entirely by the behavior of the moments $M^{(s)}_n$.

To proceed further, we need specific forms for the quantities $\Delta^{\rm vol}_{dd'}$ and $\Gamma_0$. In the spirit of our model, we treat here the special case of canonical $d$ bands, where simple analytic forms can be derived,[39,41–43] which are consistent with our first-principles results discussed above. Following the notation of Harrison,[43] both $\Delta^{\rm vol}_{dd'}$ and $\Gamma_0$ can be related to a single intra-atomic length parameter $r_d$. We find

$$\Delta^{\rm vol}_{dd'}(R_{ij})=\begin{Bmatrix}6\\-4\\1\end{Bmatrix}\times\frac{\hbar^2}{2m}\frac{15}{\pi}\frac{r_d^3}{R_{ij}^5}\quad\text{for } m=\begin{cases}0 & \text{(115a)}\\1 & \text{(115b)}\\2 & \text{(115c)}\end{cases}$$

where an overall minus sign with respect to conventional tight-binding matrix elements, as apparent from Eq. (46), has been taken into account, and

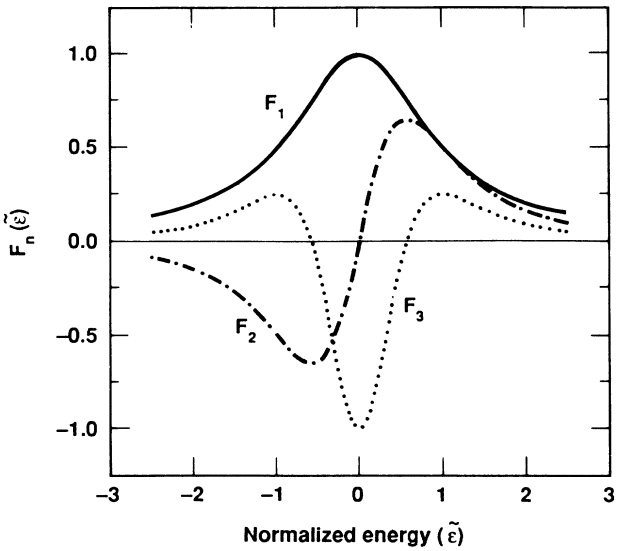


FIG. 9. Oscillatory functions $F_n(\tilde{\varepsilon})$ for $n=1$, 2, and 3 associated with $d$-band filling, as defined by Eq. (112).

$$\Gamma_0=\frac{\hbar^2}{2m}\frac{\varepsilon_F^{5/2}r_d^3}{3\pi}$$
$$=\frac{\hbar^2}{2m}\frac{15}{\pi}\frac{r_d^3}{C_Z R_{\rm WS}^5}\ , \tag{116}$$

with

$$C_Z=\frac{45}{(9\pi Z/4)^{5/3}}\ . \tag{117}$$

In obtaining the second line of Eq. (116), we have used $\varepsilon_F=(3\pi^2 Z/\Omega)^{2/3}$ from Eqs. (58) and (67). Note that both $\Delta_{dd'}^{\rm vol}$ and $\Gamma_0$ have the expected scaling property of canonical $d$ bands, namely, they vary inversely with the fifth power of distance. In addition, the ratio $\Delta_{dd'}^{\rm vol}/\Gamma_0$ which enters the moments $M_n^{(s)}$ is exactly independent of $r_d$ and depends only on the valence $Z$:

$$\frac{\Delta_{dd'}^{\rm vol}(R_{ij})}{\Gamma_0}=\begin{Bmatrix}6\\-4\\1\end{Bmatrix}\times C_Z\left[\frac{R_{\rm WS}}{R_{ij}}\right]^5 \quad \text{for } m=\begin{cases}0 & \text{(118a)}\\1 & \text{(118b)}\\2 & \text{(118c)}\end{cases}$$

As we have shown above, under normal circumstances $Z$ is rather constant for transition metals with values ranging from 1.1 to 1.7, in which case $C_Z\approx 1$ and the precise value of $Z$ is not an important issue in addressing the convergence question. Only in the extreme limit where $Z\to 0$ and the $d$ bands become decoupled from the free-electron continuum does $C_Z$ become large and our expansion obviously fail. We have here evaluated the moments $M_n^{(s)}$ using $Z=1.4$ in Eqs. (118) for the cases of (i) an fcc structure with nearest-neighbor only nonzero matrix elements and (ii) a bcc structure with nearest- and second-nearest-neighbor nonzero matrix elements. The values so obtained are listed in Table II. The dependence of the low-order moments on crystal structure is relatively weak, as expected. In both cases the largest moment is $M_2^{(2)}$ arising from two-ion pair interactions. The moments $M_3^{(3)}$ and $M_4^{(3)}$ arising from the three-ion triplet interactions are smaller but certainly not negligible, especially $M_4^{(3)}$, and can combine via Eq. (114b) to make $E_3$ comparable to $E_2$ in magnitude. In contrast, the leading four-ion moment $M_4^{(4)}$ suddenly drops below $M_4^{(3)}$ by 1–2 orders of magnitude in value, depending upon structure. This is a rather dramatic result of the well-known phenomenon of destructive interference for high- ($l\geq 2$) angular-momentum states. The increased multiplicity (i.e., the number of graphs summed) with increasing $n$ and $s$ is first balanced and then quickly overwhelmed by the alternating-sign cancellations of the $m=0$ and 1 couplings. This destructive interference applies even more strongly to the higher moments. For example, we find that the moment $M_6^{(4)}$, which arises from four-ion graphs analogous to those which contribute to the large three-ion value of $M_4^{(3)}$, is an order of magnitude smaller than $M_4^{(4)}$ in the fcc case and 2 orders of magnitude smaller in the bcc case. We conclude, therefore, that four-ion and higher interactions make only a small contribution to $E_{\rm struc}^d$, while three-ion triplet interactions can yield a contribution of comparable importance to that of two-ion pair interactions. Clearly, for the most subtle energetic questions, such as the bcc-fcc energy difference itself, even four-ion contributions cannot be neglected. For many other applications, however, it may well be sufficient to consider only $v_2^d$ and $v_3^d$.

TABLE II. Partial moments defined by Eq. (110), as evaluated for the fcc and bcc structures assuming canonical $d$ bands and $Z=1.4$.

| Moment | fcc | bcc |
|---|---|---|
| $M_2^{(2)}$ | 1.0867 | 1.1328 |
| $M_4^{(2)}$ | 0.0364 | 0.0445 |
| $M_3^{(3)}$ | 0.1146 | 0.1181 |
| $M_4^{(3)}$ | 0.4107 | 0.4304 |
| $M_4^{(4)}$ | −0.0066 | −0.0431 |

One can further use Eqs. (118) to extract explicit analytic forms for the potentials $v_2^d$ and $v_3^d$. If one neglects the small contribution associated with $M_4^{(2)}$, then it is easy to see from Eqs. (106), (110a), and (114a) that the two-ion pair potential is just

$$v_2^d(r)=-v_a\left[\frac{R_{\rm WS}}{r}\right]^{10}\ , \tag{119}$$

where $v_a$ is the *structure-independent* constant

$$v_a=\frac{140}{\pi}C_Z^2 F_1(\tilde{\varepsilon}_F)\Gamma_0\ . \tag{120}$$

The $r^{-10}$ distance dependence in $v_2^d$ comes directly from the two powers of $\Delta_{dd'}^{\rm vol}$ appearing in $M_2^{(2)}$. The constant $v_a$ is inherently positive since $F_1\geq 0$, as is clear from Fig. 9. Thus, $v_2^d$ is a purely attractive potential. Furthermore, $v_a$ and hence the strength of the potential is maximum

for half-filled $d$ bands, where $\varepsilon_F = E_d^{\rm vol}$, $\tilde{\varepsilon}_F = 0$, and $F_1 = 1$. Equation (119) is, in fact, representative of the behavior of full first-principles potentials calculated for real metals in the absence of hybridization, as shown in Fig. 10(a) for Cr.

The behavior of the three-ion triplet potential $v_3^d$ is necessarily more complicated, but nonetheless can be elaborated analytically in the context of our model. This potential is a three-dimensional function of distances $r_1$, $r_2$, and $r_3$ defining a triangle. Retaining the contributions to both $M_3^{(3)}$ and $M_4^{(3)}$, one can infer from Eq. (107) the general form

$$v_3^d(r_1,r_2,r_3) = v_b f(r_1)f(r_2)f(r_3)L(\theta_2,\theta_3) + v_c[f^2(r_1)f^2(r_2)P(\theta_3) + f^2(r_2)f^2(r_3)P(\theta_1) + f^2(r_3)f^2(r_1)P(\theta_2)] , \quad (121)$$

where $\theta_1$, $\theta_2$, and $\theta_3$ are the angles subtended by $r_1$, $r_2$, and $r_3$, respectively. For canonical $d$ bands, it follows from Eqs. (114b) and (118) that

$$f(r) = \left[\frac{R_{\rm WS}}{r}\right]^5 , \quad (122)$$

and that the *structure-independent* constants $v_b$ and $v_c$ are given by

$$v_b = \frac{180}{\pi} C_Z^3 F_2(\tilde{\varepsilon}_F)\Gamma_0 \quad (123)$$

and

$$v_c = -\frac{3620}{3\pi} C_Z^4 F_3(\tilde{\varepsilon}_F)\Gamma_0 . \quad (124)$$

The angular functions $L$ and $P$ in Eq. (121) depend only on $d$ symmetry and may be expressed entirely as polynomials involving sines and cosines.[39] The behavior of these functions, as well as $v_3$ itself, is most easily understood by considering the limit $r_2 = r_1 = d$ and $\theta_3 = \theta$, in which case $r_3 = 2d\sin(\theta/2)$ and $\theta_2 = \theta_1 = (\pi-\theta)/2$. The relevant functions $L(\theta_2,\theta)$ and $P(\theta)$ are displayed on Fig. 11. These functions are normalized to unity at $\theta = \pi$ and show local minima near $\theta = 2\pi/3$ (120°) and $\theta = \pi/2$ (90°), respectively. The full potential $v_3^d$ becomes a function of $d$ and $\theta$ only and is simplified to

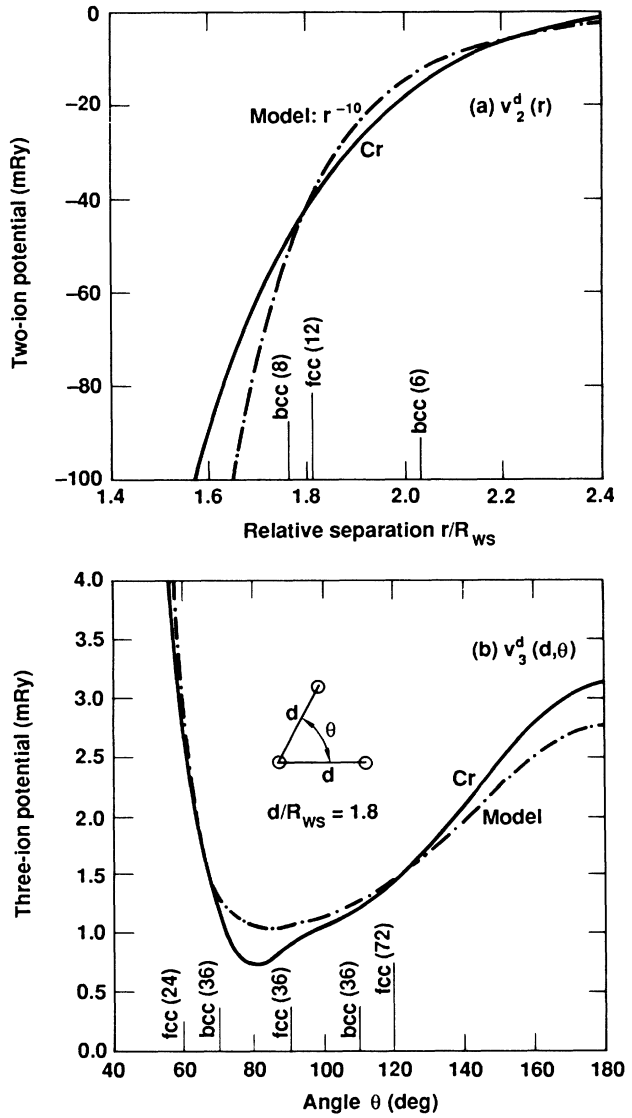


FIG. 10. Two-ion and three-ion interatomic potentials obtained from the analytic model discussed in the text for $Z = 1.4$ and $Z_d = 4.6$ and from first-principles calculations for Cr in the limit of no hybridization [$\Gamma_{dd'}^{\rm vol}(R_{ij},E) = 0$]. (a) $v_2^d(r)$, with the model result from Eq. (119). The location and number of fcc and bcc near neighbors are indicated. (b) $v_3^d(d,\theta)$, with the model result from Eq. (125). The location and number of three-ion triangles where $d$ approximates a nearest-neighbor distance in the fcc and bcc structures are indicated.

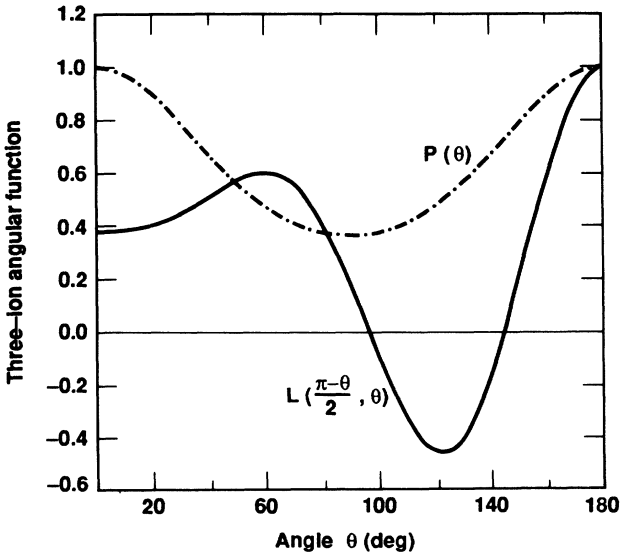


FIG. 11. Angular functions $L(\theta_2,\theta)$ and $P(\theta)$ associated with the model three-ion triplet potential $v_3^d(d,\theta)$ given by Eq. (125). Here, $\theta_2 = (\pi-\theta)/2$.

$$v_3^d(d,\theta)=v_b\left[\frac{R_{\rm WS}}{d}\right]^{15}\frac{L(\theta_2,\theta)}{32\sin^5(\theta/2)}+v_c\left[\frac{R_{\rm WS}}{d}\right]^{20}\left[P(\theta)+\frac{P(\theta_2)}{512\sin^{10}(\theta/2)}\right]. \tag{125}$$

Unlike the pair potential $v_2^d$, the triplet potential $v_3^d$ can be either attractive or repulsive depending on $d$-band filling. For half-filled $d$ bands, $v_b=0$ since $F_2=0$ and $v_c>0$ and maximum since $F_3=-1$, so that $v_3^d$ is purely repulsive. Figure 10(b) illustrates the contour $d=1.8R_{\rm WS}$ from Eq. (125) for conditions simulating Cr: $Z=1.4$ and $Z_d=4.6$. The potential exhibits a relatively deep minimum as a function of $\theta$ near 80°, in agreement with the corresponding first-principles potential for Cr calculated in the absence of hybridization, as also displayed in Fig. 10(b). For sufficiently small filling of the $d$ bands, on the other hand, $v_b<0$ and $v_c<0$, as is evident from Fig. 9, in which case $v_3^d$ is purely attractive. This condition is indeed realized in the early transition metals, as previously discussed for the case of Ba,[25] and as we will demonstrate for the $3d$ and $4d$ metals in Sec. V. In the opposite limit of large $d$-band filling, $v_b>0$ but $v_c<0$, in which case $v_3^d$ is again attractive if the magnitude of $v_c$ is greater than that of $v_b$. This is true for the late $3d$ and $4d$ metals, as we will further demonstrate in Sec. V.

It is also of interest to briefly compare and contrast our model with some of the central tight-binding ideas which have been suggested in recent work on transition-metal interatomic potentials.[20–23] The point of clearest connection is through the moments of the $d$-band density of states, which are linearly related to the moments we have defined in Eqs. (110). In the simplest tight-binding description,[44] the total $d$-band energy $E_{\rm tot}^d$ ($\equiv E_{\rm vol}^d+E_{\rm struc}^d$) is assumed to be proportional to the $d$-band width and hence to the square root of the second moment. In our notation this is a dependence of $\Gamma_0(M_2^{(2)})^{1/2}$ and for nearest-neighbor interactions implies that $E_{\rm tot}^d$ varies as the square root of the number of nearest neighbors. Further equating $E_{\rm tot}^d$ to a sum over pair potentials necessarily requires a *structure-dependent* potential which varies inversely with the square root of the number of nearest neighbors. A result of this form has been explicitly derived, for example, by Wills and Harrison,[21] and is also implicit in the work of Carlsson *et al.*[20] and MacDonald and Taylor.[22] For canonical $d$ bands, it also follows that such a pair potential must vary with interatomic distance as $r^{-5}$, as indeed found by Wills and Harrison. In contrast, our pair potential emerges from a linear relationship between $E_{\rm tot}^d$ and $M_2^{(2)}$, is independent of structure, and varies as $r^{-10}$. This behavior results directly from separating out a large volume term $E_{\rm vol}^d$ in the $d$-band energy and associating only the small residual structural energy $E_{\rm struct}^d$ with the pair potential. Ultimately, this separation is possible because of the fact that in bulk transition metals the $d$-band width is basically a volume-dependent quantity with only a weak structure dependence, as demonstrated by out zero-order pseudoatom results through Eq. (85). Likewise, the theory proposed by Dagens,[23] which does allow for a volume term in the $d$-band energy, yields a pair potential with an $r^{-10}$ dependence at short range for canonical $d$ bands. If the theory of Wills and Harrison is reformulated by expanding $E_{\rm tot}^d$ about some average structure at fixed volume, then it too yields an $r^{-10}$ dependence in the resulting pair potential, as Dagens has noted.[23]

In the tight-binding studies, only Carlsson *et al.*[20] have considered higher moments and the occurrence of nonpair interatomic potentials. However, tight-binding theory itself provides no fundamental analytic link between $E_{\rm tot}^d$ and the higher moments, so mostly what has been studied are correlations between the total energy and the third and fourth moments for various geometries and conditions of band filling, using simplifying assumptions about the density of states. In contrast, we have obtained here general linear relationships between $E_{\rm tot}^d$ and the higher moments through Eq. (114), and consequently, both well-defined and structure-independent three-ion and four-ion interatomic potentials.

## V. COMPLETION OF THE FULL THEORY

We now return to the full theory and complete the calculation of the valence-binding energy of the solid $E_{\rm bind}^{\rm solid}$, as given by Eqs. (28) and (69). Up until this point, only two classes of terms have been neglected in our development: (i) three-ion and higher exchange-correlation contributions in Eqs. (10) and (13), and (ii) two-ion and higher electron screening contributions to the valence-electron density in Eq. (76), which also make three-ion and higher contributions to $E_{\rm bind}^{\rm solid}$. If we similarly neglect all additional three-ion and higher components of the valence band-structure energy $E_{\rm band}^{\rm val}$ not already contained in Eq. (89) for $E_{\rm struc}^d$, then we can anticipate a result of the general form

$$E_{\rm bind}^{\rm solid}(Z)=E_{\rm vol}(\Omega)+\frac{1}{2N}\sum_{i,j}[v_2^d(i,j)+v_2^{\rm rest}(i,j)]+\frac{1}{6N}\sum_{i,j,k}v_3^d(i,j,k)+\frac{1}{24N}\sum_{i,j,k,l}v_4^d(i,j,k,l)+\cdots. \tag{126}$$

That is, $v_3=v_3^d$, $v_4=v_4^d$, etc. and the remaining contributions that need to be considered here are contained in either the pure volume term $E_{\rm vol}$ or the pure pair-potential term $v_2^{\rm rest}$. Moreover, at the pair-potential level of treatment essentially all total-energy contributions implicit in the local-density equations are thereby included in our formalism. Only the three-ion and higher potentials are then approximated and in each case by the dominant band-structure component of the potential through Eq. (89). The explicit derivation of $E_{\rm vol}$ and $v_2^{\rm rest}$ is similar to the corresponding development presented in paper II for empty and filled $d$-band metals and we outline the details

TABLE III. Summary of all expansion quantities entering the full transition-metal GPT, their relative order of smallness in terms of an arbitrary dimensionless scale parameter $\lambda$, and the maximum order in $\lambda$ to which they are treated in $E_{\rm vol}$, $v_2$, $v_3$, and $v_4$. Note that quantities treated to order $\lambda^2$ enter only $E_{\rm vol}$ and $v_2$.

| Quantity | Assigned order | Maximum order Treated |
|---|---|---|
| $w$, $w_{\rm pa}$, $p_c$ | $\lambda$ | $\lambda^2$ |
| $v'_{\mathbf{k}d}$, $\Delta^{\rm vol}_{\mathbf{k}d}$, $S_{\mathbf{k}d}$ [a] | $\lambda^{1/2}$ | $\lambda^2$ |
| $t^{\rm vol}_{dd'}$, $\Delta^{\rm vol}_{dd'}$, $S_{dd'}$, $\Gamma^{\rm vol}_{dd'}$ | $\lambda$ | all orders |
| $E^{\rm struc}_d$ [b] | $\lambda$ | $\lambda^2$ |
| $\Delta^{\rm struc}_{\mathbf{k}d}$ [b] | $\lambda^{3/2}$ | $\lambda^2$ |
| $W^{\rm struc}$, $\Gamma^{\rm struc}_{dd}$ [b] | $\lambda^2$ | $\lambda^2$ |
| $t^{\rm struc}_{dd'}$, $\Delta^{\rm struc}_{dd'}$, $\Gamma^{\rm struc}_{dd'}$ [c] | $\lambda^2$ | |

[a]These quantities also appear in $\Gamma^{\rm vol}_{dd'}$ and $t^{\rm vol}_{dd'}$, where they are treated to all orders.
[b]Decomposed and reabsorbed into the total energy in terms of other quantities, as discussed in Appendix D.
[c]These quantities only first appear in the theory at order $\lambda^3$ and hence are neglected in the present treatment.

in Appendix D. A summary of the small expansion quantities entering the full theory and the order to which they are thereby treated is given in Table III. We focus here on the new ingredients and the central results which emerge from them. We begin by completing the calculation of the one-ion oscillatory components of the valence-electron density contained in Eq. (76) which are required to obtain $v_2^{\rm rest}$.

### A. Oscillatory components of $n_{\rm val}$

The small one-ion components of the valence-electron density $n_{\rm val}$ can be separated into self-consistent-screening and orthogonalization-hole contributions exactly as for nontransition metals:

$$\delta n_{\rm val}(\mathbf{r}) \equiv \sum_i \delta n^i_{\rm val}(\mathbf{r}-\mathbf{R}_i) = \delta n_{\rm scr}(\mathbf{r}) + \delta n_{\rm oh}(\mathbf{r}) \ . \tag{127}$$

Neither $\delta n_{\rm scr}$ nor $\delta n_{\rm oh}$ involves any addition of electrons to the system, so that both of these densities oscillate about zero as a function of $\mathbf{r}$. The screening density is composed of all $\mathbf{k}\neq\mathbf{k}'$ terms in Eq. (76) and can be developed into the familiar reciprocal-space form

$$\delta n_{\rm scr}(\mathbf{r}) = \sum_{\mathbf{q}}{}' S(\mathbf{q}) n_{\rm scr}(q) e^{i\mathbf{q}\cdot\mathbf{r}} \ , \tag{128}$$

where the prime excludes the $\mathbf{q}=\mathbf{0}$ term from the sum, $S(\mathbf{q})$ is the usual structure factor, and using Eq. (59) of Ref. 2,

$$n_{\rm scr}(q) = \frac{4}{(2\pi)^3}\int_{k<k_F} \frac{\langle \mathbf{k}+\mathbf{q}\,|\,w\,|\,\mathbf{k}\rangle}{\varepsilon_{\mathbf{k}}-\varepsilon_{\mathbf{k}+\mathbf{q}}}d\mathbf{k} - \frac{4}{\pi\Omega}\,{\rm Im}\int_0^{\varepsilon_F}\sum_{d,\mathbf{k}} \frac{v'_{\mathbf{k}+\mathbf{q}d}v'_{d\mathbf{k}}}{(E-E_r)(E-\varepsilon_{\mathbf{k}})(\varepsilon_{\mathbf{k}}-\varepsilon_{\mathbf{k}+\mathbf{q}})}dE \ . \tag{129}$$

Here, $w$ is the one-ion component of the total pseudopotential $W$ and the sum over $d$ states is now a sum over states on one site only.[31] The first term in Eq. (129) represents the screening density arising from the $s$ and $p$ valence electrons, as in the case of simple metals, while the second term is the additional screening density produced by the $d$ electrons through hybridization. In the limit $E_r \to E_d^{\rm vol}$, the energy integral in the second term can be done analytically and, after some manipulation and making use of Eq. (B3) of Appendix B, one recovers Eq. (36) of paper II for an empty- or filled-$d$-band metal. For transition metals the contribution of this term is conceptually similar, but such energy integrals must always be done numerically. In either case, Eq. (129) represents an implicit equation for $n_{\rm scr}$ in terms of the full one-ion self-consistent potential $v$ which, in turn, depends on $n_{\rm scr}$. Using Eq. (38) of paper II for $v(q)$ in terms of $n_{\rm scr}(q)$, $v$ can be eliminated and $n_{\rm scr}$ determined self-consistently.

The orthogonalization-hole contribution in Eq. (127) consists of all remaining terms in Eq. (76) and can likewise be developed into the familiar real-space form

$$\delta n_{\rm oh}(\mathbf{r}) = \frac{Z^*-Z}{Z} n_{\rm unif} + \sum_i n_{\rm oh}(\mathbf{r}-\mathbf{R}_i) \ , \tag{130}$$

where $Z^*$ is an effective valence and $n_{\rm oh}(\mathbf{r}-\mathbf{R}_i)$ a localized depletion of electron density from within the interior of the site $i$ due to valence-core wave-function orthogonality. The latter has both an inner-core component, $n^c_{\rm oh}$, as in the case of simple metals, and a $d$-state component which is modified by hybridization:

$$n_{\rm oh}(\mathbf{r})=n^c_{\rm oh}(\mathbf{r})-\frac{2}{\pi}\,{\rm Im}\int_0^{\varepsilon_F}\sum_{d,\mathbf{k}}\left[-\frac{\langle\mathbf{r}\mid\phi_d\rangle v'_{d\mathbf{k}}v'_{\mathbf{k}d}\langle\phi_d\mid\mathbf{r}\rangle}{(E-E_r)(E-\varepsilon_{\mathbf{k}})^2}\right.$$
$$\left.+\frac{\langle\mathbf{r}\mid\phi_d\rangle v'_{d\mathbf{k}}(\langle\mathbf{k}\mid\mathbf{r}\rangle-S_{\mathbf{k}d}\langle\phi_d\mid\mathbf{r}\rangle)+\text{c.c.}}{(E-E_r)(E-\varepsilon_{\mathbf{k}})}\right]dE+\frac{\delta Z_{\rm band}}{Z_d}n_d(\mathbf{r})\ , \tag{131}$$

with

$$n^c_{\rm oh}(\mathbf{r})=-\frac{2\Omega}{(2\pi)^3}\int_{k<k_F}(\langle\mathbf{r}\mid p_c\mid\mathbf{k}\rangle\langle\mathbf{k}\mid\mathbf{r}\rangle+\langle\mathbf{r}\mid\mathbf{k}\rangle\langle\mathbf{k}\mid p_c\mid\mathbf{r}\rangle-\langle\mathbf{r}\mid p_c\mid\mathbf{k}\rangle\langle\mathbf{k}\mid p_c\mid\mathbf{r}\rangle)d\mathbf{k}\ . \tag{132}$$

Here, $p_c$ is the one-ion component of the total inner-core projection operator $P_c$. The effective valence is then

$$Z^*=Z-\int n_{\rm oh}(\mathbf{r})d\mathbf{r}=Z^*_c-\frac{2}{\pi}\,{\rm Im}\int_0^{\varepsilon_F}\sum_{d,\mathbf{k}}\frac{v'_{d\mathbf{k}}v'_{\mathbf{k}d}}{(E-E_r)(E-\varepsilon_{\mathbf{k}})^2}dE-\delta Z_{\rm band}\ , \tag{133}$$

with

$$Z^*_c\equiv Z-\int n^c_{\rm oh}(\mathbf{r})d\mathbf{r}$$
$$=Z+\frac{2\Omega}{(2\pi)^3}\int_{k<k_F}\langle\mathbf{k}\mid p_c\mid\mathbf{k}\rangle d\mathbf{k}\ . \tag{134}$$

The terms in Eqs. (131) and (133) involving the small quantity $\delta Z_{\rm band}$ arise from the Fermi-energy corrections contributions to Eq. (76), as discussed in Appendix C. In the limit $E_r\to E_d^{\rm vol}$, Eqs. (131) and (133) can be reduced to Eqs. (21) and (25), respectively, of paper II for an empty- or filled-$d$-band metal. While invariably $Z^*_c>Z$ corresponding to a net depletion of valence electrons from the inner-core region, either $Z^*>Z^*_c$ or $Z^*<Z^*_c$ is possible in transition metals. That is, the $d$-state component of $n_{\rm oh}$ can actually correspond to either a net depletion or accumulation of electrons in the outer-core region depending on $d$-band filling and other conditions. Typically, we find $Z^*>Z^*_c$ at the beginning and in the middle of the transition series and $Z^*<Z^*_c$ near the end of the series, such that in the noble metals $Z^*\approx Z$.

### B. Valence binding energy $E^{\rm solid}_{\rm bind}$

Using the above results for $\delta n_{\rm scr}$ and $\delta n_{\rm oh}$ together with Eqs. (28) and (69), the valence-binding-energy calculation can be completed. From the analysis in Appendix D, one finds

$$E^{\rm solid}_{\rm bind}(Z)=E_{\rm fe}+E^d_{\rm vol}+\frac{2\Omega}{(2\pi)^3}\int_{k<k_F}\langle\mathbf{k}\mid w_{pa}\mid\mathbf{k}\rangle(1+\langle\mathbf{k}\mid p_c\mid\mathbf{k}\rangle)d\mathbf{k}+E_{\rm oh}$$
$$-\frac{2}{\pi}\,{\rm Im}\int_0^{\varepsilon_F}\sum_{d,\mathbf{k}}\left[\frac{v'_{d\mathbf{k}}\langle\mathbf{k}\mid w_{\rm pa}\mid\mathbf{k}\rangle v'_{\mathbf{k}d}}{(E-E_r)(E-\varepsilon_{\mathbf{k}})^2}+\frac{v'_{d\mathbf{k}}\langle\mathbf{k}\mid p_c\mid\mathbf{k}\rangle v'_{\mathbf{k}d}}{(E-E_r)(E-\varepsilon_{\mathbf{k}})}\right]dE$$
$$-\tfrac{1}{2}\langle\mathbf{k}_F\mid w_{\rm pa}\mid\mathbf{k}_F\rangle\delta Z_{\rm band}+E^{\rm struc}_{\rm es}(Z^*)$$
$$+\sum_{\mathbf{q}}{}'\mid S(\mathbf{q})\mid^2F^0(q)+\frac{1}{2N}\sum_{i,j}{}'[v^d_2(i,j)+v^0_{\rm ol}(i,j)]+\frac{1}{6N}\sum_{i,j,k}{}'v^d_3(i,j,k)+\frac{1}{24N}\sum_{i,j,k,l}{}'v^d_4(i,j,k,l)+\cdots\ . \tag{135}$$

The initial eight terms of Eq. (135) all contribute to the pure volume component $E_{\rm vol}$. The first three of these are just the contributions we isolated in the zero-order pseudoatom cohesive energy, Eq. (87). The term $E_{\rm oh}$ is an orthogonalization-hole self-energy correction due to the finite size of $n_{\rm oh}$ and is given by Eq. (50) of paper II. The next four terms of Eq. (135) all contribute to the pair potential $v_2$. The first of these latter terms, $E^{\rm struc}_{\rm es}(Z^*)$, is the structural component of the electrostatic energy of point charges $Z^*e$ immersed in a uniform compensating background and is given by Eq. (44) of paper II. The second is a band-structure contribution involving an energy–wave-number characteristic $F^0(q)$ given by

$$F^0(q)=\frac{2\Omega}{(2\pi)^3}\int_{k<k_F}\frac{\mid\langle\mathbf{k}+\mathbf{q}\mid w\mid\mathbf{k}\rangle\mid^2}{\varepsilon_{\mathbf{k}}-\varepsilon_{\mathbf{k}+\mathbf{q}}}d\mathbf{k}-\frac{4}{\pi}\,{\rm Im}\int_0^{\varepsilon_F}\sum_{d,\mathbf{k}}\frac{v'_{d\mathbf{k}+\mathbf{q}}\langle\mathbf{k}+\mathbf{q}\mid w\mid\mathbf{k}\rangle v'_{\mathbf{k}d}}{(E-E_r)(E-\varepsilon_{\mathbf{k}})(\varepsilon_{\mathbf{k}}-\varepsilon_{\mathbf{k}+\mathbf{q}})}dE$$
$$-\frac{2\pi e^2\Omega}{q^2}\{G(q)[n_{\rm oh}(q)]^2+[1-G(q)][n_{\rm scr}(q)]^2\}\ . \tag{136}$$

Here, $G(q)$ is the exchange-correlation functional defined in paper I and $n_{oh}(q)$ is the Fourier transform of $n_{oh}(\mathbf{r})$. In the present work, we use the analytic expression for $G(q)$ developed by Ichimaru and Itsumi,[45] which is very similar to the form of Geldart and Taylor[46] adopted in papers I and II, but somewhat simpler to apply. The present $G(q)$, however, is still based on the Hedin-Lundqvist exchange-correlation energy.[28] The final term contributing to $v_2$ is a direct overlap potential $v_{ol}^0$, which in the shorthand notation of papers I and II and Appendix D can be expressed as

$$v_{ol}^0(i,j)=n_{core}^i\left[\left(\frac{Z_a-Z}{Z_a}\right)v_{nuc}^j+v_{core}^j+v_{xc}^j\right]+\left(\frac{Z_a+Z}{Z_a}\right)n_{nuc}^i\left[\left(\frac{Z_a-Z}{Z_a}\right)v_{nuc}^j+v_{core}^j\right]+\delta E_{xc}(i,j)+\delta E_{oh}(i,j)+\delta E_{ke}(i,j)\ , \tag{137}$$

where integrations over the volume of the solid are implied, as in Eq. (12). Here we identify $n_{core}^i$ with $n_i$ and $v_{core}^j$ with $v_j$, as in Eq. (28), while $n_{nuc}^i\equiv Z_a\delta(\mathbf{r}-\mathbf{R}_i)$ and $v_{nuc}^j\equiv Z_a e^2/|\mathbf{r}-\mathbf{R}_j|$. In addition, $v_{xc}^j$ and $\delta E_{xc}(i,j)$ are the lowest-order approximations to $\mu_{xc}^*(n_j)$ as given by Eq. (8) and $\delta\varepsilon_{xc}^*(n_i,n_j)$ as given by Eq. (15), respectively, with $n_{val}$ replaced by $n_{unif}$ in both cases. The term $\delta E_{oh}(i,j)$ is a small correction for the overlap of the orthogonalization-hole density on site $i$ with site $j$ and is given by

$$\delta E_{oh}(i,j)=2n_{oh}^i\left[\left(\frac{Z_a-Z}{Z_a}\right)v_{nuc}^j+v_{core}^j+v_{xc}^j\right]+n_{oh}^i\left[v_{oh}^j-\left(\frac{Z^*-Z}{Z_a}\right)v_{nuc}^j\right]+(n_{oh}^i+n_{oh}^j)\delta v_{xc}^{ij}\ , \tag{138}$$

where $n_{oh}^i\equiv n_{oh}(\mathbf{r}-\mathbf{R}_i)$, $v_{oh}^j$ is the Coulomb potential arising from $n_{oh}^j$, and $\delta v_{xc}^{ij}\equiv\delta v_{xc}(\mathbf{r}-\mathbf{R}_i,\mathbf{r}-\mathbf{R}_j)$, as defined in Eq. (83). However, $\delta E_{oh}$ is largely compensated for by orthogonalization-hole contributions to $\Delta_{dd'}$ in the valence band-structure energy. Since we are here neglecting the latter contributions in Eq. (83) for $\Delta_{dd'}^{vol}$, it is also appropriate to neglect $\delta E_{oh}$. This has been done in all of our preliminary applications of the transition-metal GPT.[24–26] as well as in the calculations presented below. The final term $\delta E_{ke}(i,j)$ in Eq. (137) is a correction for the increased kinetic energy due to the overlap of $d$ states on site $i$ with the inner-core states of site $j$ and vice versa. This correction becomes important for nearly filled $d$ bands and is discussed in detail in the next section.

The two-ion terms in Eq. (135) for $E_{bind}^{solid}(Z)$ are in a mixed reciprocal-space and real-space representation. To convert this equation to the real-space form (126) requires only standard transformations. The total pair potential $v_2(r)$ becomes

$$v_2(r)=v_2^d(r)+v_2^{rest}(r)=\frac{(Z^*e)^2}{r}\left[1-\frac{2}{\pi}\int_0^\infty F_N^0(q)\frac{\sin(qr)}{q}dq\right]+v_2^d(r)+v_{ol}^0(r)\ , \tag{139}$$

where $F_N^0$ is the normalized energy–wave-number characteristic

$$F_N^0(q)=-\frac{q^2\Omega}{2\pi(Z^*e)^2}F^0(q)\ . \tag{140}$$

In addition, if we denote the pure volume terms in Eq. (135) as $E_{vol}^0$, then the total volume contribution $E_{vol}$ in Eq. (126) is

$$E_{vol}=E_{vol}^0+\tfrac{1}{2}(Z^*e)^2\left[\frac{1.8}{R_{WS}}-\frac{2}{\pi}\int_0^\infty F_N^0(q)dq+\frac{2\pi}{\Omega}\frac{d^2F_N^0(0)}{dq^2}\right]. \tag{141}$$

Likewise, one can convert Eq. (135) into a reciprocal-space representation which parallels the result obtained in paper II for empty- and filled-$d$-band metals. This can be done by first subtracting from $v_2^d$ its long-range hybridization tail to create the short-range overlap potential

$$v_{ol}(r)=v_2^d(r)+\frac{2}{\pi}\,\mathrm{Im}\int_0^{\varepsilon_F}\sum_{d,d'}\frac{\Gamma_{dd'}^{vol}(r,E)\Gamma_{d'd}^{vol}(r,E)}{(E-E_r)^2}dE+v_{ol}^0(r)\ , \tag{142}$$

and then adding this tail back in reciprocal space to create the total energy–wave-number characteristic

$$F(q)=F^0(q)-\frac{2}{\pi}\,\mathrm{Im}\int_0^{\varepsilon_F}\sum_{\mathbf{k}}\frac{\left[\sum_d v'_{\mathbf{k}+\mathbf{q}d}v'_{d\mathbf{k}}\right]^2}{(E-E_r)^2(E-\varepsilon_{\mathbf{k}})(\varepsilon_{\mathbf{k}}-\varepsilon_{\mathbf{k}+\mathbf{q}})}dE\ . \tag{143}$$

In this representation, the pair potential $v_2$ can be written

$$v_2(r)=\frac{(Z^*e)^2}{r}\left[1-\frac{2}{\pi}\int_0^\infty F_N(q)\frac{\sin(qr)}{q}dq\right]+v_{ol}(r)\ , \tag{144}$$

with $F_N(q)$ related to $F(q)$ as in Eq. (140). This result, of course, is exactly equivalent to Eq. (139) and, in practice, the correspondence is a useful check on the numerical methods used to perform the numerical integrations. Finally, in subtracting and adding the hybridization tail,

$i=j$ and $\mathbf{q}=0$ terms are absorbed into the volume term, which then becomes

$$E'_{\rm vol}=E^0_{\rm vol}+\frac{1}{\pi}\,{\rm Im}\int_0^{\epsilon_F}\left[\sum_d \frac{[\Gamma^{\rm vol}_{dd}(E)]^2}{(E-E_r)^2} - \sum_{\mathbf{k}} \frac{\left[\sum_d v'_{\mathbf{k}d}v'_{d\mathbf{k}}\right]^2}{(E-E_r)^2(E-\epsilon_{\mathbf{k}})^2}\right]dE \ . \tag{145}$$

Figure 12 illustrates the impact of $v_2^{\rm rest}$ on the total pair potential $v_2$ for the case of Cr. In the vicinity of near neighbors, the net effect is to make $v_2$ more attractive. This is primarily the result of hybridization acting through the oscillatory electron density $\delta n_{\rm val}$. In Cr the effect is seen to be relatively large compared to the direct effect of the hybridization term $\Gamma^{\rm vol}_{dd'}$ on $v_2^d$ alone. However, the increased attractive nature of $v_2$ relative to $v_2^d$ for the central transition metals is largely countered by the more repulsive nature of $v_3$ due to hybridization, as will be demonstrated below. In addition, at sufficiently short distances the attractive components of $v_2$ will be balanced by the combined repulsive behavior of the Coulomb potential $(Z^*e)^2/r$ and the increased kinetic energy of overlapping $d$ and inner-core states. This typically results in a deep minimum in the potential, which for the central transition metals can lie well inside nearest-neighbor distances for metallic structures, as shown in Fig. 12 for Cr. But, again, the corresponding repulsive nature of $v_3$ makes this minimum physically inaccessible in such cases.

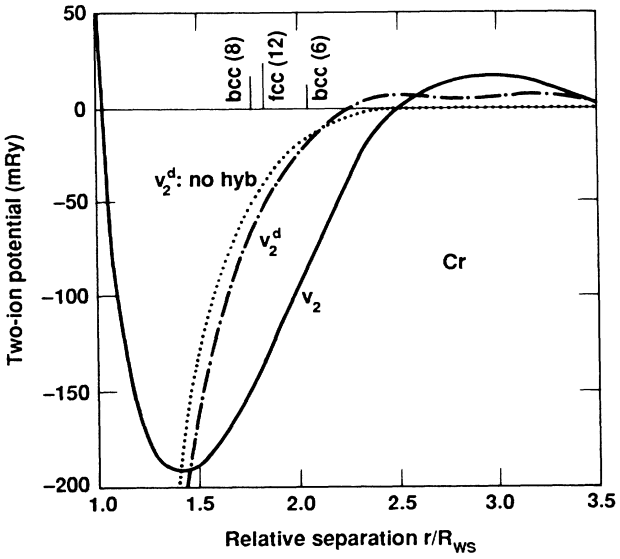


FIG. 12. Relationship of the full two-ion pair potential $v_2(r)$ in Cr to its band-structure $d$-state component $v_2^d(r)$. Also shown for comparison is $v_2^d(r)$ calculated in the limit of no hybridization $[\Gamma^{\rm vol}_{dd'}(R_{ij},E)=0]$, as in Fig. 10(a). The location and number of fcc and bcc near neighbors are indicated.

### C. Calculation of $\delta E_{\rm ke}(i,j)$

We now turn briefly to the kinetic-energy correction term $\delta E_{\rm ke}(i,j)$ introduced into Eq. (137) for $v^0_{\rm ol}$. The attractive electrostatic and exchange-correlation contributions to the $d$-state–inner-core-state overlap have already been included in Eq. (137). To obtain the compensating repulsive kinetic-energy contribution to this overlap, we proceed in the spirit of the cluster expansion developed in Sec. II for the exchange-correlation energy, which yielded the corresponding term $\delta E_{\rm xc}(i,j)$. Specifically, we introduce the kinetic-energy functional

$$\epsilon_{\rm ke}(n)\equiv\frac{3}{5}\frac{\hbar^2}{2m}(3\pi^2)^{2/3}n^{5/3} \tag{146}$$

and the related localized functional

$$\epsilon^*_{\rm ke}(n_i)\equiv\epsilon_{\rm ke}(n_{\rm val}+n_i)-\epsilon_{\rm ke}(n_{\rm val}) \ , \tag{147}$$

as in Eqs. (8) and (9). In analogy with Eqs. (10) and (13), the two-ion overlap contribution to the kinetic energy is then just

$$E_{\rm ke}(i,j)=\epsilon^*_{\rm ke}(n_i+n_j)-\epsilon^*_{\rm ke}(n_i)-\epsilon^*_{\rm ke}(n_j) \ , \tag{148}$$

where, as in $\delta E_{\rm xc}$, we identify $n_i$ with $n^i_{\rm core}$, replace $n_{\rm val}$ with $n_{\rm unif}$, and an integration over all space of the right-hand side of Eq. (148) is implied. From this result for $E_{\rm ke}(i,j)$ we must subtract the kinetic-energy contribution associated with $d$-state overlap alone, which is already contained in $v_2^d$. This is given to a good approximation by

$$E^0_{\rm ke}(i,j)=4\left[\frac{Z_d}{10}\right]\sum_{d,d'}\frac{S_{dd'}(R_{ij})\Delta^{\rm vol}_{d'd}(R_{ij})}{1-S^2_{ij}} =4\left[\frac{Z_d}{10}\right]\sum_{d,d'}S_{dd'}(R_{ij})\Delta^{\rm vol}_{d'd}(R_{ij})+\cdots \ , \tag{149}$$

where

$$S^2_{ij}=\sum_{d,d'}S_{dd'}(R_{ij})S_{d'd}(R_{ij}) \ . \tag{150}$$

The first line in Eq. (149) is an exact result in the limit $Z_d\to 10$ (or $Z_d\to 0$) where the $d$ band is completely filled (or empty). The second line appears explicitly in Eq. (52) of paper II for $v_{\rm ol}$ in a filled (or empty) $d$-band metal. Our final kinetic-energy correction is then taken to be

$$\delta E_{\rm ke}(i,j)=E_{\rm ke}(i,j)-E^0_{\rm ke}(i,j) \ . \tag{151}$$

At sufficiently large separation where the overlap is confined entirely to $d$ states, $E_{\rm ke}(i,j)$ does indeed approach $E^0_{\rm ke}(i,j)$, as shown in Fig. 13 for Cu. At smaller separations, $\delta E_{\rm ke}(i,j)>0$ as expected, and in the case of Cu this correction amounts to 50% of $E_{\rm ke}(i,j)$ at the fcc nearest-neighbor distance. However, the percentage contribution of $\delta E_{\rm ke}(i,j)$ drops steadily as one moves to the left in the transition series away from the noble metals. In the central transition metals, the nearest-neighbor contribution of $\delta E_{\rm ke}(i,j)$ is typically only 10% or 15% of $E_{\rm ke}(i,j)$.

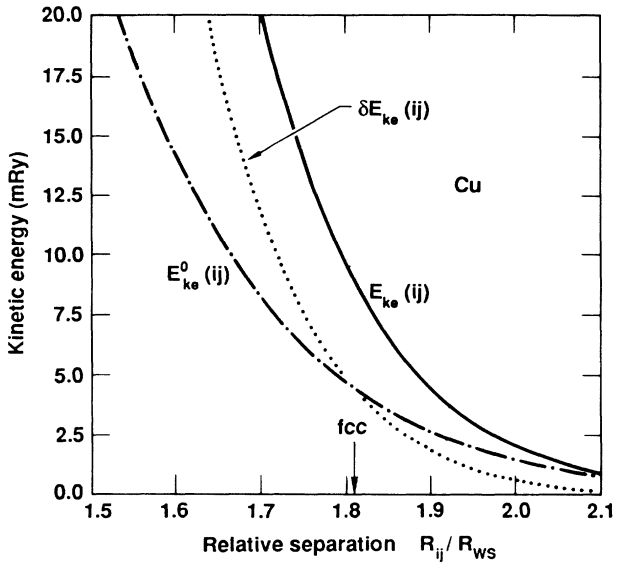


FIG. 13. Two-ion overlap kinetic-energy contributions to the full pair potential $v_2(R_{ij})$ for Cu, as discussed in the text. The location of the fcc nearest-neighbor distance is indicated.

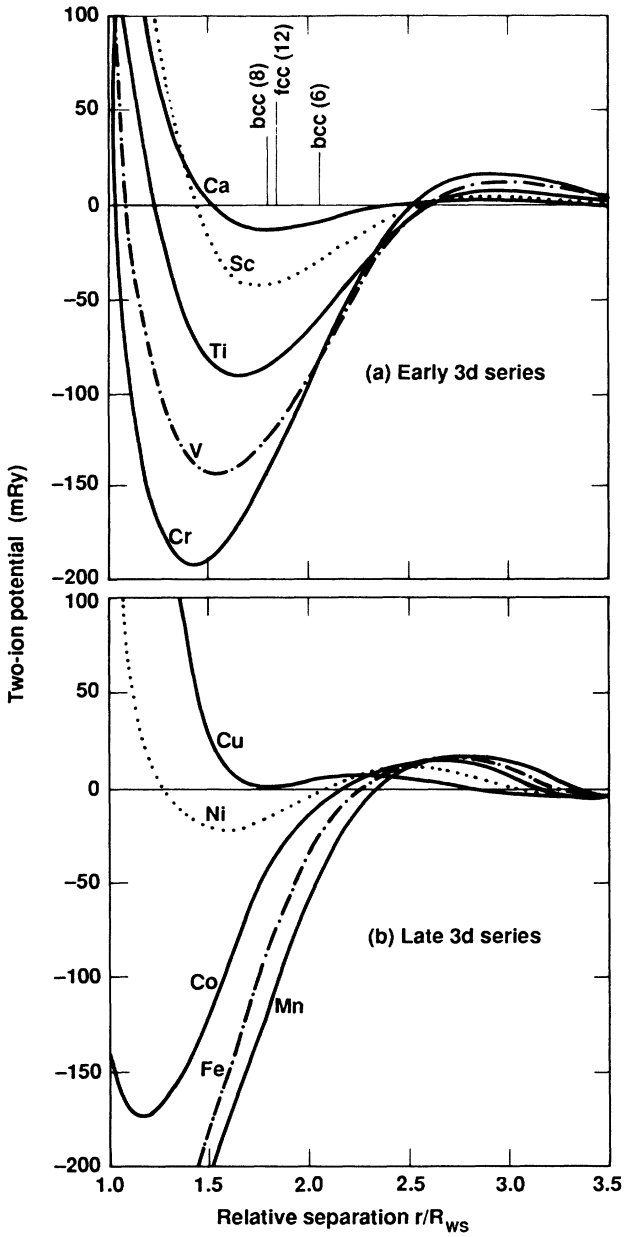


FIG. 14. Two-ion pair potential $v_2(r)$ for the $3d$ transition metals, as calculated from the full theory of Sec. V. The location and number of fcc and bcc near neighbors are indicated.

### D. Interatomic potentials for $3d$ and $4d$ metals

The full theory developed above has been applied to calculate two-ion pair potentials $v_2$ and three-ion triplet potentials $v_3$ for all 20 of the $3d$ and $4d$ transition metals. The two-ion potentials have been obtained using Eqs. (97), (98), (137), (142)–(144), and (151), with all quantities entering these equations evaluated from first principles. Our calculated $v_2(r)$ for the $3d$ series are illustrated in Fig. 14 and those for the $4d$ series in Fig. 15. Both series show systematic behavior which is driven in large part by the $d$-electron physics we have elaborated on here. Beginning on the left-hand side of these series with Ca and Sr, $v_2(r)$ displays a shallow minimum in the vicinity of the fcc nearest-neighbor distance and weak Friedel-like oscillations at long range. The potentials for Ca and Sr are qualitatively similar to those for simple metals on the left-hand side of the Periodic Table, although quantitatively the $d$-state hybridization is essential, as we have previously emphasized in paper II. As one moves to the right in the Periodic Table, the depth of the first minimum increases, its position moves to shorter distances, and the amplitude of the long-range oscillation increases. This behavior primarily reflects the effects of $d$-band filling, but is strongly amplified by the $d$-state hybridization as in Fig. 12. These trends continue through the center of each series and then begin to reverse themselves as one moves towards the end of each series. At the same time, the repulsive overlap kinetic energy $E_{ke}(i,j)$ is growing such that by the time Cu and Ag are reached the potential in the vicinity of near neighbors has been pushed entirely to positive energy. The resulting picture of the noble metals as having purely repulsive near-neighbor potentials, while at the same time an increased cohesive energy due to $E^d_{vol}$, appears to be consistent with both a band-theory description of cohesion and the observed behavior of intermetallic compounds involving noble-metal atoms.[47]

The corresponding three-ion potentials have been obtained using Eqs. (99)–(101), again with all quantities evaluated from first principles. As in our model results of Sec. IV B, the full three-dimensional triplet potential $v_3(r_1,r_2,r_3)$ is most easily discussed by considering the limit $r_1=r_2$, where $r_3=2d\sin(\theta/2)$ and the potential is a function of distance $d$ and angle $\theta$ only. Figures 16 and 17 illustrate two of the most prominent types of behavior that we find for $v_3(d,\theta)$ in the transition metals. Figure 16 shows the dominantly attractive nature of $v_3$ for Sc,

which is typical of the early transition metals, while Fig. 17 shows the dominantly repulsive nature of $v_3$ for Cr, typical of the central transition metals. These results also demonstrate that $v_3(d,\theta)$ is a rapid function of both $d$ and $\theta$, in each case increasing in magnitude with decreasing $d$ and exhibiting minima or maxima at intermediate angles $\theta$. The general magnitude of $v_3$ also varies rapidly with atomic number, as shown for the $3d$ and $4d$ series in Figs. 18 and 19, respectively, and near each series end $v_3$ again becomes primarily attractive. As with $v_2$, these trends reflect the effects of $d$-band filling, with the maximum strength of $v_3$ occurring near the center of each series. In addition, the relative importance of $v_3$ compared to $v_2$ also tends to be greatest for the central transition metals. At the ends of the series in Ca, Sr, Cu, and Ag, we find $v_3$ to be negligibly small. At the same time and as in the case of $v_2$, $d$-state hybridization strongly amplifies the magnitude of $v_3$ for a given element. In the central transition metals, this results in a great deal of cancellation of the hybridization contributions due to the opposite signs of $v_2$ and $v_3$. This cancellation is readily evident in calculated physical properties. One can show this explicitly by multiplying each interatomic hybridization term coupling sites $i$ and $j$ in the total energy by $\exp[-\alpha(R_{ij}/R_{\rm WS})^2]$ and allowing $\alpha^{-1}$ to grow from zero. Figure 20 illustrates the behavior of the pair-potential energy $E_2$, the triplet energy $E_3$, and their sum for bcc Cr as a function of $\alpha^{-1}$. While the magnitudes of

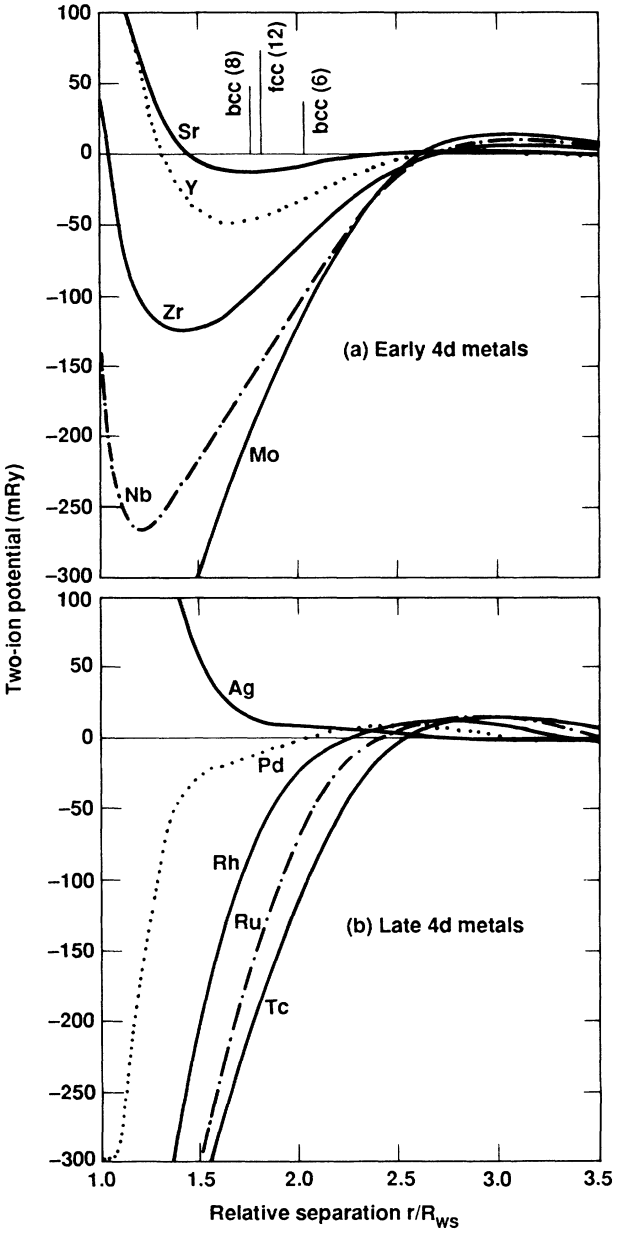


FIG. 15. Two-ion pair potential $v_2(r)$ for the $4d$ transition metals, as calculated from the full theory of Sec. V. The location and number of fcc and bcc near neighbors are indicated.

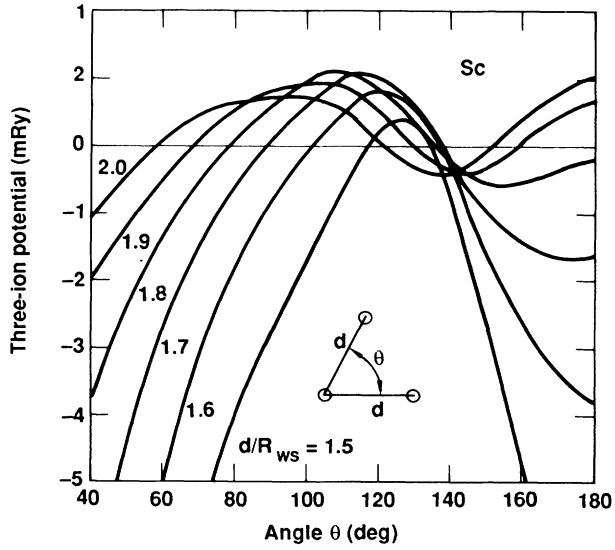


FIG. 16. Three-ion triplet potential $v_3(d,\theta)$ for Sc, as calculated from the full theory of Sec. V in the range $1.5 \le d/R_{\rm WS} \le 2.0$.

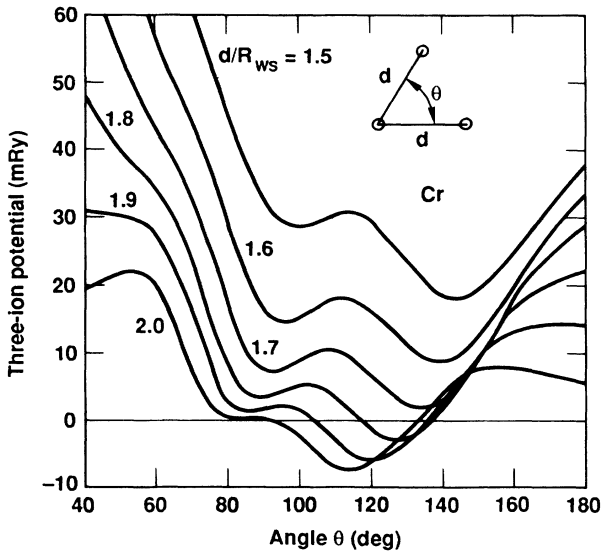


FIG. 17. Three-ion triplet potential $v_3(d,\theta)$ for Cr, as calculated from the full theory of Sec. V in the range $1.5 \le d/R_{\rm WS} \le 2.0$.

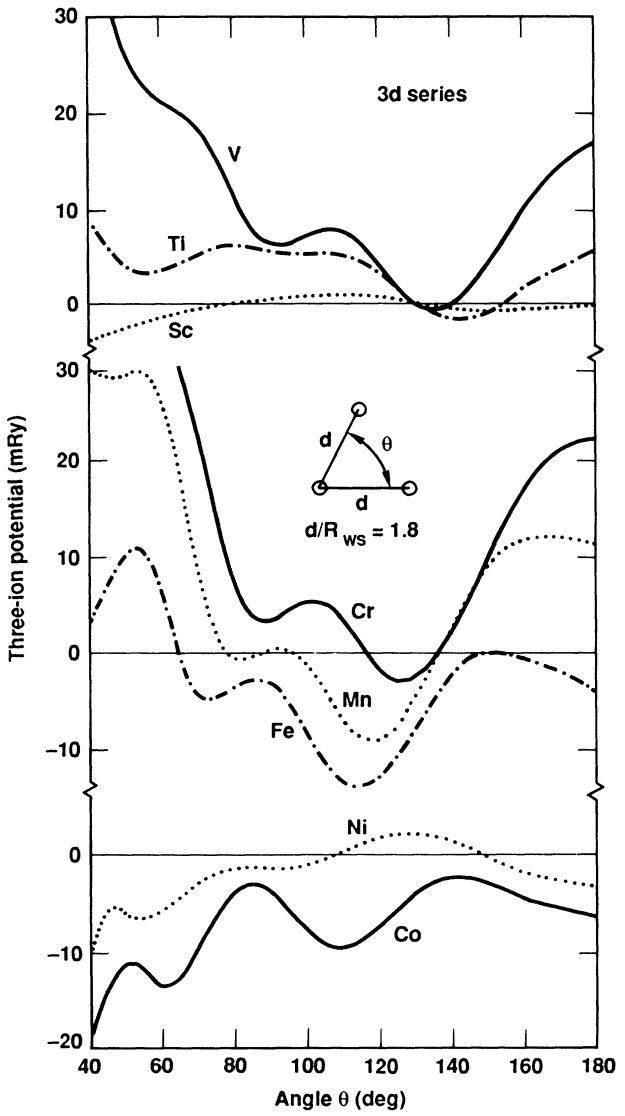


FIG. 18. Three-ion triplet potential $v_3(d,\theta)$ for the $3d$ transition metals, as calculated from the full theory of Sec. V with $d/R_{\rm WS}=1.8$.

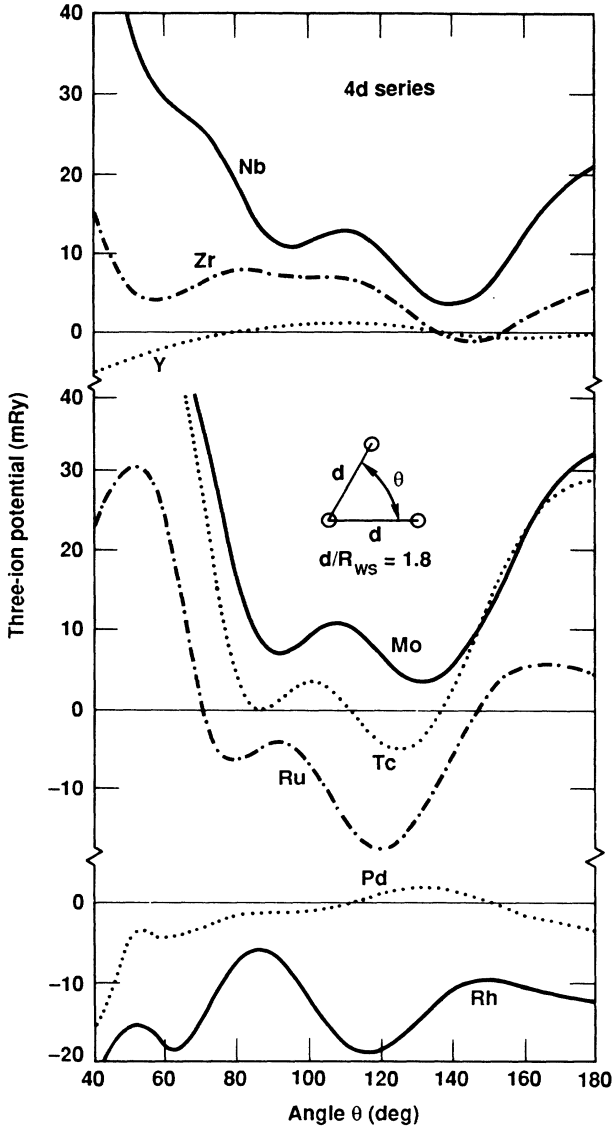


FIG. 19. Three-ion triplet potential $v_3(d,\theta)$ for the $4d$ transition metals, as calculated from the full theory of Sec. V with $d/R_{\rm WS}=1.8$.

$E_2$ and $E_3$ increase rapidly as the hybridization strength grows, $E_2+E_3$ remains relatively small and tends to oscillate about zero.

This effective cancellation of hybridization contributions has, we believe, a fundamental physical origin, as well as important practical consequences. The physical origin lies in the very nonspherical nature of the Fermi surface in transition metals, which implies that any net long-range Friedel-type interaction should be strongly damped or screened. In the present theory, the long-range tails of the potentials $v_2$, $v_3$, $v_4$, etc. are dominated by hybridization contributions and screening is only formally achieved through destructive interference among the various multi-ion interactions. In real-space calculations with full hybridization tails included this presents some difficult convergence problems in most cases. One alternative is to transfer part of the total energy to reciprocal space where the convergence is greatly improved. This is readily achieved for the two-ion interactions through the energy–wave-number characteristic $F(q)$, but is very cumbersome for the remaining multi-ion interactions and, consequently, has not as yet been successfully developed in the present context. A more attractive alternative is to simply screen the real-space hybridization interactions from the outset. We have developed several closely related schemes to do this,[24,39] including that discussed above in connection with Fig. 20. These schemes still require more rigorous justification, but as a practical matter they are extremely effective. An example of their use is shown in Fig. 21, where we display calculated [100] phonon spectra for bcc V and Cr obtained using pair and triplet potentials with interatomic hybridization contributions screened in the manner of Fig. 20. In both cases, pair interactions alone

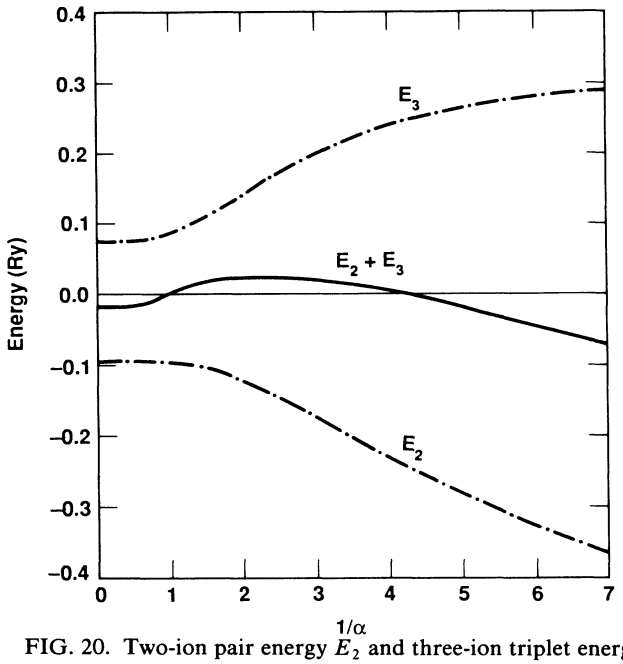


FIG. 20. Two-ion pair energy $E_2$ and three-ion triplet energy $E_3$ for bcc Cr calculated as the interatomic hybridization strength is increased from zero. (Note that $\alpha = \infty$ corresponds to no hybridization and $\alpha = 0$ to full hybridization.)

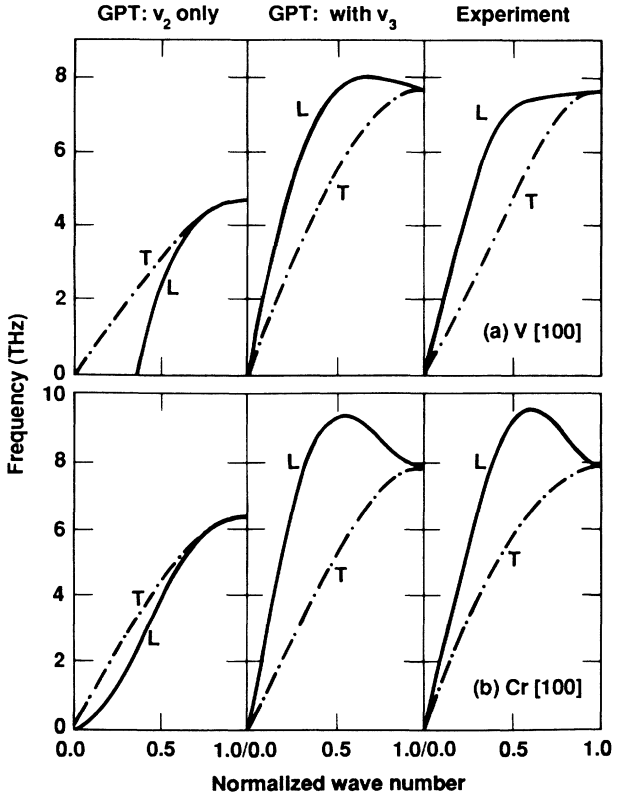


FIG. 21. Phonon spectrum in the [100] direction for the 3*d* bcc metals, as calculated with two-ion pair potential $v_2$ only, with the three-ion triplet potential $v_3$ included, and as observed experimentally. In the theoretical results, the interatomic hybridization contributions have been screened in the manner discussed in the text. (a) *V*, with $D_2^* = -2.0$ and the experimental results from Ref. 48; (b) Cr, with $D_2^* = -2.25$ and the experimental results from Ref. 49.

are seen to be inadequate to explain the observed spectra, with the frequencies too low in magnitude and the longitudinal branch lying below the transverse branch and either soft or unstable low-*q* modes. Addition of the triplet potential in both cases raises the calculated frequencies, pushes the longitudinal branch above the transverse branch, and accounts well for the prominant peaking of the longitudinal branch near the center of the zone in Cr. None of these results is qualitatively sensitive to the details of the screening.

## VI. DISCUSSION

The formal similarity between the present interatomic potential expansion for transition metals, Eq. (1), and the corresponding result for simple metals immediately suggests that the range of application of our potentials should include the vast majority of structural, thermal, and mechanical properties of both the bulk solid and the liquid. Examples of properties on which we have obtained encouraging preliminary results[24–26,39] include cohesion, the vacancy-formation energy, phonons, structural phase stability, melting, and both the solid and liquid equation of state. More generally, we anticipate that these potentials can be useful not only in connection with analytic calculation of physical properties, but also in computer-simulation studies with Monte Carlo and molecular-dynamics techniques. In this regard, simplified analytic fits of the multi-ion potentials will clearly be desirable. While the multi-ion potentials may be calculated without difficulty for any given ion configuration, efficient storage of the potentials for the enormous number of configurations which must be considered with three-ion and four-ion interactions is still an unsolved problem. One possibility we are exploring is to fit the potentials to appropriate separable forms, such as Eq. (121) for $v_3$. Another tract we are pursuing is to develop the model results of Sec. IV B into a complete parametrized version of the transition-metal GPT.[39]

There are only two obvious limits in which the transition-metal GPT developed here is expected to fail. The first of these is in the ultrahigh-pressure regime where the $s \rightarrow d$ transition has been completed and $Z \rightarrow 0$. Even for most high-pressure applications,[26,39] however, this is not a severe limitation, and near normal solid or liquid density, of course, is of no concern at all. The second limit is when the average near-neighbor environment ceases to be bulklike, such as occurs at free surfaces, near cracks or large voids in the solid, or at heterojunctions. In these instances, the valence *s*- and *p*-electron density is very nonuniform and our zero-order psuedoatom is no longer an adequate starting description of the system. Neglected higher-order multi-ion contributions to both the electron density and the total energy become large and essential to a proper treatment. On the other hand, extended defects of the homogeneous system, such as stacking faults, dislocations, and grain boundaries, are much more favorable cases and should be treatable with the present potentials.

There are also two natural extensions of the present theory which we are currently attempting to implement.[39] The first is to *AB* binary systems including in-

termetallic compounds, metallic glasses, quasicrystals, and disordered alloys. Except for the relatively new case of quasicrystals, such extensions have been successfully carried out in the case of simple metals.[50] In the context of the GPT, it should be possible to treat systems in which $A$ is a transition metal and $B$ is either a simple metal or another transition metal. The second possible extension of the present theory is to the light actinide metals, where the $5f$ electrons play the role of the $d$ electrons in transition metals and the $6d$, $7s$, and $7p$ electrons play the role of the valence $s$ and $p$ electrons, as model studies have suggested.[51] All of the methodology we have developed here for localized $d$ states should apply to localized $f$ states in a straightforward way. The only additional complication is the clear need for a relativistic treatment of the inner core in such heavy metals. The same relativistic treatment, of course, could also extend the transition-metal GPT directly to the $5d$-series metals.

Other refinements and extensions of the present theory are also possible. If one so desires, those particular expansions carried out here only to second order, as summarized in Table III, may be systematically developed to higher order. This will mainly produce additional contributions to $v_3$ and $v_4$. However, we expect these contributions to be small and that one will rapidly approach a point of diminishing returns with such refinements. Another possible extension of the transition-metal GPT is to magnetic systems. For a ferromagnetic metal like Fe this is clearly necessary for a realistic treatment of its structural and vibrational properties. The replacement of our local-density formalism with a corresponding local-spin-density (LSD) formalism would allow the incorporation of spin-polarization effects in the same manner as LSD band theory.[9]


## ACKNOWLEDGMENTS

The author wishes to thank Dr. A. K. McMahan for kindly providing the LMTO computer program used in connection with the present research. This work was performed under the auspices of the U. S. Department of Energy by Lawrence Livermore National Laboratory under Contract No. W-7405-Eng-48.


## APPENDIX A

In this appendix we derive Eq. (22) for the atomic promotion energy and discuss its accuracy for transition metals. The LD total energy of the unpromoted free atom with electron density $n_0$ can be written in the shorthand notation of the text as

$$E_{\rm tot}^{\rm atom}(n_0)=\sum_m \alpha_m^0 \varepsilon_m^0 - \tfrac{1}{2} n_0 v(n_0) + n_0[\varepsilon_{\rm xc}(n_0)-\mu_{\rm xc}(n_0)] , \tag{A1}$$

where $v(n_0)$ is the Coulomb potential arising from $n_0$. The electron density of the promoted atom, $n$, differs from $n_0$ by some small amount $\delta n$:

$$n = n_0 + \delta n . \tag{A2}$$

The promoted-atom orbital energies $\varepsilon_m$ are shifted from the $\varepsilon_m^0$ of the unpromoted atom by the extra Coulomb and exchange-correlation potentials accompanying $\delta n$ and, to a lesser extent, by the small amount of relaxation in the orbital wave functions. It is straightforward to show that

$$\sum_m \alpha_m \varepsilon_m = \sum_m \alpha_m \varepsilon_m^0 + (n_0+\delta n)[v(\delta n)+\mu_{\rm xc}(n_0+\delta n)-\mu_{\rm xc}(n_0)] + \sum_m \alpha_m \delta\varepsilon_m^0 , \tag{A3}$$

where $\delta\varepsilon_m^0$ represents the orbital-relaxation contribution. Using the corresponding expression to Eq. (A1) for the promoted atom and Eq. (A3), one finds

$$E_{\rm tot}^{\rm atom}(n_0+\delta n)=\sum_m \alpha_m \varepsilon_m^0 - \tfrac{1}{2} n_0 v(n_0) + \tfrac{1}{2}\delta n\, v(\delta n) + n[\varepsilon_{\rm xc}(n)-\mu_{\rm xc}(n_0)] + \sum_m \alpha_m \delta\varepsilon_m^0 . \tag{A4}$$

An exact form of the promotion energy is thus

$$\begin{aligned} E_{\rm pro}^0 &= E_{\rm tot}^{\rm atom}(n_0+\delta n) - E_{\rm tot}^{\rm atom}(n_0) \\ &= \sum_m (\alpha_m-\alpha_m^0)\varepsilon_m^0 + \tfrac{1}{2}\delta n\, v(\delta n) + n\varepsilon_{\rm xc}(n) - n_0\varepsilon_{\rm xc}(n_0) - \delta n\, \mu_{\rm xc}(n_0) + \sum_m \alpha_m \delta\varepsilon_m^0 . \end{aligned} \tag{A5}$$

The most commonly used approximation to the promotion energy is just the first term in Eq. (A5):

$$E_{\rm pro}^0 = \sum_m (\alpha_m-\alpha_m^0)\varepsilon_m^0 . \tag{A6}$$

The Coulomb correction to this result in Eq. (A5) is clearly of order $(\delta n)^2$. Expanding $n\varepsilon_{\rm xc}(n)$ in powers of $\delta n$ and using Eq. (6), it is also easy to show that the exchange-correlation corrections are of the same order. Thus, neglecting orbital relaxation, Eq. (A6) is correct to first order in $\delta n$. As we demonstrate below, however, this is *not* an adequate approximation for transition metals, where $\delta n$ arises from the transfer of electrons between orbitals of rather different spatial extent. The much more accurate result (22) can be obtained using Eq. (A5) and the analogous expression developed in terms of the promoted-atom energies $\varepsilon_m$:

$$E^1_{\rm pro} \equiv E^{\rm atom}_{\rm tot}(n) - E^{\rm atom}_{\rm tot}(n-\delta n)$$
$$= \sum_m (\alpha_m - \alpha^0_m)\varepsilon_m - \tfrac{1}{2}\delta n\, v(\delta n) + n\varepsilon_{\rm xc}(n) - n_0\varepsilon_{\rm xc}(n_0) - \delta n\, \mu_{\rm xc}(n) + \sum_m \alpha^0_m\, \delta\varepsilon_m \ . \quad \text{(A7)}$$

Averaging Eqs. (A5) and (A7) cancels the Coulomb correction exactly and gives

$$E_{\rm pro} = \tfrac{1}{2}(E^0_{\rm pro} + E^1_{\rm pro})$$
$$= \tfrac{1}{2}\sum_m (\alpha_m - \alpha^0_m)(\varepsilon_m + \varepsilon^0_m) + n\varepsilon_{\rm xc}(n) - n_0\varepsilon_{\rm xc}(n_0) - \tfrac{1}{2}\delta n[\mu_{\rm xc}(n) + \mu_{\rm xc}(n_0)] + \tfrac{1}{2}\sum_m (\alpha_m\, \delta\varepsilon^0_m + \alpha^0_m\, \delta\varepsilon_m) \ . \quad \text{(A8)}$$

The first term is this result is Eq. (22) and the leading correction now involves only exchange-correlation contributions and is readily shown to be of order $(\delta n)^3$. Thus, neglecting orbital relaxation, Eq. (22) is correct to order $(\delta n)^2$.

In order to illustrate the accuracy of Eq. (22) for transition metals, as well as the inadequacy of Eq. (A6), we consider the case of Cu as a function of volume. Then, $Z_0 = 1$ and the promotion involves the transfer of $Z-1$ electrons from the $3d$ to the $4s$ orbital, with $Z-1$ increasing in value as the volume is decreased, as shown in Fig. 5. Equations (A6) and (22) in this case reduce, respectively, to the simple formulas[29]

$$E^0_{\rm pro} = (Z-1)(\varepsilon^0_{4s} - \varepsilon^0_{3d}) \quad \text{(A9)}$$

and

$$E_{\rm pro} = \tfrac{1}{2}(Z-1)[(\varepsilon_{4s} - \varepsilon_{3d}) + (\varepsilon^0_{4s} - \varepsilon^0_{3d})] \ . \quad \text{(A10)}$$

Figure 22 compares these results for $E^0_{\rm pro}$ and $E_{\rm pro}$ with the exact promotion energy obtained from direct total-energy subtraction, over a range of electron transfer from about 0.45 to 1.2. Over this range, $E^0_{\rm pro}$ underestimates the promotion energy by up to 75%, whereas $E_{\rm pro}$ is accurate to within about 5% and always represents an upper bound to the exact result. For a typical transfer of 0.5 electrons, Eqs. (22) and (A10) are accurate to better than 2% and this level of accuracy is reflected in Table I for all of the transition metals.

It is finally of some interest to point out the relationship between Eq. (22) and Slater's transition-state approximation[52] for calculating free-atom excitation energies. Such a result follows from Eq. (22) if one further notes that the eigenvalue $\varepsilon_m$ is approximately linear in the occupation number $\alpha_m$. Replacing $(\varepsilon_m + \varepsilon^0_m)/2$ by the eigenvalue obtained from a parallel atomic calculation in which exactly one-half of the electrons in question are promoted then produces the transition-state approximation.

## APPENDIX B

With the zero of energy taken at the bottom of the valence bands, the nonlocal pseudopotential (34) is, to lowest order, of the theoretically optimized form for simple metals.[53] This form of pseudopotential also enters the present pseudo-Green's-function formalism for $d$-band metals in a natural and convenient way. In fact, useful simplifications in the analysis of Sec. III are possible if one begins with the closely related pseudopotential

$$W = V + P_c(E - H) \ , \quad \text{(B1)}$$

and notes that for $E = \varepsilon_{\mathbf{k}}$ the plane-wave matrix elements $\langle \mathbf{k}+\mathbf{q} \mid W \mid \mathbf{k} \rangle$ of Eqs. (34) and (B1) are identical. This latter replacement is just the effect achieved in the energy integrations over the poles $(E - \varepsilon_{\mathbf{k}})^{-1}$ and $(E - \varepsilon_{\mathbf{k}})^{-2}$ which occur in Eq. (69) for the valence band-structure energy and Eq. (76) for the valence-electron density. At the same time, the Hermitian nature of Eq. (B1) allows for some easier manipulations, especially with respect to the valence-electron density, as discussed in Ref. 2.

The plane-wave matrix elements of Eq. (34) can be separated to lowest order into a structure factor and a form factor in the usual way:

$$\langle \mathbf{k}+\mathbf{q} \mid W \mid \mathbf{k} \rangle = S(\mathbf{q}) \langle \mathbf{k}+\mathbf{q} \mid w \mid \mathbf{k} \rangle + \langle \mathbf{k}+\mathbf{q} \mid W^{\rm struc} \mid \mathbf{k} \rangle \ , \quad \text{(B2)}$$

where the form factor is[31]

$$\langle \mathbf{k}+\mathbf{q} \mid w \mid \mathbf{k} \rangle = v(q) + \sum_c (\varepsilon_{\mathbf{k}} - E^{\rm vol}_c) \langle \mathbf{k}+\mathbf{q} \mid \phi_c \rangle \langle \phi_c \mid \mathbf{k} \rangle \ . \quad \text{(B3)}$$

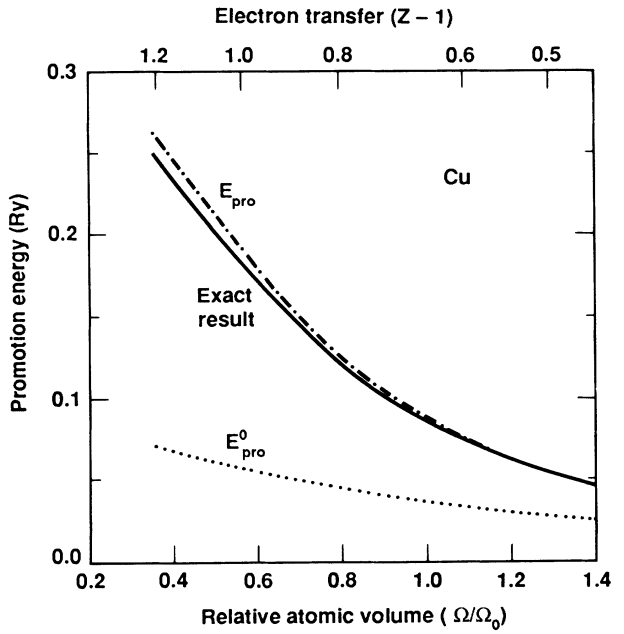


FIG. 22. Promotion energy in Cu as a function of relative atomic volume and electron transfer $Z-1$ between the $3d$ and $4s$ orbitals. The approximate results $E^0_{\rm pro}$ and $E_{\rm pro}$ have been calculated from Eqs. (A9) and (A10), respectively.

with $v(q)$ the Fourier transform of the one-ion component of the potential, as given by Eq. (38) of paper II, and with

$$E_c^{\rm vol}=E_c^{\rm pa}-\langle\phi_c\,|\,\delta V_{\rm unif}\,|\,\phi_c\rangle-V_0' \ . \tag{B4}$$

The core energies $E_c^{\rm vol}$ (as well as the $d$-state energy $E_d^{\rm vol}$) are the same as used in paper II apart from the small constant $V_0'$ determined by the choice of the zero of energy. This constant affects only the repulsive part of the pseudopotential and in paper II we implicitly made the choice $V_0'=0$. The form factor (B3) enters directly in Eq. (129) for the screening electron density and Eq. (136) for the energy–wave-number characteristic. The higher-order structural component of the pseudopotential, $W^{\rm struc}$, is separated from $W$ and then reabsorbed into the total-energy calculation in terms of other quantities, as discussed in Appendix D.

Similarly, the diagonal matrix element $\langle\mathbf{k}\,|\,w_{\rm pa}\,|\,\mathbf{k}\rangle$ appearing in Eq. (87) for the pseudoatom cohesive energy and Eq. (135) for the valence binding energy is given by

$$\langle\mathbf{k}\,|\,w_{\rm pa}\,|\,\mathbf{k}\rangle=\langle\mathbf{k}\,|\,v_{\rm pa}\,|\,\mathbf{k}\rangle-V_0'+\sum_c(\varepsilon_{\mathbf{k}}-E_c^{\rm vol})\langle\mathbf{k}\,|\,\phi_c\rangle\langle\phi_c\,|\,\mathbf{k}\rangle \ . \tag{B5}$$

In addition, placing the zero of energy at the bottom of the valence bands leads to the $\mathbf{k}=\mathbf{0}$ condition

$$\langle 0\,|\,w_{\rm pa}\,|\,0\rangle=0 \ . \tag{B6}$$

Using Eqs. (B4) and (B5), this yields for $V_0'$ the result

$$V_0'=\frac{\langle 0\,|\,v_{\rm pa}\,|\,0\rangle-\sum_c(E_c^{\rm pa}-\langle\phi_c\,|\,\delta V_{\rm unif}\,|\,\phi_c\rangle)\langle 0\,|\,\phi_c\rangle\langle\phi_c\,|\,0\rangle}{1-\langle 0\,|\,p_c\,|\,0\rangle} \ . \tag{B7}$$

For all 20 $3d$ and $4d$ transition metals, we calculate $|V_0'|<0.2$ Ry at normal density with Eq. (B7).

## APPENDIX C

In this appendix we consider the Fermi-energy correction terms $\delta E_{\rm band}$ and $\delta n_{\rm band}(\mathbf{r})$, appearing in Eq. (69) for the valence band-structure energy and in Eq. (76) for the valence-electron density, respectively. We begin by expanding the integrated density of states $\mathcal{N}(E)$ about the zero-order Fermi energy $\varepsilon_F$:

$$\mathcal{N}(E)=\mathcal{N}(\varepsilon_F)+\frac{d\mathcal{N}(\varepsilon_F)}{dE}(E-\varepsilon_F)+\cdots$$
$$=\mathcal{N}(\varepsilon_F)+\rho(\varepsilon_F)(E-\varepsilon_F)+\cdots \ . \tag{C1}$$

Noting that $\mathcal{N}(E_F)=\mathcal{N}_0(\varepsilon_F)+\mathcal{N}_d(\varepsilon_F)=N(Z+Z_d)$, Eq. (C1) can be used to solve for the true Fermi energy $E_F$. One finds

$$E_F=\varepsilon_F-\frac{[\delta\mathcal{N}_{sp}(\varepsilon_F)+\delta\mathcal{N}_d(\varepsilon_F)]}{\rho(\varepsilon_F)}+\cdots \ . \tag{C2}$$

Then, using Eqs. (C1) and (C2) it is straightforward to evaluate Eq. (71) for $\delta E_{\rm band}$. This leads to the general result

$$\delta E_{\rm band}=\tfrac{1}{2}\rho(\varepsilon_F)(E_F-\varepsilon_F)^2+\cdots$$
$$=\frac{1}{2}\frac{[\delta\mathcal{N}_{sp}(\varepsilon_F)+\delta\mathcal{N}_d(\varepsilon_F)]^2}{\rho(\varepsilon_F)}+\cdots \ . \tag{C3}$$

Note that $\delta E_{\rm band}$ is inherently small because $\delta\mathcal{N}_{sp}(\varepsilon_F)$ and $\delta\mathcal{N}_d(\varepsilon_F)$ are both small while $\rho(\varepsilon_F)$ is large. We proceed further by evaluating these latter components only to lowest order. From Eq. (59) one obtains

$$\delta\mathcal{N}_{sp}(\varepsilon_F)=\frac{2}{\pi}\,{\rm Im}\sum_{\mathbf{k}}\frac{W_{\mathbf{kk}}}{\varepsilon_F-\varepsilon_{\mathbf{k}}}+\cdots$$
$$=-\langle\mathbf{k}_F\,|\,w_{\rm pa}\,|\,\mathbf{k}_F\rangle\rho_0(\varepsilon_F)+\cdots \ . \tag{C4}$$

Likewise, using Eq. (64) and expanding the logarithm in the first term one finds

$$\delta\mathcal{N}_d(\varepsilon_F)=\frac{2}{\pi}\sum_d\frac{E_d^{\rm struc}}{\varepsilon_F-E_r}+\cdots$$
$$=-E_d^{\rm struc}\rho_d(\varepsilon_F)+\cdots \ . \tag{C5}$$

Approximating $\rho=\rho_0+\rho_d$ and noting that the formally first-order quantity $E_d^{\rm struc}$ is very small in practice, $\delta E_{\rm band}$ is then taken to be

$$\delta E_{\rm band}=N\left\{\frac{1}{2}\langle\mathbf{k}_F\,|\,w_{\rm pa}\,|\,\mathbf{k}_F\rangle\delta Z_{\rm band}\frac{\rho_0(\varepsilon_F)}{\rho_d(\varepsilon_F)}+E_d^{\rm struc}\delta Z_{\rm band}+\cdots\right\}, \tag{C6}$$

where we have defined

$$\delta Z_{\rm band}\equiv\langle\mathbf{k}_F\,|\,w_{\rm pa}\,|\,\mathbf{k}_F\rangle\frac{\rho_0(\varepsilon_F)\rho_d(\varepsilon_F)}{N[\rho_0(\varepsilon_F)+\rho_d(\varepsilon_F)]} \ . \tag{C7}$$

Similarly, $\delta n_{\rm band}(\mathbf{r})$ is derived from the energy contributions between $\varepsilon_F$ and $E_F$ in the integral on the right-hand side of Eq. (74). Retaining the dominant electron-density terms involving $n_{\rm unif}$ and $n_d$, this leads to

$$\delta n_{\text{band}}(\mathbf{r}) = -\frac{2}{\pi}\,\text{Im}\int_{\varepsilon_F}^{E_F}\left[\sum_{\mathbf{k}}\frac{\langle\mathbf{r}\,|\,\mathbf{k}\rangle\langle\mathbf{k}\,|\,\mathbf{r}\rangle}{E-\varepsilon_{\mathbf{k}}}+\sum_{d}\frac{\langle\mathbf{r}\,|\,\phi_d\rangle\langle\phi_d\,|\,\mathbf{r}\rangle}{E-E_r}+\cdots\right]dE$$
$$=(E_F-\varepsilon_F)\left[\frac{\rho_0(\varepsilon_F)}{NZ}n_{\text{unif}}+\frac{\rho_d(\varepsilon_F)}{NZ_d}\sum_i n_d(\mathbf{r}-\mathbf{R}_i)+\cdots\right], \tag{C8}$$

Finally, using Eqs. (C2), (C4), (C5), and (C7) and keeping only volume and one-ion terms, one has

$$\delta n_{\text{band}}(\mathbf{r})=\frac{\delta Z_{\text{band}}}{2}\frac{\rho_0(\varepsilon_F)}{\rho_d(\varepsilon_F)}n_{\text{unif}}+\frac{\delta Z_{\text{band}}}{Z_d}\sum_i n_d(\mathbf{r}-\mathbf{R}_i)+\cdots . \tag{C9}$$

We note that the second term in Eq. (C9) contributes directly to the orthogonalization-hole density $n_{\text{oh}}$, as given by Eq. (131). The first term in Eq. (C9), on the other hand, combines with a similar contribution from the term involving $W_{\mathbf{kk}}/(E-\varepsilon_{\mathbf{k}})^2$ in Eq. (76) to yield a net compensating uniform density $-(\delta Z_{\text{band}}/Z)n_{\text{unif}}$, which contributes to Eq. (130).

## APPENDIX D

In this appendix we outline the derivation of Eq. (135) for the valence binding energy $E_{\text{bind}}^{\text{solid}}$ from Eqs. (28) and (69). The first step is to add and subtract a term $n_{\text{unif}}(V+V_0')$ from Eq. (69) for $E_{\text{band}}^{\text{val}}$ and write

$$E_{\text{band}}^{\text{val}}=\tfrac{3}{5}NZ\varepsilon_F+n_{\text{unif}}(V+V_0')+NE_d^{\text{vol}}+E_{\text{rest}}\ , \tag{D1}$$

where we have set

$$E_{\text{rest}}\equiv -n_{\text{unif}}(V+V_0')-\int_0^{\varepsilon_F}[\delta\mathcal{N}_{sp}(E)+\delta\mathcal{N}_d(E)]dE - NZ_dE_d^{\text{struc}}+\delta E_{\text{band}} \tag{D2}$$

Using Eq. (D1) in Eq. (28), one can then manipulate the electrostatic quantities exactly and expand the exchange-correlation terms in powers of $\delta n_{\text{val}}$ to obtain

$$NE_{\text{bind}}^{\text{solid}}(Z)=N[\tfrac{3}{5}Z\varepsilon_F+Z\varepsilon_{\text{xc}}(n_{\text{unif}})+ZV_0'+E_d^{\text{vol}}]+E_{\text{rest}}+E_{\text{es}}(Z)$$
$$+n_{\text{unif}}\sum_i v^i_{\text{nuc-core}}-\tfrac{1}{2}\delta n_{\text{val}}\left[\delta V_{\text{val}}+\frac{d\mu_{\text{xc}}(n_{\text{unif}})}{dn}\delta n_{\text{val}}\right]$$
$$+\tfrac{1}{2}{\sum_{i,j}}'\left\{n^i_{\text{core}}v^j_{\text{nuc-core}}+\left[\frac{Z_a+Z}{Z_a}\right]n^i_{\text{nuc}}\left[\left[\frac{Z_a-Z}{Z_a}\right]v^j_{\text{nuc}}+v^j_{\text{core}}\right]+\delta E_{\text{xc}}(i,j)\right\}, \tag{D3}$$

where we have defined

$$v^i_{\text{nuc-core}}\equiv\left[\frac{Z_a-Z}{Z_a}\right]v^i_{\text{nuc}}+v^i_{\text{core}}+v^i_{\text{xc}}\ . \tag{D4}$$

The result (D3) is analogous to Eq. (A1) of paper II, except that we now retain for completeness the small electrostatic term involving $n^i_{\text{nuc}}$, as in Eq. (21) of paper I, and the new exchange-correlation terms from Eq. (28).

In the present development, $\mu^*_{\text{xc}}(n_i)$ and $\varepsilon^*_{\text{xc}}(n_i,n_j)$ are replaced by $v^i_{\text{xc}}$ and $\delta E_{\text{xc}}(i,j)$, respectively, as discussed in connection with Eq. (137), while the higher-order contribution $\delta n_{\text{val}}\delta\mu^*_{\text{xc}}(n_i,n_j)$ is dropped. We may then evaluate the quantity $E_{\text{rest}}$ from Eq. (D2) by using Eqs. (59), (64), and (C6). Expanding the logarithms in Eq. (64), separating volume and structure components, and further using Eqs. (63) and (89) leads to

$$E_{\text{rest}}=-\frac{2}{\pi}\,\text{Im}\int_0^{\varepsilon_F}\left[\sum_{\mathbf{k}}\left[\frac{\langle\mathbf{k}\,|\,W-(V+V_0')\mathbf{k}\rangle}{E-\varepsilon_{\mathbf{k}}}+\frac{1}{2}\frac{(\langle\mathbf{k}\,|\,W\,|\,\mathbf{k}\rangle)^2}{(E-\varepsilon_{\mathbf{k}})^2}+{\sum_{\mathbf{q}}}'\frac{|\langle\mathbf{k}+\mathbf{q}\,|\,W\,|\,\mathbf{k}\rangle|^2}{(E-\varepsilon_{\mathbf{k}})(\varepsilon_{\mathbf{k}}-\varepsilon_{\mathbf{k}+\mathbf{q}})}\right]\right.$$
$$\left.+\sum_d\left[\frac{E_d^{\text{struc}}(d\Gamma_{dd}^{\text{vol}}/dE)+\Gamma_{dd}^{\text{struc}}}{E-E_r}+\frac{\Lambda_{dd}^{\text{vol}}}{E-E_r}\right]\right]dE+NE^d_{\text{struc}}+\delta E_{\text{band}}+\cdots\ , \tag{D5}$$

where we have assumed the Hermitian representation of the pseudopotential $W$ given by Eq. (B1) and we have used the integral representation of $n_{\text{unif}}$ in Eq. (78) to combine $V+V_0'$ with $W$ in the first term. This latter term may be manipulated exactly as in Eq. (A3) of paper II to yield

$$N\frac{2\Omega}{(2\pi)^3}\int_{k<k_F}\langle\mathbf{k}\,|\,W-(V+V_0')\,|\,\mathbf{k}\rangle d\mathbf{k}=N\frac{2\Omega}{(2\pi)^3}\int_{k<k_F}\langle\mathbf{k}\,|\,w_{\text{pa}}\,|\,\mathbf{k}\rangle d\mathbf{k}-n_{\text{unif}}\sum_i v^i_{\text{pa}}-\sum_i(n^c_{\text{oh}})^i\delta V^i_{\text{struc}}\ . \tag{D6}$$

The terms in Eq. (D5) involving $E_d^{\text{struc}}$ and $\Gamma_{dd}^{\text{struc}}$ represent the net contribution to $E_{\text{bind}}^{\text{solid}}$ from the structure-dependent

part of the hybridization potential and, as in paper II for an empty- or filled-$d$-band metal, can be collapsed into the form $-\sum_i n^i_{\rm oh}\delta V^i_{\rm struc}$:

$$-\sum_i n^i_{\rm oh}\,\delta V^i_{\rm struc}=-\sum_i (n^c_{\rm oh})^i\delta V^i_{\rm struc}-\frac{2}{\pi}\,{\rm Im}\int_0^{\epsilon_F}\sum_d\left[\frac{E_d^{\rm struc}(d\Gamma_{dd}^{\rm vol}/dE)+\Gamma_{dd}^{\rm struc}}{E-E_r}\right]dE+NE_d^{\rm struc}\delta Z_{\rm band}\ . \tag{D7}$$

Equation (D7) can be verified directly by using Eq. (131) for $n_{\rm oh}(\mathbf{r})$ and noting the definitions of the various quantities. The remaining terms in Eq. (D5) may be evaluated in a straightforward manner to give the result

$$N(E_{\rm fe}+E_d^{\rm vol})+E_{\rm rest}=NE^0_{\rm vol}-n_{\rm unif}\sum_i v^i_{\rm pa}+\frac{Z^*-Z}{Z}n_{\rm unif}\left[V_{\rm unif}-\sum_i v^i_{\rm unif}\right]$$
$$+\sum_i n^i_{\rm oh}\,\delta V^i_{\rm struc}+N\sum_{\mathbf{q}}{}'\,|\,S(\mathbf{q})\,|^2\,\delta F^0(q)+NE^d_{\rm struc}\ , \tag{D8}$$

where $\delta F^0(q)$ represents the first two terms in Eq. (136) involving the form factor of $w$. The final step is to manipulate the orthogonalization-hole terms left in Eqs. (D3) and (D8) by adding and subtracting a term $\delta n_{\rm oh}\,\delta V_{\rm oh}$ in Eq. (D3), noting that

$$-\sum_i n^i_{\rm oh}\,\delta V^i_{\rm struc}=\sum_{i,j} n^i_{\rm oh}\left[\frac{Z}{Z_a}v^j_{\rm nuc}+v^j_{\rm nuc\text{-}core}+\delta v^{ij}_{\rm xc}\right]+\delta n_{\rm oh}\left[\delta V_{\rm val}+\frac{d\mu_{\rm xc}(n_{\rm unif})}{dn}\delta n_{\rm val}\right]\ , \tag{D9}$$

and using Eqs. (A8) and (A9) of paper II. Equation (135) then follows immediately with the inclusion of the overlap kinetic-energy term $\delta E_{\rm ke}$ discussed in Sec. V.

---


[1]W. A. Harrison, Phys. Rev. **181**, 1036 (1969).

[2]J. A. Moriarty, Phys. Rev. B **5**, 2066 (1972).

[3]L. Dagens, J. Phys. F **6**, 1801 (1976); **7**, 1167 (1977); Phys. Status Solidi B **84**, 311 (1977).

[4]J. A. Moriarty, Phys. Rev. B **16**, 2537 (1977) (referred to as paper I in the text).

[5]J. A. Moriarty, Phys. Rev. B **26**, 1754 (1982) (referred to as paper II in the text).

[6]J. A. Moriarty, Int. J. Quantum Chem. Quantum Chem. Symp. **17**, 541 (1983), and additional references therein.

[7]J. C. Upadhyaya and L. Dagens, J. Phys. F **8**, L21 (1978); **9**, 2177 (1978); **12**, L137 (1982); Phys. Rev. B **26**, 743 (1982).

[8]W. Kohn and L. J. Sham, Phys. Rev. **140**, A1133 (1965).

[9]V. L. Moruzzi, J. F. Janak, and A. R. Williams, *Calculated Electronic Properties of Metals* (Pergamon, New York, 1978).

[10]H. L. Skriver, Phys. Rev. B **31**, 1909 (1985).

[11]K.-M. Ho, C. L. Fu, and B. N. Harmon, Phys. Rev. B **29**, 1575 (1984).

[12]See, for example, L. Dagens, M. Rasolt, and R. Taylor, Phys. Rev. B **11**, 2726 (1975); J. Hafner, J. Non-Cryst. Solids **61-62**, 175 (1984).

[13]See, for example, R. A. Johnson, J. Phys. F **3**, 295 (1973), and references therein.

[14]A. E. Carlsson, C. D. Gelatt, Jr., and H. Ehrenreich, Philos. Mag. **41**, 241 (1980).

[15]D. M. Esterling and A. Swaroop, Phys. Status Solidi B **96**, 401 (1979); A. Swaroop and D. M. Esterling, *ibid.* **96**, 691 (1979).

[16]C. C. Matthai, P. J. Grout, and N. H. March, J. Phys. Chem. Solids **42**, 317 (1981), and refereinces therein.

[17]E. S. Machlin and J. Shao, J. Phys. Chem. Solids **44**, 435 (1983).

[18]M. S. Daw and M. I. Baskes, Phys. Rev. B **29**, 6443 (1984).

[19]M. W. Finnis and J. E. Sinclair, Philos. Mag. A **50**, 45 (1984).

[20]A. E. Carlsson and N. W. Ashcroft, Phys. Rev. B **27**, 2101 (1983); R. H. Brown and A. E. Carlsson, *ibid.* **32**, 6125 (1985).

[21]J. M. Wills and W. A. Harrison, Phys. Rev. B **28**, 4363 (1983).

[22]A. H. MacDonald and R. Taylor, Can. J. Phys. **62**, 796 (1984).

[23]L. Dagens, J. Phys. F **16**, 1705 (1986).

[24]J. A. Moriarty, Phys. Rev. Lett. **55**, 1502 (1985).

[25]J. A. Moriarty, Phys. Rev. B **34**, 6738 (1986).

[26]J. A. Moriarty, in *Shock Waves in Condensed Matter,* edited by Y. M. Gupta (Plenum, New York, 1986), p. 101.

[27]The difficulty in treating the noble metals Cu and Ag as having completely filled $d$ bands is discussed in details in paper II and reflects the fact that the metallic valence $Z$ is some 65% larger than the atomic valence $Z_0$. In the alkaline-earth metals Ca and Sr, on the other hand, $Z$ is only about 20% smaller than $Z_0$, so that these metals are accurately treated in the empty-$d$-band limit of the GPT. For the third alkaline-earth metal Ba, however, $Z_0-Z$ is considerably larger and a transition-metal treatment is required (see Ref. 25).

[28]L. Hedin and B. I. Lundqvist, J. Phys. C **4**, 2064 (1971).

[29]In the rare case where $Z>2$, such as occurs in Cu under extreme compression, the extra $Z-2$ electrons are promoted to the next unoccupied $p$ orbitals. The general result for the promotion energy, Eq. (22), remains valid, but the specific forms, Eqs. (A9) and (A10), must be suitably generalized.

[30]J. A. Moriarty, Phys. Rev. B **19**, 609 (1979).

[31]In Secs. IV and V and Appendix B, we revert to the convention of papers I and II and remove the implicit summation over ion sites in $\sum_c$ and $\sum_d$, so that these sums are then over states on one particular site.

[32]One can alternatively define a logarithmic derivative $D_2$ directly in terms of $\phi_d(\mathbf{r})$, as in Eqs. (63)–(65) of paper II. For $E_d^{\rm vol}=E_d^0$, which is approximately the case in empty- and filled-$d$-band metals, one has $D_2^*=D_2$. In pure transition metals, on the other hand, $E_d^{\rm vol}$ lies somewhat below $E_d^0$ in energy, and the definition (81) is preferred.

[33]O. K. Andersen, Phys. Rev. B **12**, 3060 (1975); O. K. Andersen and O. Jepsen, Physica **91B**, 317 (1977).

[34]H. L. Skriver, *The LMTO Method* (Springer, Berlin, 1984).

[35]The present self-consistent LMTO calculations have been car-

ried out for all $3d$ and $4d$ transition metals within the nonrelativistic local-density framework (Ref. 8), using the Hedin-Lundqvist exchange-correlation potential (Ref. 28). The calculations employ the atomic-sphere approximation, the combined-correction term to this approximation, and $s$, $p$, $d$, and $f$ angular-momentum components of the valence-electron density (Ref. 34). For a consistent comparison with our GPT results, a fcc structure and the observed equilibrium atomic volume have been assumed in each case and the electrostatic Ewald or muffin-tin correction (Ref. 34) has been included in the cohesive energy results presented in Fig. 7. In the case of Mo, similar calculations for both the fcc and bcc structures have been performed over a volume range corresponding to Fig. 5.

[36]As calculated in the LMTO method, the number of non-$d$ valence electrons within the atomic sphere contains a slight structure dependence. For the case of Mo at its observed equilibrium atomic volume, we find the difference between the fcc and bcc values to be about 6%.

[37]R. C. Albers, A. K. McMahan, and J. E. Müller, Phys. Rev. B **31**, 3435 (1985); A. K. McMahan (private communication).

[38]While Eq. (98) is an exact result for $L_{ij}$, Eq. (100) for $L_{ijk}$ and Eq. (103) for $L_{ijkl}$ are exact only for site orientations where all of the matrices $T_{ij}$, $T_{jk}$, etc. involved in these expressions mutually commute. For arbitrary site orientations these matrices will not all commute, and there are correction terms which are formally fifth order in the $T_{ij}$. In practice, such corrections are typically very small and are here neglected.

[39]J. A. Moriarty (unpublished).

[40]In dropping the energy dependence of $\Gamma_{dd}^{\mathrm{vol}}(E)$ in Eq. (109), it is appropriate to extend also the lower limit of integration in Eqs. (106)–(108) to $-\infty$ to avoid any spurious contributions from this limit.

[41]J. A. Moriarty, J. Phys. F **5**, 873 (1975).

[42]D. G. Pettifor, J. Phys. F **7**, 613 (1977).

[43]W. A. Harrison, *Electronic Structure and the Properties of Solids* (Freeman, San Francisco, 1980), pp. 500–517.

[44]For the general tight-binding argument, see V. Heine, in *Solid State Physics*, edited by H. Ehrenreich, F. Seitz, and D. Turnbull (Academic, New York, 1980), Vol. 35, pp. 80–83.

[45]S. Ichimaru and K. Utsumi, Phys. Rev. B **24**, 7385 (1981).

[46]D. J. W. Geldart and R. Taylor, Can. J. Phys. **48**, 167 (1970).

[47]N. E. Christensen and V. Heine, Phys. Rev. B **32**, 6145 (1985).

[48]R. Colella and B. W. Batterman, Phys. Rev. B **1**, 3913 (1970).

[49]M. W. Shaw and L. D. Muhlestein, Phys. Rev. B **4**, 969 (1971).

[50]See, for example, J. Hafner, Phys. Rev. B **21**, 406 (1980); **16**, 351 (1977); **15**, 617 (1977); J. Phys. F **6**, 1243 (1976).

[51]W. A. Harrison, Phys. Rev. B **28**, 550 (1983).

[52]J. C. Slater, *The Self-Consistent Field for Molecules and Solids: Quantum Theory of Molecules and Solids* (McGraw-Hill, New York, 1974), Vol. 4, pp. 51–55.

[53]W. A. Harrison, *Pseudopotentials in the Theory of Metals* (Benjamin, New York, 1966).